Layout and Connectivity of Orientation Domains in Mammalian Visual Cortex: A Physiological Description

by

Louis J. Toth

S.B. Aeronautical and Astronautical Engineering
Massachusetts Institute of Technology, 1989

SUBMITTED TO THE DEPARTMENT OF BRAIN AND COGNITIVE SCIENCES IN PARTIAL FULFILLMENT OF THE REQUIREMENTS FOR THE DEGREE OF

DOCTOR OF PHILOSOPHY IN BRAIN AND COGNITIVE SCIENCES
AT THE
MASSACHUSETTS INSTITUTE OF TECHNOLOGY

SEPTEMBER 1995

Signature of Author:_____
Department of Brain and Cognitive Sciences
6 September 1995

Certified by:_____
Mriganka Sur
Professor of Neuroscience
Thesis supervisor

Accepted by:_____
Gerald E. Schneider
Chariman, Department Graduate Committee

Layout and Connectivity of Orientation Domains in Mammalian Visual Cortex: A Physiological Description

by

Louis J. Toth

Submitted to the department of Brain and Cognitive Sciences
on 6 September 1995 in Partial Fulfillment of the
Requirements for the Degree of Doctor of Philosophy in
Brain and Cognitive Sciences

ABSTRACT

Four experiments using newly developed techniques were used to better understand how orientation selectivity relates to the cortical connectivity and receptive field organization.

1) Comparative imaging of intrinsic signals from cat and ferret cortices showed much smaller distances between iso-orientation domains in ferret. Single-unit properties and anatomical connectivity can be correctly predicted from the imaging results. Since it was strongly expected that the distance between iso-orientation domains in ferret would be larger than in cat, we suggest that cat cortex may employ a novel organization strategy.

2) Imaging of intrinsic signals in cats viewing "center" and "surround" visual stimuli in combination with single-unit recording of receptive fields showed that lateral spreads exclusively between iso-orientation domains, and into regions far beyond what would be predicted from knowledge of the "classical" receptive fields. Stimuli in the extra-classical receptive field can facilitate or suppress iso-orientation responses, depending on the level of center contrast.

3) Using the technique of *in vivo* whole-cell recording, we studied the responses of cells to small bars flashed at various positions in the receptive field. Cells responded at multiple, discrete latencies, generally separated in time by 70-100 msec. At distant locations outside of the "classical" receptive field, EPSPs were found only at the longer latencies. These results suggest that the "extra-classical" receptive field does not influence the fastest response of cells, and that information traveling laterally in cortex is carefully synchronized, perhaps by an intracolumnar mechanism.

4) Intrinsic signals were imaged before, during and after iontophoresis of drugs that selectively influence the inhibitory circuitry of the cortex. The antagonist bicuculline increased both the magnitude and lateral spread of the iso-orientation response, changing the orientation preference of a cortical region of 1.5 mm radius around the injection. Agonists GABA and muscimol changed the orientation preference towards orthogonal orientations. The results are most consistent with a model of cortical function where inhibition serves to non-specifically limit the spread of excitation.

Thesis Supervisor: Mriganka Sur
Title: Professor of Neuroscience

Dedicated to Louis Toth, 1908-1992,
in partial fulfillment of his dreams.

ACKNOWLEDGMENTS

The author wishes to thank his experimental colleagues who cheerfully endured an uncountable number of long, painful, multi-day experiments: Young Kwon, Manny Esguerra, Sarah Pallas, Sacha Nelson, Chenchal Rao, Dae-Shik Kim, Jitendra Sharma.

The author especially thanks Sacha Nelson, for his extensive collaboration in pioneering the *in vivo* whole-cell recording technique in our lab.

Likewise, the author thanks Chenchal Rao for extensive collaboration in setting up the intrinsic signal imaging technique in our lab, and cheerfully doing many cat and ferret surgeries.

The success of a graduate education depends most on the presence of gifted scientific mentors. The author would like to express his appreciation to those mentors who provided him this most important part of his own scientific education: Sarah Pallas, Sacha Nelson, and Dae-Shik Kim.

The author thanks those who have served on his thesis committee, for their supportive nature and their insightful criticisms: Mriganka Sur (MIT), Peter Schiller (MIT), Richard Anderson (Cal. Inst. Tech.), Matt Wilson (MIT), and Barry Connors (Brown Univ.).

The animals (and students) participating in these experiments were extremely fortunate to have received the loving care and attention of Dr. Robert P. Marini (Dr. Bob), Carson Odle, and the entire, highly competent veterinary staff of the Division of Comparative Medicine at MIT.

Most importantly, the author thanks his advisor Mriganka Sur, and his parents Louis P. and Marilyn B. Toth, for providing him not only freedom, but also the financial support to pursue whatever he wished.

Lastly, the author thanks the many makers of precision equipment who have made his graduate career especially enjoyable: F. Lorée, Rigoutat, Buffet-Crampon, Schreiber und Söhne, Geminhardt, Yamaha, and Selmer Paris.

Table of Contents:

Reproductions of the color figures contained in this work may be requested from:

Louis Toth
E25-618
45 Carleton St.
Cambridge, MA 02139
ljtoth@mit.edu

Introduction

General theories of brain function have been based on the premise that the brain can be divided into several compartments, each of which is responsible for a particular function. Originating with the phrenology of F.J. Gall, the premise received the first concrete experimental support from J. Hughlings Jackson. The foundations were laid for over a century of work in neuroanatomy and neurophysiology; work which subdived the brain into uncountable divisions in the hopes that important functional correlations could be therein discovered.

In the visual system, numerous subdivisions exist (reviewed in Schiller, 1986). On the gross level, light enters the eye, passes through structures of the lens, is transduced into an electrical signal by cells in the retina, is carried by the optic nerve to the dorsal lateral geniculate nucleus in the thalamus (LGN), and is there carried through the optic radiation to primary and a host of other "association" areas of cortex. Although this is the familiar path, the one apparently mediating visual consciousness, other paths also exist, notably those to the superior colliculus and accessory optic system in the brainstem, which mediate other, probably subconscious tasks. In each of these areas, further subdivisions exist. On a cellular level, signals from the retina pass through three forward layers of neurons (photoreceptors, bipolar cells and ganglion cells) and are modulated by two horizontal ones (horizontal and amarcine), before leaving the eye. The LGN, though only contributing one synapse to the forward visual pathway, is itself divided into many layers (three in cat, six in primates) corresponding to ocularity of the inputs, and physiological

classification of inputs fibers. In the ferret, (*Mustela putoris furo)* the LGN also contains a novel division into sublayers corresponding to cells' preference for light increment or decrement (Stryker and Zahs, 1983). LGN projections are received mainly by primary visual cortex (termed "V1" in primates, and "area 17", in analogy with Brodmann's classification scheme, in cats) though in cats several "higher" visual areas also receive direct projections (LeVay and Gilbert, 1976). All projections from retina to LGN and from LGN to cortex, are excitatory in nature, though within each structure, inhibitory interneurons exist providing forward projecting cells with fast modulation. Furthermore, a large projection exists from primary cortex back to the LGN and reticular nucleus, outnumbering the forward projection by 10:1 (Robson, 1983; Walker, 1938). Once signals arrive in the visual cortex, a bewildering array of connectivity makes dissection of the circuitry quite difficult. However, cortex (Talbot, 1940), like LGN (Bishop et al, 1962) and many other visual areas, contains a retinotopic mapping of visual space, which is preserved in the radial dimension. Similarly, many other physiological properties are preserved radially, such as orientation preference, ocular dominance, color, and more controversially ON/OFF (McConnell and LeVay, 1984; Zahs and Stryker, 1988), and directional columns (Payne et al, 1980; Rao et al, 1995) (for reviews see Valverde, 1991; LeVay and Nelson, 1991). Evidence concerning the combination of these properties in "hypercolumns" (Hubel and Wiesel, 1974) the conceptual repeat unit of the cortex, is presented in chapter 1.

Properties which are preserved in the radial dimension also form orderly maps in the lateral dimension. Maps of retinotopy, orientation and ocular dominance have been particularly well-studied in primary visual cortex by a variety of techniques. It is reasonable to ask, therefore, what role is played by lateral fibers in generating, or maintaining these properties. Lateral connections within area 17 are both local and long-range. While local connections arise from many different cell types in many layers, long-range connections arise mainly from pyramidal cells in layers II and III (Gilbert and Wiesel, 1983). In a pattern similar across many species, they tend to arborize in patchy clusters (tree shrew, Rockland et al, 1982; primate, Rockland and Lund, 1983; Blasdel et al, 1985; Livingstone and Hubel, 1984; ferret, Rockland, 1985; cat Luhmann et al, 1986; Gilbert and Wiesel, 1989), though the periodicity of these clusters may differ between species. Since the periodicity of the long-range connections is similar to the periodicity of orientation domains, it may be that long-range connections mediate some aspect of their function. The relationship of the periodicity of long-range connections to that of orientation domains is not always 1:1, and in chapter 1 we explore the possibility that it may also involve the arrangement of ocular dominance columns. Long-range connections have been shown to connect regions of similar orientation preferentially (Gilbert and Wiesel, 1989; Sharma et al, 1995). Furthermore, these connections are assumed to be excitatory only (demonstrated by Kisvárday et al, 1993 in area 18). Inhibitory connections, on the other hand, are mainly local, and do not show correlation with the orientation system (Kisvárday et al, 1994). In chapters 1 and 2, we discuss the role of long-range connectivity in generating and maintaining the orientation maps, and in chapter

4, we examine the role of the inhibitory network in maintaining orientation selective responses. Despite demonstrations that modulating inhibition pharmacologically changes the orientation tuning of cortical cells (Sillito, 1975, 1977, 1979; Crook et al, 1991), Nelson et al (1994) demonstrated that orientation selectivity is maintained if all inhibition to a single cell is blocked. In chapter 4, we propose a reconciliation of these two observations, and a non-specific role for inhibition in limiting the range over which excitatory signals propagate.

Long-range connections also serve to connect disparate points of the retinotopic mapping, and in chapters 2 and 3 we explore the possibility of their mediating modulatory effects of stimuli outside the classical receptive field. Since, by definition, stimuli outside the classical receptive field do not evoke spiking, they have in the past been studied through observation of their modulatory effects on a center stimulus (Nelson and Frost, 1978, 1985; Allman et al, 1985; Knierim and VanEssen, 1992). In chapter 2, we demonstrate that the same surround stimulus can have both excitatory and inhibitory effects depending on stimulus contrast. In chapter 3, we examine the influence of surround stimuli directly using intracellular recording techniques.

In summary, using techniques of *in vivo* whole-cell recording and intrinsic signal optical imaging, we explore the relationship of lateral connectivity within area 17 of cat to maps of retinotopy and orientation. Although this connectivity does not seem to be responsible for the generation of orientation selective responses, excitatory connections are implicated

in generating the extra-classical surround, and inhibitory connections in controlling the spread of cortically generated excitation.

General Methods

Intrinsic signal imaging

The technique of intrinsic signal imaging (Grinvald, 1986; Frostig et al, 1990) is based on the differential absorption at certain wavelengths of oxygenated and deoxygenated hemoglobin. Although other sources of intrinsic signal can also be measured, such as changes in blood volume (Frostig et al, 1990) and cell composition (reviewed in Cohen, 1973), the oxygen saturation signal is the most useful for cortical recordings because it can be measured with 600 nm (orange-red) light, which affords better penetrating ability and less absorption by the large, superficial vasculature. Another popular approach to imaging, that of voltage-sensitive dyes (reviewed in Grinvald, 1985), affords a major advantage in temporal resolution, but has the disadvantage of toxicity, complicating its use for repeated measurements of the same cortical area. Optical recording affords a major advantage over 2-deoxyglucose imaging (Sokoloff, 1977), also used for studies of cortical organization, in that it allows several experiments and several stimuli to be mapped without the need to sacrifice the animal. Intrinsic signal imaging is so non-invasive, that it has even been used to localize language areas in human cortex during surgery for removal of an epileptic focus (Haglund et al, 1992). The ability to map several stimuli has been particularly useful for studies of the orientation system, since many different orientations can be tested, and the signals combined mathematically using vector summation (Blasdel and Salama, 1986) or other approaches (see appendix) to give a composite picture of the cortical response. Details of the technique are further given in chapters 1, 2 and 4.

In vivo whole cell recording

The whole-cell patch method (Hamill et al, 1981) takes advantage from a poorly understood property of borosilicate glasses which allows the formation, under the right conditions, of electrically-tight seals with the clean surface of a cell membrane. Although the original technique involved approaching visualized cells, and "cleaning" the cell membranes prior to patching, it was later applied in tissue-slices in what has been termed the "blind-patch" technique (Blanton et al, 1989), which relies on monitoring the change in electrode resistance to locate cell membranes. Although mechanical stability of the cell being patched is a large problem, the technique has in recent years been used in several systems to study the intracellular responses of cells in intact animals (cat visual cortex, Ferster and Jagadeesh, 1992; Jagadeesh et al, 1992; Pei et al, 1994; cat motor cortex, Baranyi et al, 1993; rat auditory cortex, Metherate and Ashe, 1994; frog tectum, Nakagawa et al, 1994). The technique offers an advantage over more traditional sharp-electrode intracellular recordings in that the higher seal resistance provides greater signal-to-noise in recordings, the seal once formed is mechanically more stable, allowing longer recordings, less damage is done to the cell, and fast intracellular diffusion is possible through the pipette tip (Nelson et al, 1994). Details of our technique are given in the methods to chapter 3.

REFERENCES

Allman JM, Miezin F, McGuinness E (1985) Stimulus specific responses from beyond the classical receptive field: neurophysiological mechanisms for local-global comparisons in visual neurons. *Ann. Rev. Neurosci.* 8:407-430.

Baranyi A, Szente MB, Woody CD (1993) Electrophysiological characterization of different types of neurons recorded in vivo in the motor cortex of the cat. *J. Neurophys.* 69(6):1850-1879.

Bishop PO, Kozak W, Levick WR, Vakkur GJ (1962) The determination of the projection of the visual field on to the lateral geniculate nucleus in the cat. *J. Physiol.* 163:503-539.

Blanton MG, Lo Turco JJ, Kriegstein AR (1989) Whole cell recording from neurons in slices of reptilian and mammalian cerebral cortex. *J. Neurosci. Methods* 30:203-210.

Blasdel GG, Lund JS, Fitzpatrick D (1985) Intrinsic connections of macaque striate cortex: axonal projections of cells outside lamina 4C. *J. Neurosci.* 5:3350-3369.

Blasdel GG, Salama G (1986) Voltage-sensitive dyes reveal a modular organization in monkey striate cortex. *Nature* 321:579-585.

Brodmann K (1909) Vergleichende lokalisationslehre der Großhirnrinde. J.A. Barth, Leipzig.

Cohen LB (1973) Changes in neuron structure during action potential propagation and synaptic transmission. *Physiol. Rev.* 53:373-418.

Crook, JM, Eysel, UT, Machemer, HF (1991) Influence of GABA-induced remote inactivation on the orientation tuning of cells in area 18 of feline visual cortex: a comparison with area 17. *Neuroscience* 40(1):1-12.

Ferster D, Jagadeesh B (1992) EPSP-IPSP interactions in cat visual cortex studied with *in vivo* whole-cell patch recording. *J. Neurosci.* 12(4):1262-1274.

Frostig RD, Lieke EE, Ts'o DY, Grinvald A (1990) Cortical functional architecture and local coupling between neuronal activity and the microcirculation revealed by in vivo high-resolution optical imaging of intrinsic signals. *Proc. Nat. Acad. Sci. USA* 87:6082-6086.

Gall FJ, Spurzheim G (1810) Anatomie et physiologie du système nerveux en général, et du cerveau en particulier, avec des observations sur la possibilité de reconnoître plusieurs dispositions intellectuelles et morales de l'homme et des animaux, par la configuration de leurs têtes. Schoell, Paris.

Gilbert CD, Wiesel, TN (1989) Columnar specificity of intrinsic horizontal and corticocortical connections in cat visual cortex. *J. Neurosci.* 9(7):2432-2442.

Gilbert CD, Wiesel, TN (1983) Clustered intrinsic connections in cat visual cortex. *J. Neurosci.* 3:1116-1133.

Grinvald A (1985) Real-time optical mapping of neuronal activity: from single growth cones to the intact mammalian brain. *Ann. Rev. Neurosci.* 8:263-305.

Grinvald A, Lieke E, Frostig RD, Gilbert CD, Wiesel TN (1986) Functional architecture of cortex revealed by optical imaging of intrinsic signals. *Nature* 324:361-364.

Haglund MM, Ojemann GA, Hochman DW (1992) Optical imaging of epileptiform and functional activity in human cerebral cortex. *Nature* 358:668-671

Hamill OP, Marty A, Neher E, Sakmann B, Sigworth FJ (1981) Improved patch-clamp techniques for high-resolution current recording from cells and cell-free membrane patches. *Pflügers Arch.* 391:85-100.

Hubel DH, Wiesel TN (1974) Uniformity of monkey striate cortex: a parallel relationship between field size, scatter, and magnification factor. *J. Comp. Neurol.* 158:295-306.

Jackson JH (1884) The Croonian lectures on evolution and dissolution of the nervous system. *Br. Med. J.* 1:591-593; 660-663; 703-707.

Jagadeesh B, Gray CM, Ferster D (1992) Visually evoked oscillations of membrane potential in cells of cat visual cortex. *Science* 257:552-554.

Kisvárday ZF, Kim DS, Eysel UT, Bonhoeffer T (1993) Patchy intrinsic connections follow iso-orientation sites in cat visual cortical area 18. *Soc. Neurosci. Abstr.* 19:1499. (618.4)

Kisvárday ZF, Kim DS, Eysel UT, Bonhoeffer T (1994) Relationship between lateral inhibitory connections and the topography of the orientation map in cat visual cortex. *Eur. J. Neurosci.* 6:1619-1632.

Knierim JJ, Van Essen DC (1992) Neuronal responses to static texture patterns in area V1 of the alert macaque monkey. *J. Neurophys.* 67(4):961-980.

LeVay S, Gilbert CD (1976) Laminar patterns of geniculocortical projection in the cat. *Br. Res.* 113:1-19.

LeVay S, Nelson SB (1991) Columnar organization of the visual cortex. In: vol 4, *Vision and visual dysfunction* JR Cronly-Dillon ed., London, MacMillan Press.

Livingstone MS, Hubel DH (1982) Anatomy and physiology of a color system in the primate visual cortex. *J. Neurosci.* 4:2830-2835.

Luhmann HJ, Millan LM, Singer W (1986) Development of horizontal intrinsic connections in cat striate cortex. *Exp. Br. Res.* 63:443-448.

McConnell SK, LeVay S (1984) Anatomical organization of the visual system of the mink, Mustela vison. *J. Comp. Neurol.* 250:109-132.

Metherate R, Ashe JH (1994) Facilitation of an NMDA receptor-mediated EPSP by paired-pulse stimulation in rat neocortex via depression of GABAergic IPSPs. *J. Physiol. Lond.* 481:331-348.

Nakagawa H, Kikkawa S, Matsumoto N (1994) Synaptic connection patterns between frog retinal ganglion cells and tectal neurons revealed by whole-cell recordings in vivo. *Brain Res.* 665(2):319-322.

NelsonJI, Frost BJ (1978) Orientation-selective inhibition from beyond the classic visual receptive field. *Brain Res.* 139:359-365.

Nelson JI, Frost BJ (1985) Intracortical facilitation among co-oriented, co-axially aligned simple cells in cat striate cortex. *Exp. Br. Res.* 61:54-61.

Nelson SB, Toth LJ, Sheth BR, Sur M (1994) Orientation selectivity of cortical neurons during intracellular blockade of inhibition. *Science* 265:774-777.

Payne, BR, Berman, N, Murphy, EH (1980) Organization of direction preferences in cat visual cortex. *Br. Res.* 211:445-450.

Pei X, Vidyasagar TR, Volgushev M, Creutzfeldt OD (1994) Receptive field analysis and orientation selectivity of postsynaptic potentials of simple cells in cat visual cortex. *J. Neurosci.* 14(11:II):7130-7140.

Rao SC, Toth LJ, Kim DS, Sur M (1995) Direction selective patches revealed by optical imaging of intrinsic signals in cat primary visual cortex. *Soc. Neurosci. Abstr.* 21:392 (162.2)

Robson JA (1983) The morphology of corticofugal axons to the dorsal lateral geniculate nucleus in the cat. *J. Comp. Neurol.* 216:89-103.

Rockland KS (1985) Anatomical organization of primary visual cortex (area 17) in the ferret. *J. Comp. Neurol.* 241:225-236.

Rockland KS, Lund JS (1983) Intrinsic laminar lattice connections in primate visual cortex. *J. Comp. Neurol.* 216:303-318.

Rockland KS, Lund JS, Humphrey AL (1982) Anatomical banding of intrinsic connections in striate cortex of tree shrews (Tupaia glis). *J. Comp. Neurol.* 309:41-58.

Schiller PH (1986) The central visual system. *Vision Res.* 26(9):1351-1386.

Sharma J, Angelucci A, Rao SC Sur M (1995) Relationship of intrinsic connections to orientation maps in ferret primary visual cortex: iso-orientation domains and singularities. *Soc. Neurosci. Abstr.* 21:392. (162.3)

Sillito AM, (1975) The contribution of inhibitory mechanisms to the receptive field properties of neurones in the striate cortex of the cat. *J. Physiol.* 250:305-329.

Sillito AM (1977) Inhibitory processes underlying the directional specificity of simple, complex and hypercomplex cells in the cat's visual cortex. *J. Physiol.* 271:699-720.

Sillito AM (1979) Inhibitory mechanisms influencing complex cell orientation selectivity and their modification at high resting discharge levels. *J. Physiol.* 289:33-53.

Stryker MP, Zahs KR (1983) ON and OFF sublaminae in the lateral geniculate nucleus of the ferret. *J. Neurosci.* 3:1943-1951.

Talbot SA (1940) Arrangement of the visual field on cat's cortex. *Amer. J. Physiol.* 129:477-478P.

Valverde F (1991) The organization of the striate cortex. In: vol 3, *Vision and visual dysfunction* JR Cronly-Dillon ed., London, MacMillan Press.

Walker AE (1938) The primate thalamus. Chicago, Univ. Chicago Press.

Zahs K, Stryker MP (1988) Segregation of ON and OFF afferents to ferret visual cortex. *J. Neurophysiol.* 59:1410-1429.

FIGURE LEGEND

Fig. 1. Schematic diagram of equipment for intrinsic signal optical recording. A voltage-stabilized light source is filtered and directed onto the exposed cortex using a fiber-optic light guide. The animal is anesthetized, paralyzed (when neccessary to prevent eye-movements), and fixed in a stereotaxic frame for stability and measuring of precise coordinates. Heart rate, electroencephalogram and expired carbon dioxide are continuously monitored to ensure the animal's condition. Output of the camera, in NTSC format, is sent to the subtraction box, where it is compared with a stored reference image and then passed through an A/D converter. The process is designed to ensure that adequate signal resolution can be attained in real time (see also appendix). The data collection computer controls the timing of the experiment, and stores the relevant data on a SCSI hard drive for later back-up with a data quality DAT tape unit. The display computer, receiving stimulus and timing information, generates all relevant stimuli prior to the experiment, and readies them for instantaneous display as commanded. The stimulus monitor is positioned at the appropriate retinotopic location of the visual field (or fields, for binocular experiments), using a back-projection of the retinal vasculature, area centralis and optic disk as a guide.

Figure 1.

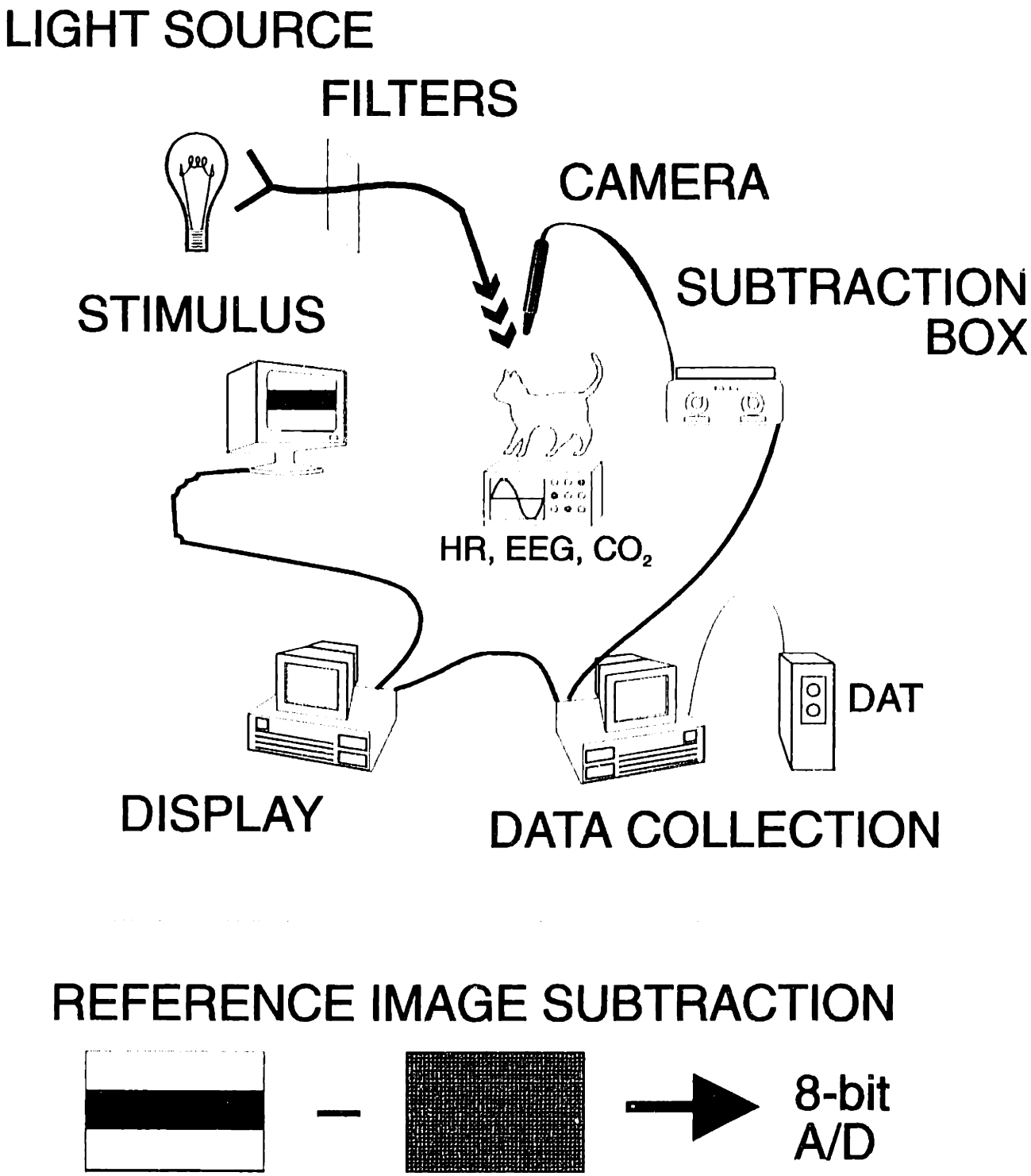
LIGHT SOURCE
FILTERS
CAMERA
STIMULUS
SUBTRACTION BOX
HR, EEG, CO_2
DAT
DISPLAY
DATA COLLECTION
REFERENCE IMAGE SUBTRACTION
8-bit A/D

Chapter 1

Spacing of Orientation Domains in Cat and Ferret Primary Visual Cortex Suggest Different Strategies of Cortical Organization

ABSTRACT

Optical imaging of activity dependent intrinsic signals in cat area 17 and ferret area 17 revealed a continuous organization of orientation preference into "pinwheel" like structures qualitatively similar to those previously described in cat area 18 and monkey V1. We observed three notable differences in intrinsic signal images of orientation preference between these two species. First, singularity points (pinwheel centers) in ferret visual cortex are much closer together; we find a value of 5.5 pinwheels/mm^2 in ferret area 17 compared to a value of 2.5 pinwheels/mm^2 in cat area 17. The density of iso-orientation domains is also nearly twice as great in ferret area 17 (2.7/mm^2) as in cat area 17 (1.5/mm^2). Second, orientation preference does not only change *more rapidly*, but also *less smoothly* across visual cortex in ferret than in cat; after controlling for density, "fracture zones" are still more apparent in the ferret cortex. Third, a comparison of the amount of cortex activated by a single orientation shows that (1) individual orientation patches in ferret are only slightly smaller and more closely spaced than in cat, and (2) iso- and cross orientation domains overlap substantially in ferret, but not in cat. These results imply that the arrangement of cells into orientation-specific columns is less orderly in ferret cortex, and that individual cells are more broadly tuned for orientation. Also, these results suggest possible differences in the organizational strategy between ferret, cat and monkey primary visual areas.

INTRODUCTION

Thousands of papers have been written describing the anatomy and physiology of primary visual cortex of the cat (*Felis domesticus)*. Although for many studies it is the animal of choice, developmental studies are complicated by the fact that many important developmental events occur *in utero*. The ferret (*Mustela putoris furo)*, however, is born at a time of relative visual system immaturity, thus making it an ideal animal for studies of development (Linden et al, 1981; Guillery et al, 1985; McConnell, 1985; reviewed in Jackson and Hickey, 1985). Though many of the same patterns of organization occur in both cat and ferret, notable differences occur. For example, although ferret LGN shares the same triple-laminated organization as cat LGN, the ferret LGN is further subdivided physiologically into sublayers responsive to light increment and light decrement (ON and OFF) (Stryker and Zahs, 1983). The few physiological studies of ferret primary visual cortex to date (Roe et al, 1992; Chapman & Stryker 1993; Redies et al, 1990) suggest that the orientation tuning of single-units is somewhat broader than in cat. Although the two species are closely related in terms of visual system structure, ferret's eyes are optically inferior to most cats, due to their small size, between 6 and 9 mm in diameter, compared with 22 mm in the cat, and larger visual angle subtended by ganglion cell receptive fields (Vitek et al, 1985; Zahs and Stryker, 1985). Since its lowered acuity results in lesser patterned information to the rest of the visual system, and since activity-dependent mechanisms are known to play a crucial

role in development, we wondered whether adaptive changes in cortical structure, specifically the density of orientation domains, might be visible.

We chose to examine these issues in primary visual cortex using the technique of intrinsic signal imaging (Grinvald et al, 1986; Frostig et al, 1990; Ts'o et al, 1990; Bonhoeffer and Grinvald, 1991). Optical imaging excels at visualizing patterns of retinotopy (Toth et al, 1994), orientation (Blasdel 1992b, Bonhoeffer and Grinvald 1993) and ocular dominance (Ts'o *et al.*, 1990, Blasdel 1992a) across the cortical surface. Intrinsic signals arise from changes in the oxygenation state of hemoglobin in response to activity-linked metabolic demands (Frostig et al., 1990). The tight spatial correlation between site of hemoglobin deoxygenation and site of neuronal activity has benefited the development of not only this technique, but also the techniques of 2-deoxyglucose radiolabeling, positron-emission tomography, and functional magnetic resonance imaging. Our intrinsic-signal data demonstrates that primary visual cortex in ferret has a unique organization, on one hand preserving the same features of orientation and retinotopy maps found in cat and monkey, but on the other hand differing in details of the mapping perhaps as an adaptive response to the quality of visual input.

METHODS

Surgery and recording chamber placement

Female cats aged 10 weeks to adult and adult female ferrets were initially anesthetized with a mixture of ketamine (cat 15 mg/kg; ferret 25 mg/kg, i.m.) and xylazine (1.5 mg/kg, i.m.). Subsequently anesthesia was maintained by continuous infusion of sodium pentobarbital (1.5-2 mg/kg/hr, i.v.) in a 50/50 mixture of 5% dextrose and lactated Ringer's solution for fluid maintenance. A tracheotomy was performed to facilitate artificial ventilation. The animal's heart rate and EEG were continuously monitored to ensure adequate levels of anesthesia. Expired CO_2 was maintained at 4% by adjusting the stroke volume and the rate of the respirator. The animal was placed on a heating blanket and the rectal temperature was maintained at 38°C. In cats, a bilateral craniotomy and durotomy was performed posterior to Horsley-Clark AP0 extending roughly 7 mm posterior and 4 mm lateral. In ferrets the craniotomy extended to 7 mm laterally and to 4 mm anterior of the posterior cortical pole, initially located using the tentorial ridge as a guide. After completion of surgery, paralysis was initiated with gallamine triethiodide (10 mg/kg/hr) to prevent eye movements. A stainless steel chamber (20 mm diameter) was cemented to the skull with dental acrylic and the inner margin was sealed with wax. In order to minimize cortical pulsations due to respiration and heart beat, the chamber was filled with silicone oil and sealed with a transparent quartz window over the chamber.

Optical recording

The cortical surface was illuminated with a bifurcated fiber-optic light guide attached to an 100W tungsten-halogen lamp source powered by a regulated power supply (Kepco ATE25-20M). The light was passed through an IR filter and filters of appropriate center wavelength, and was adjusted for even illumination of the cortical surface at an intensity within the linear range of the camera's sensitivity. We used a slow-scan video camera (Bischke CCD-5024N, RS-170, 30 Hz, 60dB s/n) fitted with a macroscope (Ratzlaff and Grinvald, 1991) consisting of two back-to-back camera lenses (50 mm *f*1.2 and 55 mm *f*1.2) that allows both a high numerical-aperture and a shallow depth of field. The camera was focused on the cortical surface by emphasizing the vasculature using light of 540 nm (maximum absorption of hemoglobin). After the pattern of cortical vasculature was imaged, the camera was focused 300 μm below this plane to minimize blood-vessel artifacts. Light of 600 nm (10 nm bandpass) was used to image activity dependent intrinsic oximetric signals. Data collection was under the control of the Imager 2001 system (Optical Imaging Inc.) which performed analog subtraction of a stored reference image (collected during presentation of a neutral gray screen) from the stimulus image (collected during presentation of an oriented grating), such that the image could be digitized in real time (Matrox image processor, 8 bit, 15 MHz) without sacrificing the signal-to-noise ratio of the camera.

Visual stimulation

Except where indicated, all visual stimuli were presented binocularly. Appropriate contact lenses were fitted in order to focus the eyes on the monitor, typically 30 cm away. Eye position was checked by projecting the location of the optic disk onto the monitor with a reversible ophthalmoscope. Refraction in ferret was judged by slit retinoscopy and direct opthalmoscopy. The presence of a strongly reflective retinal epithelium in cat allowed judgment of refraction by reverse opthalmoscopy (focusing the pattern of retinal vasculature onto the display screen directly.) Correction in the ferret was often minimal, since the ferret's smaller pupil diameter provides a naturally larger depth of field. Stimuli were generated by an IBM-compatible computer running STIM (K. Christian, Rockefeller, Univ.), using a Sgt. Pepper + graphics board with 4 MB memory (Number Nine Corp.) at a resolution of 640x480 pixels. They were shown at a 60 Hz frame rate on a Sony Trinitron 14" monitor positioned approximately 30 cm away from the animal. Individual frames were computed prior to the beginning of the experiment and shown under the timing control of the data-collection computer.

Full-field square-wave gratings of 0.375 cyc/deg were shown as sets of 8 or 16 stimuli (45° or 22.5° apart, respectively). The timing of the stimulus was chosen to give the maximum optical signal, as determined by previous reports of optical imaging in cat area 18 (Bonhoeffer and Grinvald 1993) and by our initial experiments. The oriented grating was shown in a stationary position for 5 sec, and then drifted at a rate of 1.5 Hz. for the duration of data collection. Grating orientations were randomly interleaved.

Single-unit recording

In some experiments optical recording was stopped before the signal had deteriorated, the chamber was opened, and single units were recorded with tungsten microelectrodes of impedance 2-4 MΩ. The signal was amplified (BAK, RP-1) filtered at 1 - 10 kHz, digitally windowed (Harvard Apparatus, PSD-1) and collected on an IBM 486 computer using a 200 MHz A/D board (AT-16-F-5, National Instruments) and software written in-house. High-contrast, oriented bar stimuli of optimal dimensions were shown under computer control at orientations corresponding to those used for optical recording, and a tuning curve for 10 responses to each orientation was plotted on-line. All orientations were randomly interleaved.

Data analysis

The timing of the data collection was chosen based on pilot experiments to bracket the time of maximum signal strength. 30 Hz camera frames were summed into between 5 and 8 larger time blocks, and collected between 400 ms and 5500 ms after the start of stimulus motion. Frames between approximately 1300 ms and 4600 ms after the start of stimulus motion were selected for further analysis. *Single-condition maps* were created by dividing the summed differential response to all presentations of a particular orientation with image obtained for the blank stimulus. *Angle maps* were created, where the value of each pixel codes the vector angle obtained from the formula: $= \Sigma_i p_i(2\alpha_i)$ where p_i is the signal strength in the ith map, and α_i the stimulus

orientation corresponding to the ith map. These orientation preference ("angle") maps were displayed in color by choosing the number of colors to be equal to the number of different stimulus orientations and binning the pixels to the closest stimulus angle.

RESULTS

Images of iso-orientation domains

Single condition maps were obtained by summing responses to stimulus of an oriented grating divided by responses to blank stimulus. Single condition maps for area 17 of cat (fig. 1a and b) and ferret (fig. 2a and b) show a patchy distribution of activity, termed "orientation domains", in a spatially complimentary manner for orthogonal stimulus orientations. Intermediate stimulus orientations generated qualitatively similar maps with a smooth change in the spatial location of the orientation domains. Significant contrast improvement for visualizing differential activity can be achieved by dividing single condition maps obtained for orthogonal orientations (fig. 1c for cat, 22.5°/112.5°; fig. 2c for ferret, 0°/90°), though at the expense of losing information about the size of orientation domains. We use the term "orientation domain" to mean a region of the cortical surface activated by a particular orientation, as seen in a single-condition map. The use of the term "orientation column" is reserved for the area over which a given small range of orientations are preferred, such as seen in an angle map, or in the limit, corresponding perhaps to anatomically distinct columns. Since a cortical region can be activated by orientations that are not its preferred orientation, orientation domains are generally larger than orientation columns.

Spacing of iso-orientation domains

Our single-unit recordings in ferret suggest that the average degree of orientation tuning is low, compared to cat. We therefore examined the strength of tuning in the optical data. If a region of cortex is broadly tuned for orientation, we would expect to see overlapping orientation domains in the single condition maps at that point, indicating activation of that point by several of the stimuli. Orientation domains may come to overlap more if they are a) closer together, or b) larger. To show that orientation domains are closer together, and to compare our results with published anatomical data, we measured the distribution of center-to-center spacing between nearest-neighbor iso-orientation domains, judged qualitatively. Histograms of data obtained from single condition maps of cat and ferret (fig. 3) show the distribution of this spacing. The iso-orientation domains are more closely spaced in ferret area 17, with a mean of 0.68±0.15 mm as compared to a value of 1.01±0.22 mm for cat.

Spread of signal from an iso-orientation domain

The second possibility to explain broader orientation tuning seen in single units is that orientation domains in ferret are larger; that is, a larger area of the cortex responds to a given stimulus orientation. We constructed line profiles from the single-condition maps, starting in each case at a location of maximal activity, and ending at a point of minimal activity (which we took to be the same point in which the cross-orientation map shows maximal activity). Furthermore, we only selected lines that traversed roughly linear regions of orientation change in the angle map, and

avoided orientation singularities. Figure 4 shows an average of 10 such line profiles obtained for both cat and ferret. The slope of the signal strength vs. cortical distance graph over the initial 400 μm is 2.3 ± 0.09 for ferret (n=10) which is significantly steeper ($p>.05$, Student's *t* test) than a value of 1.62 ± 0.13 for cat (n=10). Thus the size of the orientation domain activated for a particular stimulus orientation is *smaller* in ferret than in cat area 17. Moreover, in cat, beyond about 500 μm, there is a zone of low signal strength marking the beginning of the cross-orientation domain. Such a distinct region is absent in the ferret, with the activity of cross-orientation domain beginning even before the activity of the iso-orientation domain has decayed to its lowest value.

Maps of spatial frequency

Although the locations of orientation domains are considered to be markedly stable, we wished to rule out the hypothesis that any stimulus-specific features dynamically affect the locations of orientation domains. Furthermore, it has recently been claimed that differential effects of varying stimulus spatial frequency can be observed in optical images (Hübener et al, 1995). We obtained single condition maps obtained for different spatial frequencies in cat area 17 (fig. 5a 0.38 cyc/deg; fig. 5b 0.78 cyc/deg). As can be seen, the locations and spacing of the iso-orientation domains are independent of the spatial frequency of the stimulus. However, when using higher spatial frequency stimuli, the activity was lower in peripheral (anterior in cortex, inferior in visual space) iso-orientation domains. Our imaging data agrees with the known, eccentricity-dependent

decrease in response properties of cortical cells to changes in spatial frequency of the stimulus (Movshon et al, 1978; Tootell et al, 1988).

Periodicity of orientation domains

Angle maps derived from eight single condition maps by vector average method are shown in fig 6a for cat and fig. 6c for ferret area 17. The most obvious feature of an "angle" map is the radial arrangement of orientation preference in a "pinwheel-like" manner as previously described in cat area 18 (Bonhoeffer and Grinvald 1993) and the periodicity of these structures. We measured periodicity by counting both the number of "pinwheel" centers and the number of orientation domains within the valid (flat and artifact free) region of the map, and dividing by the area of that region. We found a pinwheel density in cat of 2.5 /mm^2 and in ferret of 5.5/mm^2. The density of iso-orientation domains in ferret area 17 is 2.73 ± 0.35 /mm^2 compared 1.49 ± 0.19 /mm^2 in cat. As expected for a continuous mapping of orientation, the pinwheel density is approximately twice the orientation column density. Furthermore, the density of pinwheels found in ferret area 17 is twice that found in cat area 17.

Discontinuities of the orientation map

In order to establish whether orientation maps in ferrets show as much organization and regularity as those of cats, we looked for discontinuities by calculating the two-dimensional spatial derivative of the orientation preference maps. On a discrete image, the spatial derivative is

estimated by: $\frac{\delta\theta}{\delta x} = (\theta_{i+1,j} - \theta_{i,j})$ and $\frac{\delta\theta}{\delta y} = (\theta_{i,j+1} - \theta_{i,j})$, where $\theta_{i,j}$, representing the vector angle at map coordinate (i,j), is a circular variable ranging between 0° and 180° (Blasdel, 1992b). Such maps are shown for cat (fig. 6 b) and ferret (fig. 6 d). In these maps, note that although pinwheel centers are clearly seen, there also exist discrete "fracture zones" extending from the centers, representing regions of especially high rate of change in the angle of the orientation vector. For purposes of comparison we counted the percentage of points within the signal region of the derivative map which represented vector shifts of more than 22.5 degrees in the angle map. For the cat map shown in figure 6 b, only 0.78% of the pixels (582/74798) fell into this range. In contrast, for the ferret map shown in figure 6 d, 4.65% (2102/45251) of the image was in this range. Since the rate of change of the orientation vector angle across the surface of the cortex is larger in ferret, a relative undersampling of the ferret cortex could account for this difference. We therefore recomputed the derivative map for the cat using input data where each pixel represented 2x2 pixels in the original, thus making the rate of change of the orientation vector angle per image pixel greater than that in the ferret map. Still, by this method, only 1.51% of the image (285/18911) represented angle shifts more than 22.5 degrees. Hence we conclude that the organization of the orientation map in the ferret area 17 is noticeably less *smooth* than that in cat area 17.

DISCUSSION

Correspondence with 2-deoxyglucose studies

All our single condition maps show a patchy pattern of organization of iso-orientation zones as distinct from a pattern of iso-orientation "bands" or "beads" in area 17 labeled by 2-deoxyglucose autoradiography (Schoppmann and Stryker, 1981; Löwel et al, 1987). Such banded pattern could be a result of non-specific labeling of cortical tissue in regions containing high cytochrome oxidase activity (Horton and Hubel 1980), or could be an adaptation artifact resulting from the need to present single orientations for prolonged time periods. Despite the difference in the pattern of iso-orientation activity, our finding of the average spacing of 1.01 mm for iso-orientation domains by optical recording in cat area 17 corresponds well with a spacing of 1.08 mm suggested Albus and Sieber (1984) using 2-DG methods. Ferret area 17 shows a higher periodicity of 1.4 cycles/mm (Redies *et al.* 1990) for iso-orientation domains, consistent with closer spacing of iso-orientation domains (0.68 mm) found in the present study.

A major advantage of the optical imaging technique is the ability to compare data from tests of multiple orientations. By identifying not just the orientation but also the orientation gradient of a given point we are able to see columns that may blur together in the single-condition map similar to overlap of metabolic activity seen in the 2-deoxyglucose map of orientation domains in ferret

visual cortex (Redies *et al.* 1990). In fact, one can see from the data we present that, far from there being a uniform size for an orientation module, there is a huge diversity in sizes.

Properties of cells in ferret V1

Based on our optical recording data, we can make some predictions about the average response properties of neurons in ferret area 17. Since the radius of cortical activation for a particular orientation is similar to that in cat, but the spacing is tighter, it follows that a given point in ferret cortex responds to a wider range of orientations. Cells in the ferret area 17 should therefore show less selectivity (more broad tuning) for orientation, and increased stimulus-driven activity even at cross-orientations. Our own experience with ferret single-unit recording is in agreement with these predictions. There are two published reports that describe the tuning of single-unit orientation tuning for cells in ferret area 17 (Roe et al, 1992; Chapman and Stryker, 1993). Chapman finds that a significantly broader average tuning exists in ferret cortex than cat cortex. Although Roe et al did not compare their results to cat, they find a mean orientation tuning index in ferret of 0.39 (where 1.0 = perfectly oriented, 0.0 = unoriented), and a mean tuning width of 72.5°, which is much broader than values commonly observed in cat (for example, Nelson, 1991, figure 3 measures an orientation index near 0.2 where 0.0 = perfectly oriented, 1.0 = unoriented). Furthermore, both studies support the finding that most ferret cells, unlike cat cells, do respond at orientations 90° from optimal. In cat cortex, the variance in preferred orientation radially within a single column is on the order of 5-10° (Albus, 1975). If we take a value of 40° for the

average tuning width of cells in cat visual cortex, the population tuning curve should have a width on the order of 50°. We might then predict that the percentage of cortex activated by a single orientation in cat should be roughly 50/90, or 56%. This value is in reasonable agreement with our data, suggesting that optically-derived measurements of activity over baseline are in reasonable accord with actual neuronal activity.

What controls orientation domain size?

One might expect that the repeat distance of the orientation system has something to do with anatomical constraints, such as the extent of cortical cell arborizations, the pattern of horizontal connections, or the point spread of geniculocortical axons. There are currently no studies of thalamocortical or intracortical axon arborizations in ferret primary visual cortex that can shed light on this issue. In cat and monkey, the most likely candidate for an anatomical correlation with orientation domain density is the patchy intrinsic connectivity of the horizontal connections from layers 2-3. These connections have been observed to be orientation specific (in cat, Gilbert and Wiesel, 1989; Kisvárday et al, 1993; in ferret, Sharma et al, 1995; in monkey, Malach et al, 1993). Furthermore, although exact measurements of patch densities are complicated by issues about completeness of axon terminal labeling, experiments using the same technique of extracellular biocytin injection in monkey (Amir et al, 1993; Lund et al, 1993), cat (Kisvárday and Eysel, 1992), and ferret (Sheth et al, 1993), suggest that the distance between patches follows the

same comparative sequence as the distance between orientation domains; that is, monkey (0.64) < ferret (0.68) < cat (1.01).

The above experiments address the question of whether all biocytin labeled patches connect iso-orientation domains; however an equally interesting question is whether all iso-orientation domains within a certain distance of each other are interconnected. Malach et al (1993) observe that biocytin label in monkey V1 is specific not only for orientation, but also for ocular dominance. Thus, at least two (ipsilateral, contralateral), and possibly three (including binocular) intermixed but separate systems of connections exist in monkey V1, as a point injection of biocytin apparently labels only every second to third iso-orientation column (Malach et al, 1993). Though this experiment has not been attempted in cat or in ferret, it seems necessary in cat that all iso-orientation domains are interconnected due to the close correspondence of values for center-to-center distance between anatomically defined patches (1.050 mm (WGA-HRP), Luhmann et al, 1989; 1.1 mm (biocytin), Kisvárady and Eysel, 1992) and between orientation domains (1.01 mm, this paper).

Physiological correlates of orientation domain density

Prior to our results, it was reasonable to assume that the much higher density of orientation centers in macaque V1 was due to the vast difference in the number of cells in the visual systems of cat and monkey. The average density of orientation centers (singularities or pinwheel centers)

is 8.1/mm^2 in macaque V1 (Obermeyer and Blasdel 1991) and 2.5/mm^2 in cat area 17 (reported in this paper). If the differences in the density of pinwheels between monkey and cat area 17 is related to the number of cells present, then one would expect an even lower value of pinwheel density in the ferret. Monkey retina contains 1,500,000 ganglion cells, reaching a peak density of 33,000 /mm^2 in the fovea centralis (Perry and Cowey, 1985). Cat retinas contain 217,000 ganglion cells, with a peak density of 9-10,000 cells/mm^2 (Hughes, 1975). It is interesting to note that the ratio of maximum ganglion cell density in cat vs. monkey retina is exactly equal to the ratio of the pinwheel densities in area 17 (30%). Ferret retinas, by a liberal estimate, contain 88,000 ganglion cells, with a peak density of 5,200 cells/mm^2 (Vitek et al, 1985). Using the central field estimates, available axons in the ferret optic nerve to carry foveal information is therefore 55% that in cat, and only 16% that in monkey. If the ratio of pinwheel density to information capacity were constant, we would expect a pinwheel density of 1.3 /mm^2 in ferret. In fact, this hypothesis is wrong; our measured pinwheel density of 5.5 /mm^2 in ferret 17 actually lies between that of cat and monkey.

A similarly flawed hypothesis is that the need to represent the visual field within a smaller surface area of visual cortex could account for the variation in the observed density of pinwheels. Although morphometric measurements are made difficult by the convoluted patterns of gyri and sulci, estimates of the total area of V1 in a single hemisphere have been attempted in ferret, cat and monkey. The best estimates for the areas of primary visual cortex for ferret is 80 mm^2 (Law

et al. 1988), for cat is 380 mm^2 (Tusa *et al.*, 1978), and for macaque is 1200 mm^2 (Van Essen 1984). With these numbers in hand, and assuming no variation in pinwheel density with eccentricity, we can calculate the total number of pinwheels that must exist in a typical V1 of each species. Thus ferret area 17 may contain up to 550 pinwheels while cat and monkey cortices contain 950 and 9720, respectively. Thus, we conclude that not only does the pinwheel density per unit area of cortex vary among different species, but pinwheel density per unit visual field area also varies.

In the monkey, it has been suggested that there is a relationship between the spatial organization of the orientation and ocular dominance systems; namely, that the regions of high orientation gradient ("fracture zones") tend to lie on ocular dominance column centers, or to intersect ocular dominance column boundaries at right angles (Blasdel and Salama 1986; Obermayer and Blasdel 1993; but see Bartfeld and Grinvald, 1992). This suggests the possibility of a modular arrangement of cortex in which the basic unit is one set of orientation domains, all receiving their primary input from one eye. Such a unit would be repeated in ipsilateral and contralateral eye columns. Although spatial segregation of inputs by ocularity does exist in cat cortex, the methods of 2-deoxyglucose labeling (Löwel and Singer 1993) and intrinsic signal imaging (Rao *et al.*, 1994) both fail to show ocular dominance structure in visual cortex of the anesthetized adult cat. Strabismic cats, however, which do show ocular dominance columns, have iso-orientation connectivity restricted to same eye columns only (Schmidt et al, 1995), and have an increased

orientation pinwheel density approximately double that of normal cats (2.8 per mm, Schmidt et al, 1994). Evidence would thus seem to suggest that normal cat cortex has a different interrelation of ocular dominance and orientation domains from monkey.

We suggest that ferret and monkey may be similar, in that connections between iso-orientation domains also respect ocular dominance. If we assume that the possible range of the patchy long-range connectivity within area 17 is limited (perhaps by a space constraint), then orientation domains must repeat at roughly twice the frequency in ferret and monkey relative to cat in order that iso-orientation iso-ocularity patches can be connected by the same lengths of fibers (Fig. 7). Following this hypothesis, differences in other types of connectivity between species may also affect the maximum range of connectivity, accounting for differences in the periodicity of the anatomically observed patches.

In summary, we have used intrinsic signal imaging of orientation-specific activity to compare the pattern of orientation preference in primary visual cortex of cats and ferrets. Though the size of cortical patches activated by a particular orientation is similar between ferret and cat, the patches are closer together in ferret, thus predicting broader tuning properties of single units, and greater response to orthogonal orientations, both of which have been observed. The orientation gradient across ferret visual cortex is even steeper than would be predicted based on orientation domain spacing alone. This may be an adaptation to the smaller quantity of visual input available during

development available to shape the map. Finally, the correlation of intrinsic signal orientation maps with anatomical labeling support the view that the cat has a fundamentally different form of cortical organization from ferret or monkey, in that all iso-orientation domains are interconnected, without regard to ocular dominance preference.

REFERENCES

Albus K, Sieber B (1984) On the spatial arrangement of iso-orientation bands in cat's visual cortical areas 17 and 18: A ^{14}C-deoxyglucose study. *Exp. Br. Res.* 56:384-388.

Albus K (1975) A quantitative study of the projection of the central and the paracentral visual field in area 17 of the cat II. the spatial organization of orientation domains. *Exp. Br. Res.* 24:81-202.

Amir Y, Harel M, Malach R (1993) Cortical hierarchy reflected in the organization of intrinsic connections in macaque monkey visual cortex. *J. Comp. Neurol.* 334:19-46.

Bartfeld E, Grinvald A (1992) Architecture of processing modules in primate striate cortex underlying color, orientation and depth perception. *Proc. Nat. Acad. Sci. USA* 89:11905-11909.

Blasdel GG, Salama G (1986) Voltage-sensitive dyes reveal a modular organization in monkey striate cortex. *Nature* 321:579-585.

Blasdel GG (1992a) Differential imaging of ocular dominance and orientation selectivity in monkey striate cortex. *J. Neurosci.* 12:3115-3138.

Blasdel GG (1992b) Orientation selectivity, preference, and continuity in monkey striate cortex. *J. Neurosci.* 12:3139-3161.

Bonhoeffer T, Grinvald A (1991) Iso-orientation domains in cat visual cortex are arranged in pinwheel-like patterns. *Nature* 353:429-431.

Chapman B, Stryker MP (1993) Development of orientation selectivity in ferret visual cortex and effects of deprivation. *J. Neurosci.* 13(12):5251-5262.

Frostig RD, Lieke EE, Ts'o DY, Grinvald A (1990) Cortical functional architecture and local coupling between neuronal activity and the microcirculation revealed by *in vivo* high-resolution optical imaging of intrinsic signals. *Proc. Natl. Acad. Sci. USA* 87:6082-6086.

Gilbert CD, Wiesel TN (1989) Columnar specificity of intrinsic horizontal and corticocortical connections in cat visual cortex. *J. Neurosci.* 9:2432-2442.

Henderson, Z (1985) Distribution of ganglion cells in the retina of adult pigmented ferret. *Brain Res.* 358:221-228.

Grinvald A, Lieke EE, Frostig RD, Gilbert CD, Wiesel TN (1986) Functional architecture of cortex revealed by optical imaging of intrinsic signals. *Nature* 324:361-364.

Guillery RW, Ombrellaro M, LaMantia AL (1985) The organization of the lateral geniculate nucleus and of the geniculocortical pathway that develops without retinal afferents. *Brain Res.* 358:213-220.

Hubel DH, Wiesel TN (1974) Sequence regularity and geometry of orientation columns in monkey striate cortex. *J. Comp. Neurol.* 158:267-293.

Hubel DH, Wiesel TN (1963) Shape and arrangement of columns in cat's striate cortex. *J. Physiol. (Lond.)* 160:106-154.

Hübener M, Shoham D, Grinvald A, Bonhoeffer T (1995) Spatial frequency, ocular dominance, and orientation maps and their relationship in kitten visual cortex. *Soc. Neurosci. Abstr.* 21:771 (311.5)

Hughes, A. (1975) A quantitative analysis of the cat retinal ganglion cell topography. *J. Comp. Neurol.* 163:107-128.

Jackson CA, Hickey TL (1985) Use of ferrets in studies of the visual system. *Lab Anim. Sci.* 35:211-215.

Kisvárday ZF, Kim DS, Eysel UT, Bonhoeffer T (1993) Patchy intrinsic connections follow iso-orientation sites in cat visual cortical area 18. *Soc. Neurosci. Abstr.* 19:1499. (618.4)

Kisvarday ZF, Eysel UT (1992) Cellular organization of reciprocal patchy networks in layer III of cat visual cortex (area 17). *Neuroscience* 46:275-286.

Law MI, Zahs KR, Stryker MP (1988) Organization of primary visual cortex (area 17) in the ferret. *J. Comp. Neurol.* 278:157-180.

Linden DC, Guillery RW, Cucchiaro J (1981) The dorsal lateral geniculate nucleus of the normal ferret and its postnatal development. *J. Comp. Neurol.* 203:189-211.

Löwel S, Singer W (1993a) Monocularly induced 2-deoxyglucose patterns in the visual cortex and lateral geniculate nucleus of the cat I. anesthetized and paralyzed animals. *Eur. J. Neurosci.* 5:846-856.

Löwel S, Singer W (1993b) Monocularly induced 2-deoxyglucose patterns in the visual cortex and lateral geniculate nucleus of the cat II. awake animals and strabismic animals. *Eur. J. Neurosci.* 5:857-869.

Löwel S, Singer W (1987) The pattern of ocular dominance columns in flat-mounts of the cat visual cortex. *Exp. Br. Res.* 68:661-666.

Luhmann HJ, Singer W, Martínez-Millán L (1989) Horizontal interactions in cat striate cortex: I. anatomical substrate and postnatal development. *Eur. J. Neurosci.* 2:344-357.

Lund JS, Yoshioka T, Levitt JB (1993) Comparison of intrinsic connectivity in different areas of macaque monkey cerebral cortex. *Cereb. Cortex* 3:148-162.

Malach R, Amir Y, Harel M, Grinvald A (1993) Relationship between intrinsic connections and functional architecture revealed by optical imaging and *in vivo* targeted biocytin injections in primate striate cortex. *Proc. Nat. Acad. Sci. USA* 90:10469-10473.

McConnell SK (1985) Migration and differentiation of cerebral cortical neurons after transplantation into the brains of ferrets. *Science* 229:1268-1271.

Movshon JA, Thompson ID, Tolhurst DJ (1978) Spatial summation in the receptive fields of simple cells in the cat's striate cortex. *J. Physiol. Lond.* 282:101-120.

Nelson SB (1991) Temporal interactions in the cat visual system. I. orientation-selective suppression in the visual cortex. *J. Neurosci.* 11(2):344-356.

Obermayer K, Blasdel GG (1993) Geometry of orientation and ocular dominance columns in monkey striate cortex. *J. Neurosci.* 13:4114-4129.

Perry VH, Cowey A (1985) The ganglion cell and cone distributions in the monkey's retina: implications for central magnification factors. *Vis. Res.* 25:1795-1810.

Ratzlaff EH, Grinvald A (1991) A tandem-lens epifluorescence macroscope: Hundred-fold brightness advantage for wide-field imaging. *J. Neurosci. Methods* 36:127-137.

Redies C, Diksic M, Riml H (1990) Functional organization in the ferret visual cortex: A double-label 2-deoxyglucose study. *J. Neurosci.* 10:2791-2803.

Roe, AW, Pallas, SL, Kwon, YH, Sur, M (1992) Visual projections routed to the auditory pathway in ferrets: receptive fields of visual neurons in primary auditory cortex. *J. Neurosci.* 12(9) 3651-3664.

Schmidt KE, Kim DS, Singer W, Bonhoeffer T, Löwel S (1994) Optical imaging of the orientation map and horizontal intrinsic connections in strabismic cats. *Soc. Neurosci. Abstr.* 20:313 (137.7)

Schmidt KE, Kim DS, Singer W, Bonhoeffer T, Löwel S (1995) Functional specificities of long-range intrinsic and interhemispheric connections in strabismic cats. submitted

Schoppmann A, Stryker MP (1981) Physiological evidence that the 2-deoxyglucose method reveals orientation columns in cat visual cortex. *Nature* 293:574-576.

Sharma J, Angelucci A, Rao SC, Sur M (1995) Relationship of intrinsic connections to orientation maps in ferret primary visual cortex: iso-orientation domains and singularities. *Soc. Neurosci. Abstr.* 21:392. (162.3)

Sheth BR, Rao SC, Toth LJ, Sur M (1993) Patchy intrinsic connections within ferret primary visual cortex. *Soc. Neurosci. Abstr.* 19:139.8 (pp. 333).

Stryker MP, Zahs KR (1983) ON and OFF sublaminae in the lateral geniculate nucleus of the ferret. *J. Neurosci.* 3:1943-1951.

Swindale NV, Matsubara JA, Cynader MS (1987) Surface organization of orientation and direction selectivity in cat area 18. *J. Neurosci.* 7:1414-1427.

Tootell RBH, Silverman MS, Hamilton SL, Switkes E, De Valois RL (1988) Functional anatomy of macaque striate cortex. V. spatial frequency. *J. Neurosci.* 8(5):1610-1624.

Toth LJ, Rao SC, Sheth, BR, Sur M (1994) Orientation-specific spread of activation in primary visual cortex measured by optical recording of intrinsic signals. *Soc. Neurosci. Abstr.* 20:836 (349.2).

Ts'o DY, Frostig RD, Lieke EE, Grinvald A (1990) Functional organization of primate visual cortex revealed by high-resolution optical imaging. *Science* 249:417-420.

Tusa RJ, Palmer LA, Rosenquist AC (1978) The retinotopic organization of area 17 (striate cortex) in the cat. *J. Comp. Neurol.* 177:213-236.

Van Essen DC, Newsome WT, Maunsell JHR (1984) The visual field representation in striate cortex of the macaque monkey: asymmetries, anisotropies, and individual variability. *Vision Res.* 24:429-448.

Vitek DJ, Schall JD, Leventhal AG (1985) Morphology, central projections and dendritic field orientation of retinal ganglion cells in the ferret. *J. Comp. Neurol.* 241:1-11.

Zahs KR, Stryker MP (1988) Segregation of ON and OFF afferents to ferret visual cortex. *J. Neurophysiol.* 59:1410-1429.

FIGURE LEGENDS

Fig 1. Orientation specific intrinsic signals from cat area 17. **(A)** single condition map showing segregation of iso-orientation patches of intrinsic cortical activity (dark areas represent higher cortical activity) when the cat is viewing a moving grating oriented at 22.5 degrees (cortical activities for gratings moving in opposite directions were averaged). **(B)** single condition map as in (a), but when the cat is viewing moving gratings of orthogonal orientation, 112.5 degrees. Note orthogonal gratings activate complimentary spatial locations of the cortex. **(C)** contrast enhancement achieved for a differential image obtained by dividing the single condition map obtained for a stimulus orientation (a) by single condition map obtained for an orthogonal stimulus orientation (b). **(D)** pattern of cortical vasculature of the functionally imaged region obtained by illuminating with light of wavelength 540 nm. Scale bar 1 mm. A : Anterior, L : Lateral.

Fig. 2. Orientation specific intrinsic signals from ferret area 17. **(A)** single condition map when the ferret is viewing a moving grating of 0 degree orientation. **(B)** similar to map in (a), but obtained when the animal is viewing a moving grating of orientation orthogonal (90 degrees) to (a). **(C)** differential image showing improved contrast obtained by dividing map (a) by map (b). **(D)** pattern of cortical vasculature corresponding to the imaged region. Scale bar 1 mm. A : Anterior, M : Medial.

Fig. 3. Distribution of the spacing of iso-orientation domains in cat and ferret are 17. We measured the distance between nearest iso-orientation domains in each of the eight single condition maps for cat (n=108) and ferret (n=110). These distances were binned to the nearest 100 μm. The mean inter-domain spacing for ferret (open bars) is 0.68 ± 0.15 mm and for cat (filled bars) is 1.01 ± 0.22 mm.

Fig. 4. Spatial spread of orientation specific activity in cat and ferret area 17. Values are obtained from single condition maps for lines connecting the center of an orientation domain to the center of its orthogonal domain. Each line ends at the location of highest cross-orientation activity (see text); thus the lack of a flat region at the tail of the ferret activation curve is due to the relative closeness of the next iso-orientation domain, and indicates that some stimulus-specific response occurs for any cortical point. ΔR is change in the signal from blank image (spontaneous activity when the animal was viewing a neutral gray screen). R is the signal from blank image. Since there is a variation in the spontaneous activity both due to species difference and in spatial location, the values were normalized to the range of signal for each line to facilitate inter-species comparison. Means of 10 lines were used for this plot. Bars denote standard error.

Fig. 5. Spatial frequency dependent activation of orientation domains for cat area 17. The stimulus orientation for both the maps was 0 degrees. (a) moving grating of spatial frequency

0.38 cycles/deg. was used to obtain this single condition map. (b) single condition map similar to (a), but the spatial frequency of the moving grating was 0.78 cycles/deg. Foveal representation is towards the right of the map. Arrows mark approximately 5 degrees separation in eccentricity. Note similarity in the spatial location of patchy activity. A marked decrease in activity for grating of higher spatial frequency in (b) at the parafoveal region to the left of the map. Scale bar 1 mm. P : Posterior, M : Medial.

Figure 6. Organization of orientation preference in cat and ferret area 17. (a) composite orientation preference map of cat area 17 obtained by vector averaging of signal on a pixel-by-pixel basis of eight single condition maps. The eight single condition maps were obtained when the animal was viewing moving gratings of orientations spaced 22.5 degrees apart. (b) gradient map of (a) showing rate of change of orientation preference across cortical surface. This map was obtained by applying a two-dimensional gradient operator on the orientation preference map in (a). Dark areas correspond to regions where the orientation preference of adjacent pixels differ by 22.5 degrees or more. (c) orientation preference map of ferret area 17. This map is got in a similar manner as (a). (d) map of orientation gradient obtained from (c). For maps (a) and (b) lateral is up and anterior is left. For maps (c) and (d) anterior is up and medial is left.

Figure 7. Schematic to partly explain the difference in orientation domain density in cat and ferret. Circles represent iso-orientation domains; thick lines, representative cortical connections.

Assuming that the average lateral distance over which cortical fibers can arborize is relatively fixed (all lines of the same length), the necessity to repeat orientation structures in adjacent ocular dominance columns forces an increased density of orientation domains. Also, the necessity to repeat connections across ocular dominance domains necessitates double the amount of fibers running laterally through the cortex in the case of monkey and ferret. Crowding of fibers may thus be a further constraint on the maximum distance of arborization, necessitating even denser packing of iso-orientation domains in a crowded cortex.

Figure 1.

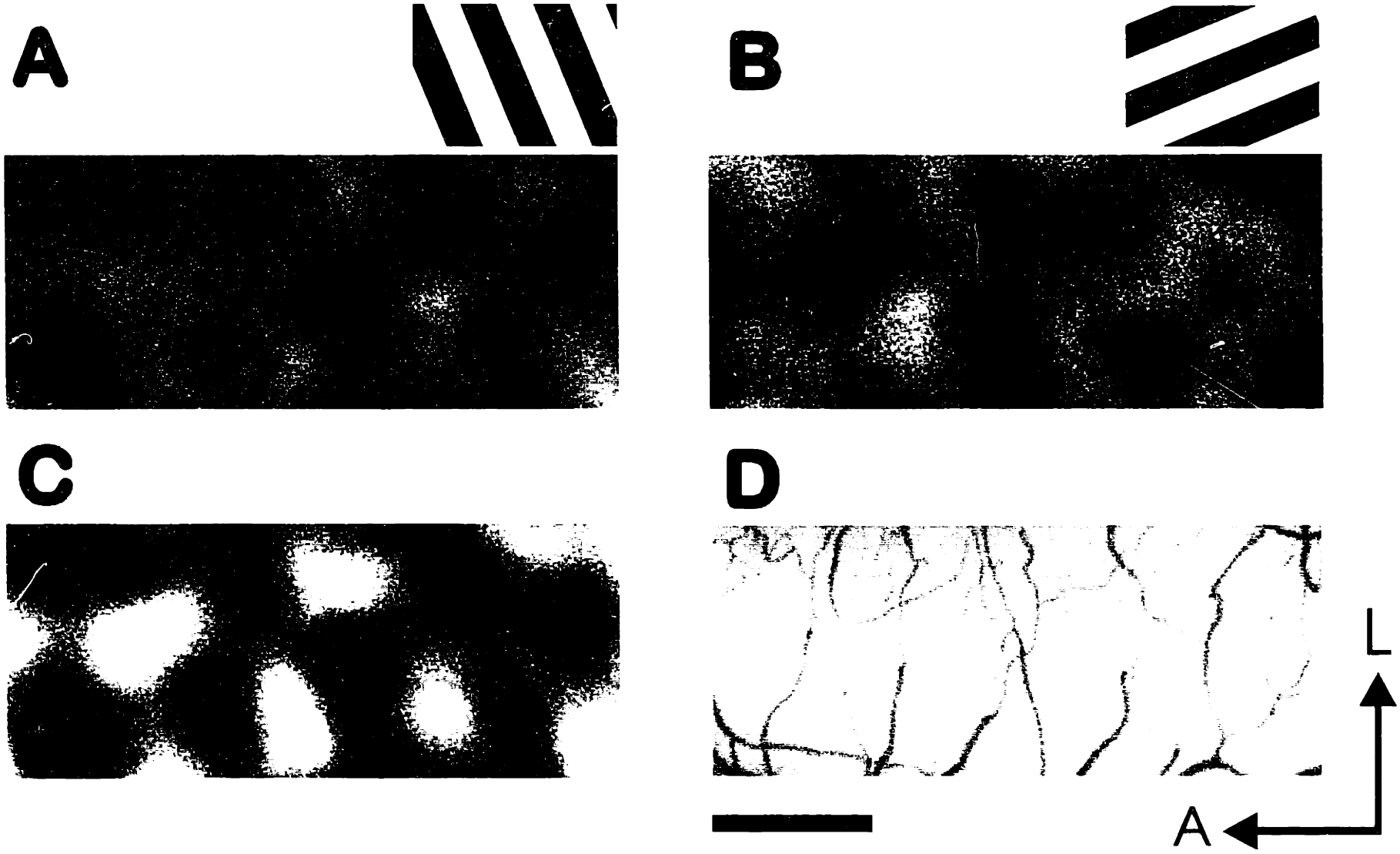

Figure 2.

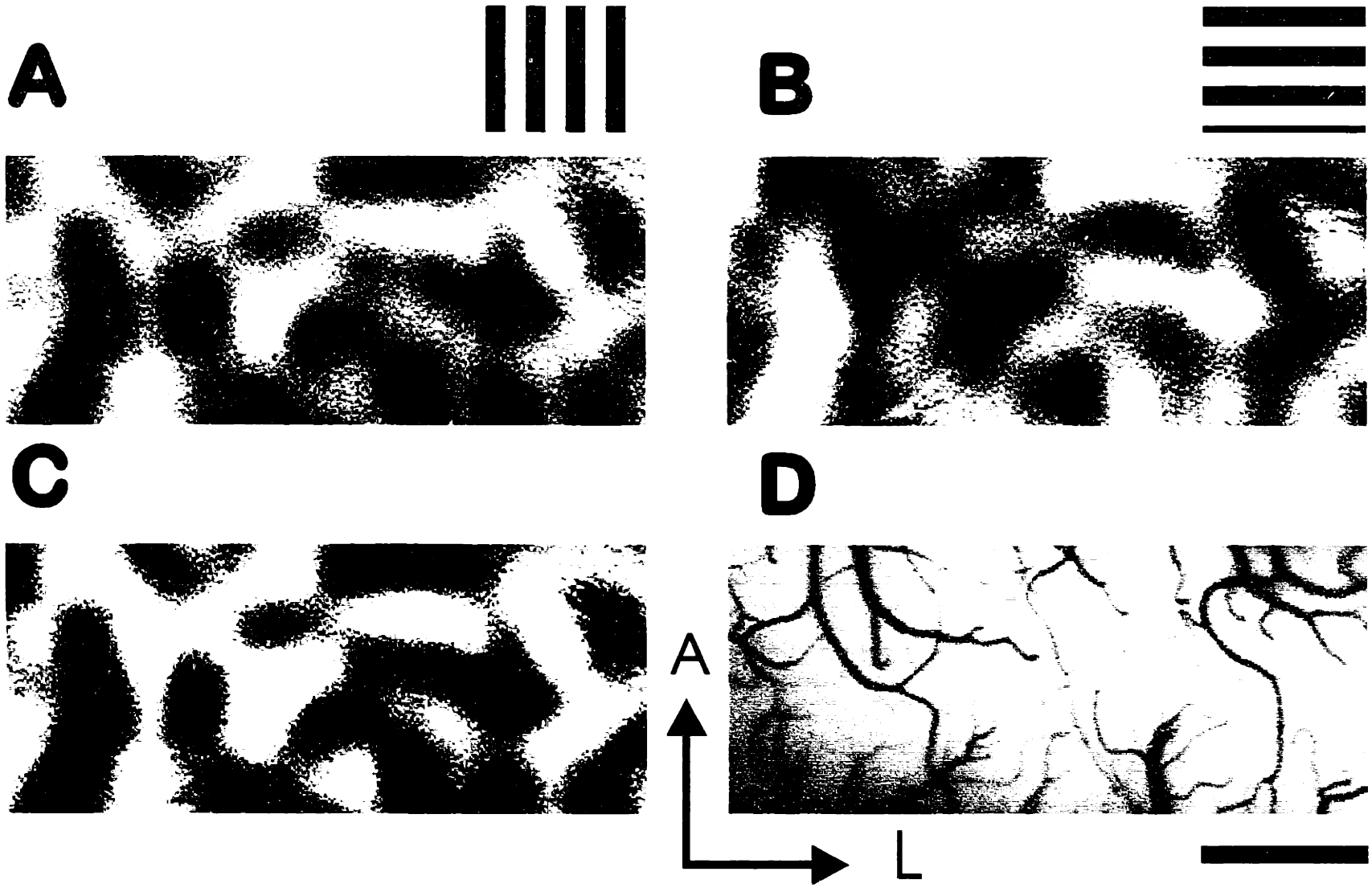

Figure 3.

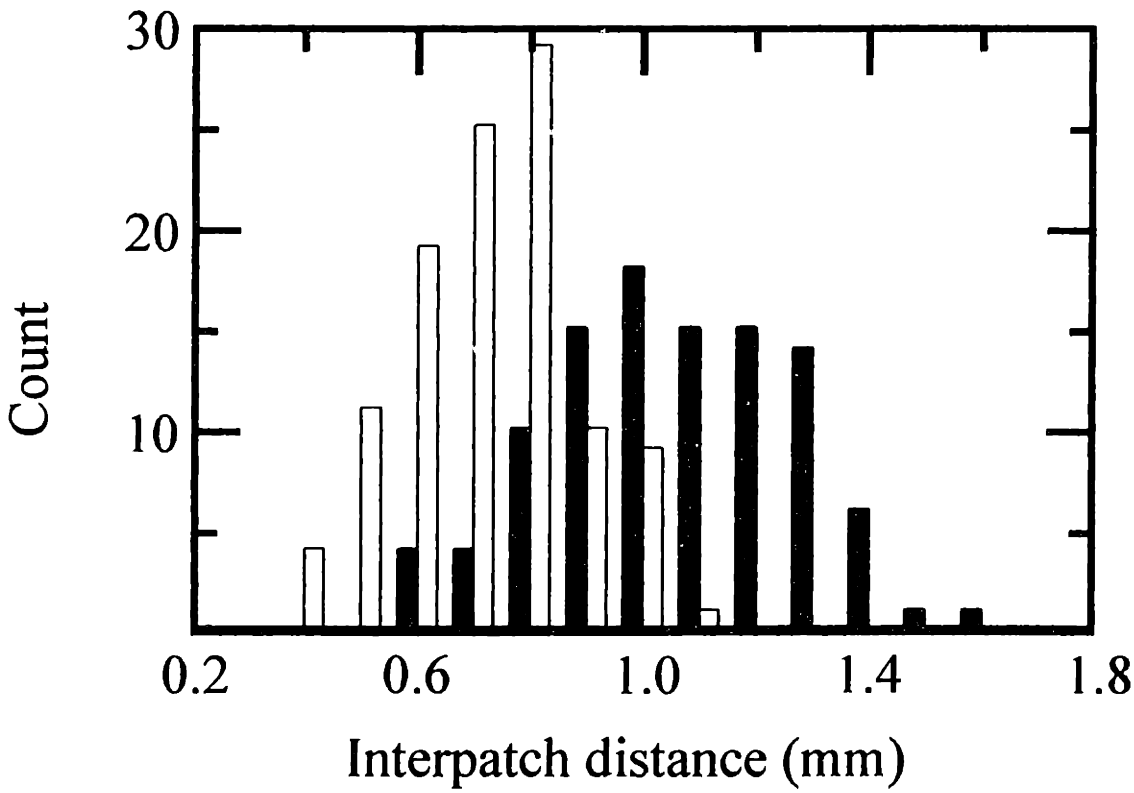

Figure 4.

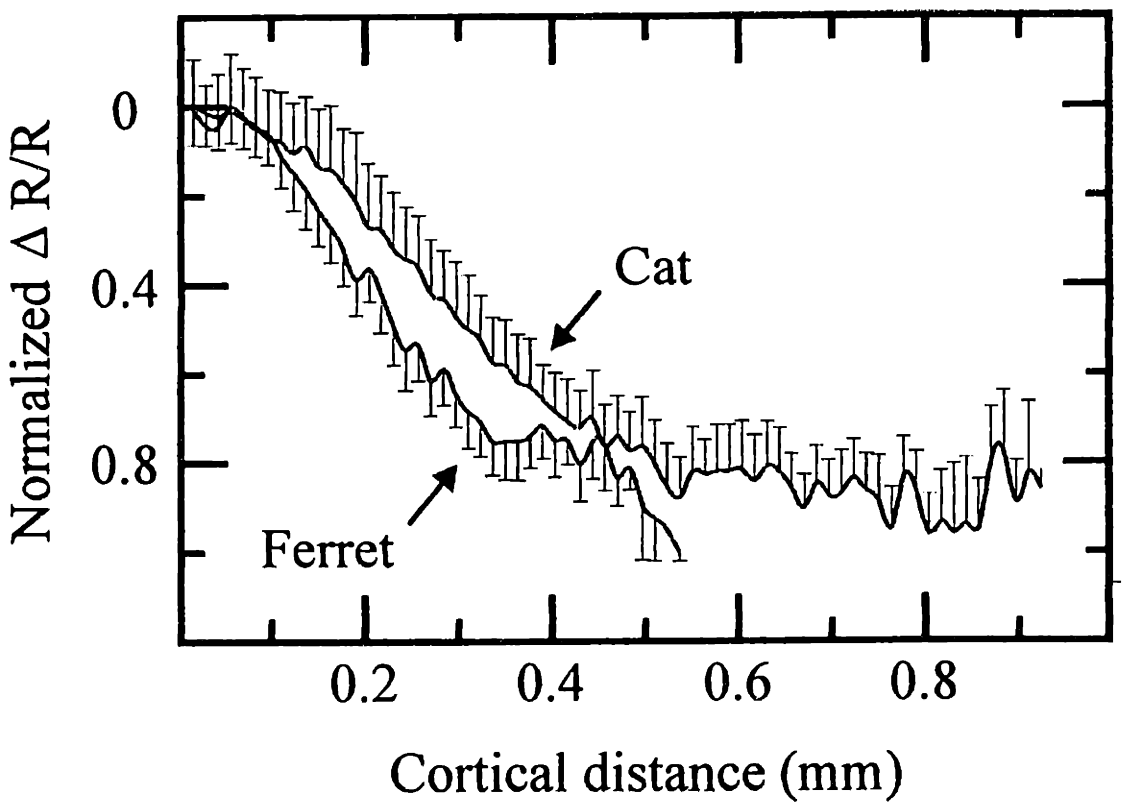
Normalized Δ R/R
0
0.4
0.8
Cat
Ferret
0.2
0.4
0.6
0.8
Cortical distance (mm)

Figure 5.

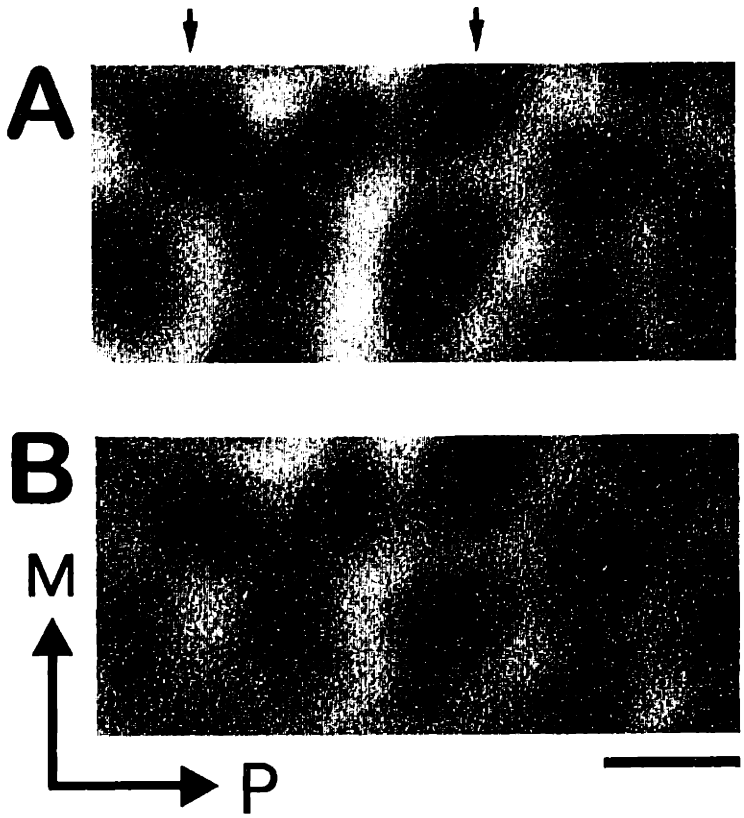

Figure 6.

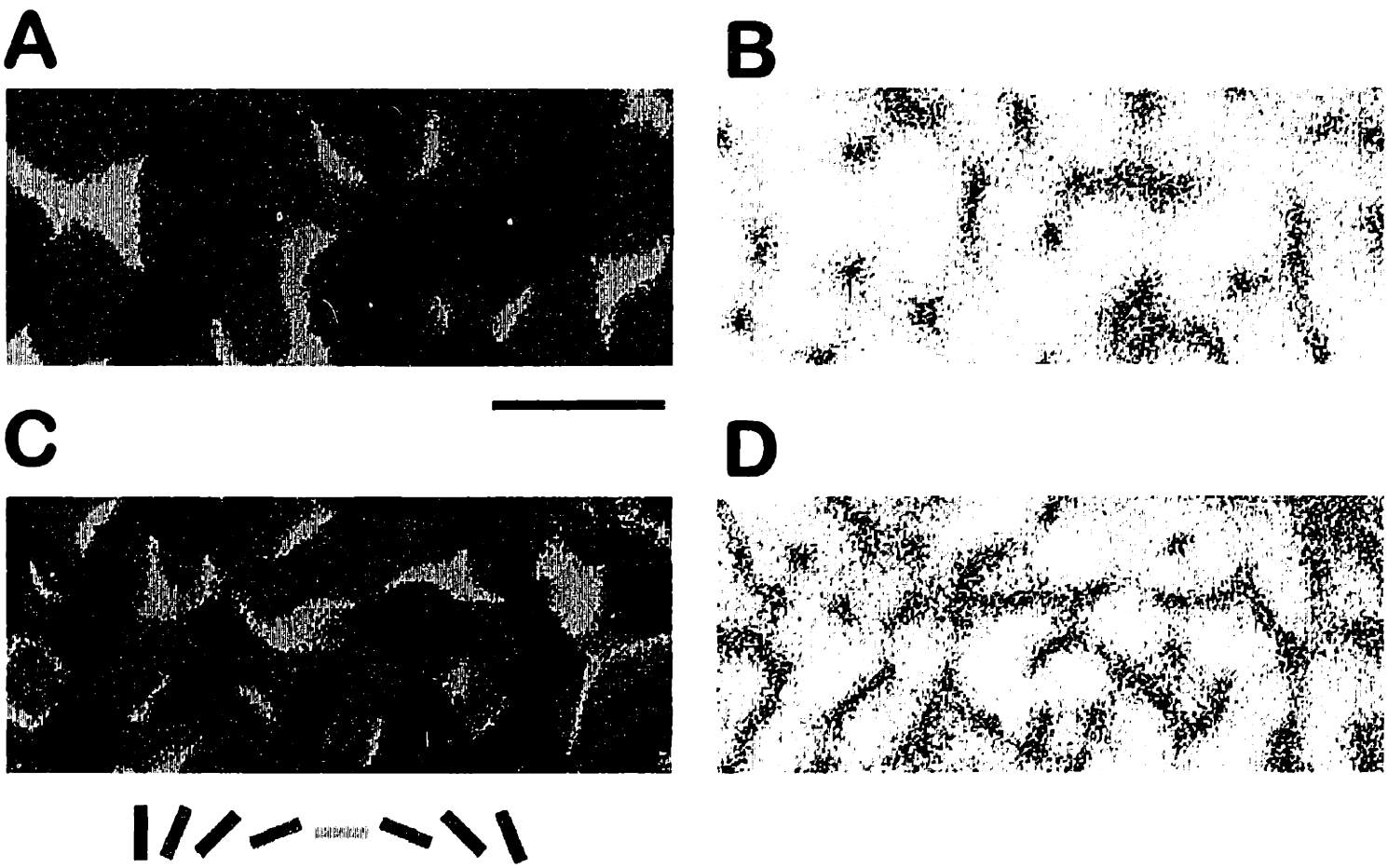

Figure 7.

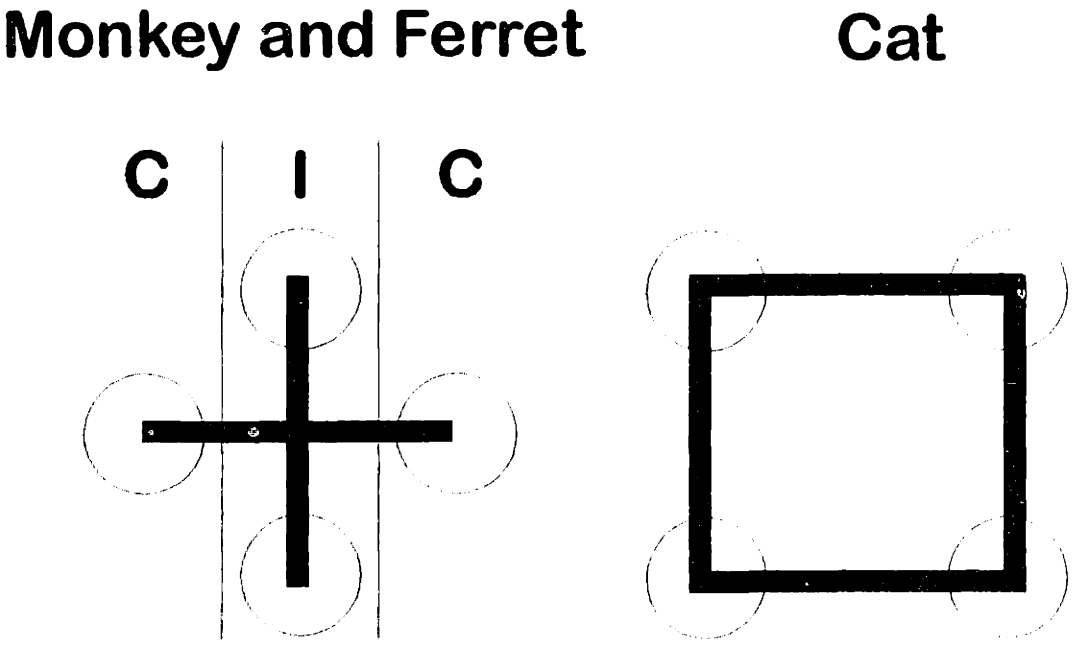

Chapter 2

Lateral Connectivity in Visual Cortex Imaged Through Intrinsic Signals: A Substrate for Extra-Classical Receptive Field Influences and Psychophysical "Filling-in"

ABSTRACT

In mammalian visual cortex, the importance of lateral connectivity in establishing orientation selective responses is widely acknowledged, though little understood. We have used the technique of intrinsic signal imaging in anesthetized cats to directly view the physiological spread of activation away from localized sources in order to understand the properties of the lateral connections. First, we demonstrate that lateral activation of cortex always occurs in an orientation specific manner. Activity contained in single orientation columns spreads to iso-orientation columns specifically. Second, by mapping the response properties of single units within the imaged region, we demonstrate that a large percentage of the optical signal must represent subthreshold responses. Single-unit receptive field mapping allows us to divide the imaged cortex into "center" and "surround" regions. We find that iso-orientation surround stimuli suppress high-contrast center responses, however they facilitate low-contrast center responses. Our stimuli are comparable to those used to create "artificial scotomas," which in human subjects are associated with perceptual filling-in of surface features. We therefore suggest that subthreshold responses mediated by the lateral connectivity may form the neural substrate for perceptual filling-in phenomena.

INTRODUCTION

Intrinsic signal imaging (Grinvald et al, 1986) is a powerful technique for investigating functional subdivisions of the cortical surface *in vivo*. In the primary visual cortex of mammals, organizations that can be seen by optical imaging techniques include orientation preference (Bonhoeffer and Grinvald, 1991; Blasdel, 1992), ocular dominance (Blasdel, 1992) and retinotopy (Toth et al, 1994). While the global structure of cortex has been increasingly well defined through optical imaging, traditional views of single cell receptive field structures have been upended. DeAngelis *et al.* (1993) showed a surprising temporal dependence to the excitation/inhibition structure of receptive fields. An experiment by Pettet and Gilbert (1992) suggested the idea that the spatial extent of a receptive field is a function of the stimulus used to measure it, and of the cell's history of stimulation. And finally, hypotheses on the possible modulatory effects of stimuli presented outside the "classical" receptive field, have begun to be explored directly by the technique of *in vivo* whole-cell recording (Toth et al, 1993). In this study, we demonstrate that optical imaging is also a useful tool for exploring issues of dynamic receptive field changes, as well as properties of the extra-classical receptive field (ECRF).

The size of a cortical cell's ECRF is a significant fraction of the entire visual space, suggesting a large physiological divergence of the visual pathway between retina and cortex. Some of this divergence occurs as a result of cortical cells communicating with neighboring cells via lateral connections within area 17. Optical imaging techniques have

already demonstrated (Grinvald et al, 1994) that focal stimulation spreads over an unexpectedly large region of cortex, presumably through this network of lateral connectivity. In this paper, we demonstrate that the spread of activity in cortex occurs in an orientation-specific manner. Further, by comparing our data with neuronal responses recorded extracellularly, we demonstrate that a significant fraction of the activity we measure is due to subthreshold sources, and represents effects of ECRF stimulation.

Surgery and recording chamber placement

Female cats aged 10 weeks to adult were initially anesthetized with a mixture of ketamine (15 mg/kg) and xylazine (1.5 mg/kg, i.m.). Subsequently anesthesia was maintained either by continuous infusion of sodium pentobarbital (1.5-2 mg/kg/hr, i.v.), or by isofluorane (0.5-1.5%) in a 70/30 mixture of N_2O/O_2. A tracheotomy was performed to facilitate artificial ventilation. The animal's heart rate and EEG were continuously monitored to ensure adequate levels of anesthesia. Expired CO_2 was maintained at 4% by adjusting the stroke volume and the rate of the respirator. The animal was placed on a heating blanket and the rectal temperature was maintained at 38°C. A mixture of 5% dextrose and lactated Ringers for fluid maintenance was given by continuous i.v. infusion. Craniotomy and durotomy were performed posterior to Horsley-Clark AP0 extending roughly 7 mm posterior and 4 mm lateral. After completion of surgery, paralysis was initiated with gallamine triethiodide (10 mg/kg/hr) to prevent eye movements. A stainless steel chamber (20 mm diameter) was cemented to the skull with dental acrylic and the inner margin was sealed with wax. In order to minimize cortical pulsations due to respiration and heart beat, the chamber was filled with silicone oil and sealed with a transparent quartz window over the chamber. Synchronization of the respirator, heart beat and data collection was attempted in some experiments, but was not routinely used as it was not observed to influence the signal magnitude or localization.

Optical recording

The cortical surface was illuminated with a bifurcated fiber-optic light guide attached to an 100W tungsten-halogen lamp source powered by a regulated power supply (Kepco ATE25-20M) to minimize variations in overall illumination level during the experiment. The light was passed through an IR filter and filters of appropriate center wavelength, and was adjusted for even illumination of the cortical surface at an intensity within the linear range of the camera's sensitivity. We used a slow-scan video camera (Bischke CCD-5024N, RS-170, 30 Hz, 60 dB s/n) fitted with a macroscope (Ratzlaff and Grinvald, 1991) consisting of two back-to-back camera lenses (50 and 55 mm, *f*1.2) allowing both a high numerical-aperture and a shallow depth of field. The camera was focused on the cortical surface by emphasizing the vasculature using light of 540 nm (maximum absorption of hemoglobin). After the pattern of cortical vasculature was imaged, the camera was focused 300 μm below this plane to minimize blood-vessel artifacts. Light of 600 nm (10 nm bandpass) was used to image activity dependent intrinsic oximetric signals. Data collection was under the control of the Imager 2001 system (Optical Imaging Inc.) which performed analog subtraction of a stored reference image (collected during presentation of a neutral gray screen) from the stimulus image (collected during presentation of an oriented grating), such that the image could be digitized in real time (Matrox image processor, 15 MHz) without sacrificing the signal-to-noise ratio of the camera.

Visual stimulation

All visual stimuli were presented to the contralateral eye, with the ipsilateral eye covered. The animal's eyes were focused on the monitor by back-projecting the retinal vasculature pattern with a reversible opthalmoscope and fitting the eyes with appropriate contact lenses. Constancy of eye position was verified before and after every experiment to within 0.4°. Stimuli were generated by an IBM-compatible computer running STIM (K. Christian, Rockefeller, Univ.), using a Sgt. Pepper + graphics board with 4 MB memory (Number Nine Corp.) at a resolution of 640x480. They were shown at a 60 Hz frame rate on a Sony Trinitron 14" monitor positioned approximately 30 cm away from the animal. Individual frames were computed prior to the beginning of the experiment and shown under the timing control of the data-collection computer.

A typical experiment consisted of four center stimuli, four surround stimuli, four full-field stimuli (equivalent to center + surround with no phase difference), and one neutral gray screen, presented in an interleaved manner. Four center stimuli were generated by presenting against a neutral gray background a small circular window within which a square-wave grating of 0.75 cyc/deg was shown at one of four orientations of motion (0° to 135° in 45° increments). Four surround stimuli were constructed in a identical manner, except that the grating was shown outside the circular window, and neutral gray shown inside. As discussed in the text, in some experiments the window was changed from a circular aperture to a square aperture with sides oriented along the 0° and 90° directions. In such experiments, only the horizontal sides of the rectangle were seen in the image, since the cortical representation of the vertical sides fell outside the imaged area.

The timing of the stimulus was chosen to give the maximum optical signal, as determined by our preliminary experiments with full-field gratings in area 17, and by others (Frostig, et al, 1990). The oriented grating was shown in a stationary position for 5 sec, and then was drifted at a rate of 1.5 Hz. 30 Hz camera frames were summed into 5 larger time blocks of 900 ms each. The first and last frames were discarded for the purposes of analysis; thus the data represents the summed signal from 1300 ms to 4600 ms after the start of stimulus motion. This timing scheme is summarized in fig. 1.

Single-unit recording

Single units were recorded with tungsten microelectrodes of impedance 2-4 MΩ. The signal was amplified (BAK, RP-1) filtered at 1 - 10 kHz, digitally windowed (Harvard Apparatus, PSD-1) and collected on an IBM 486 computer using a 200 MHz A/D board (AT-16-F-5, National Instruments) and software written in-house. Receptive fields were hand plotted using the minimum response field technique, and verified with a small, high-contrast bars moving through the receptive field under computer control.

RESULTS

We evaluated the data based on 40-70 tests of interleaved center/surround stimuli per experiment in 12 animals. While we attempted as many experiments as possible in each animal, the number that could be performed was limited due to the fact that after 8 to 14 hours of imaging, the magnitude of the optical signal dropped significantly below that of other artifacts in the image. The largest such artifacts were usually the result of brain or blood vessel pulsation. We noted that synchronizing the data collection periods to the animal's heart rate and/or respiration was not effective in reducing these artifacts. Since each experiment, consisting of 12 or more interleaved center, surround and full-field stimuli, occupied from 3 to 5 hours, depending on the amount of signal averaging needed, we usually obtained a maximum of four useful tests per animal. We presented our stimuli monocularly to avoid the need of aligning the two eyes. Parcellation of activity into ocular dominance regions has not been seen in anesthetized cats either with 2-deoxyglucose activity imaging (Löwel and Singer, 1993) or with intrinsic signal imaging (Rao et al, 1994), suggesting that similar results would have been obtained with binocular presentation.

Activation induced by center and surround stimuli

Figure 2 shows representative plots of the cortical activity generated from center (fig. 2A) and surround stimuli (fig. 2B). One can see that the area of highest activity is approximately complementary in these maps. The spatial location of this activity is in

agreement with standard maps of retinotopy in cat area 17 (Tusa et al, 1986), since the top edge of the spot is positioned 3 degrees below the area centralis, and on the vertical meridian. However, two other features appear in this image apart from this retinotopic correspondence. First, the border zone between the active areas of the two images is fuzzy. Some columns appear strongly activated by both stimuli. This fuzziness is not surprising, as a particular point of the retinal image is known to be capable of directly activating a whole population of cortical cells, with a spatial spread of perhaps a few millimeters (Albus, 1975). The second feature to note, however, is that one can discern localized activation even as far as the edge of the optical image, quite far from the stimulus border. Fig. 3 shows a second example of center (fig. 3A) and surround (fig 3B) activation, where the stimulus border is even less distinct. To obtain the border location accurately, we compared the magnitude of the center and surround stimulus-specific signals at each pixel in the image. Figure 2C shows the result of this comparison. Regions which gave a greater response to the center stimulus are shown in white, while regions which gave greater response to the surround stimulus are shown in black. The area thus delimited defined the cortical center representation in the optical image.

Lateral spread of signal

Although activity in response to center and surround stimuli was to a large degree spatially localized, we found it possible to obtain maps of orientation preference even in the lesser activated regions several millimeters away from the stimulus border. Fig. 4 shows an example of such maps, computed from the same cortex as fig. 3 such that preferred angle

is coded by the color scheme shown, and strength of orientation-specific signal (magnitude of the vector summation) is coded by intensity of color. Regions outside the region of maximal activation always retain the same orientation specificity as when those regions are maximally activated. One can see that the center stimulus (fig. 4A) continues to activate orientation columns at the image edge, and that the surround stimulus (fig. 4B) completely activates the center region with strength sufficient to generate a robust orientation map over the entire cortical area. In this experiment, a surround stimulus of 6 degrees continued to generate an orientation map in which all orientation domains present in the full field orientation map could still be discerned, whereas a surround stimulus of 9 degrees generated a map with some domains, 5 to 6 mm away, providing undetectable signal levels. The orientation response to a full field grating, shown in fig 4C, confirms that activation is always orientation specific; that is, stimuli always activate iso-orientation domains, regardless of whether they are activating center or surround regions.

Response to the stimulus edge

Since a large proportion of cells in area 17 are known to have end-stopped characteristics, we wondered whether the presence of the stimulus edge itself might be causing much of this activity. To test this possibility, we compared responses to the full-field grating as shown in fig. 1B with a stimulus where the grating over the center region was out of phase with the surround, but in all other respects identical. We failed to see any differential activation between the two images. Furthermore, a full-field vector angle map computed from a phase-shifted 0° stimulus, and three in-phase stimuli at 45°, 90° and 135°, did not

show any significant difference in the 0° representation area from a normally-computed angle map. We see no evidence in the optical signal for any novel response to the presence of the stimulus edge.

Correspondence with single-unit physiology

Having obtained the result that distant regions of cortex are activated in an orientation-specific manner, we wished to show that such activation did not result merely from divergence in the visual pathway prior to the cortex. In two cats, microelectrode recordings were made in order to verify that the receptive field positions of the underlying cells were in correspondence with the data obtained from optical imaging. Receptive field locations are shown in figure 5A and C. Recording sites were chosen to show that the optical map is large enough to contain regions of non-overlapping receptive fields. Fig. 5 B and D show the locations from which single units were obtained, relative to the map of the stimulus edge calculated by the same method as in fig. 3C. Penetrations within the center region (white) are coded red; those in the surround region (black) are coded blue. Note that in the first case (fig. 5 A and B) the center spot is below the area centralis, and thus the top edge is being imaged, whereas in the second case (fig 5 C and D) the center spot covers area centralis, and thus the bottom edge is the one imaged. We found an excellent correlation between the centers of single-unit receptive fields, and their expected position relative to the spot border as defined by the optical imaging method. Furthermore, the data suggest that the anterior and posterior penetrations within the imaged area are sufficiently distant to have non-overlapping receptive fields. Since we

always imaged a spot border between 3° and 5° below area centralis, these receptive field positions and sizes shown here are representative for all the data shown. (Orientation preference of single-units generally agreed with that of the imaged map, though describing that correspondence is beyond the scope of this study.)

Surround inhibition

When comparing population signals under different stimulus conditions, we make the assumption that activity at a particular point is always originating in the same cells. Another possibility, though somewhat unlikely, is that a given cortical region contains two sub-populations of cells which react differently to the stimuli, but do not interact with each other. If our results were due to the activity of two different populations of cells, one should expect the activity to the full-field stimulus in the spot region to be equal to the summation of the center and surround activities in that region. To calculate absolute amounts of activity, the vector magnitudes over a roughly 1.3 mm^2 area of the center region of cortex were averaged for each stimulus type. To avoid the inaccuracies involved in measuring small differences between small signals, we confined our analysis to those experiments which gave exceptionally high overall signal magnitudes. Also, since signal magnitude falls as a function of distance from the retinotopic stimulus border, we chose for each case regions 2.5 mm from the calculated border. Results for the two best 8-orientation experiments are shown in figure 6. Surprisingly, the greatest signal occurred not for the full-field stimulus, but rather for the center stimulus. We confirmed this finding by single-unit recordings (see legend to figure 7A). Averaged over these two

experiments, the intrinsic signal response to the surround stimulus comprised 62% of the response to the center. Response to full-field stimulation comprised 92% of the response to the center. Since our single unit recordings indicate that receptive fields in the measured region fall within the stimulus border, we interpret these findings as direct evidence for inhibition from the extra-classical receptive field.

How much of the intrinsic signal is subthreshold?

We reasoned that if we could estimate a population sum of single-unit responses to the experimental stimuli, we could calculate what fraction of the intrinsic signal represents the subthreshold response. For comparing with the values of vector magnitude reported above, we measured the response to stimuli of optimal orientation, and subtracted the response to the blank stimulus (spontaneous activity). Recordings occurred under identical conditions to those during the imaging session. For each cell (n=30), we calculated the surround response as a percentage of the center response after subtracting the background response. A histogram of this index across the entire population of cells appears in figure 7B. Calculated in this manner, spiking response to the surround stimulus across the population was 6.8% of the response to the center stimulus. The magnitude of intrinsic signal response to the surround stimulus was 52% to 72% that of the center. If we make the assumption that equal amounts of subthreshold activity exist in the center region during center and surround stimulation, we can then estimate that over half of the intrinsic signal response to the center stimulus represents subthreshold activity.

Single-unit recordings demonstrate biphasic surround effects.

We have demonstrated that a high-contrast surround inhibits the response to a high-contrast center. Since optical recording does not distinguish between signals from excitatory or inhibitory sources, we are left with the problem of whether the largely subthreshold, iso-orientation activity generated in the center region by the surround stimulus is inhibitory or excitatory. In 20 of the single-unit recordings represented in figure 7A and B, we presented two novel stimuli, in order to answer the question of whether the surround could also be facilitory. These were 1) a center stimulus of low contrast and neutral surround, and 2) a center stimulus of low contrast with a high contrast surround. Responses to these stimuli from two representative cells are shown in figure 7C and D. In cells which also demonstrated the suppressive effect of the high-contrast surround on a high-contrast center, we observed small but present facilitory effects of the same high-contrast surround on a low contrast center, close to physiological threshold. We conclude that the surround can have both facilitory and suppressive effects, depending on the stimulus configuration, and (since a zero contrast center is the limiting case of a low contrast center) that the subthreshold iso-orientation signal observed optically is largely from excitatory sources.

Point spread in cortex

The question of the amount of cortex capable of responding to a given point in the visual field is both one of anatomy and of physiology. Previous studies suggest that thalamocortical afferents arborize at most over a maximum area of 1.8 mm^2 (Humphrey et al, 1985) or a maximum lateral distance of 1.0 to 1.5 mm. Similarly, physiological studies of the point spread distance from retina to cortex have suggested values on the order of 1 to 2 mm (Hubel and Wiesel, 1974; Albus, 1975; Tootell, 1988; Das and Gilbert 1995). These values are clearly too small to account for the amount of signal spread that we (up to 6 mm) and others (Grinvald et al, 1994 (up to 10 mm); Das and Gilbert, 1995 (3.2 to 5.2 mm)) observe optically, suggesting that the lateral activity is mediated by a cortical mechanism. Within area 17, Gilbert and Wiesel claim a value of 6 to 8 mm for the range of cortical connectivity from a given cell, though these are mainly large pyramidal cells, and 4 mm is perhaps a more typical value for our purposes (Gilbert and Wiesel, 1979; Gilbert and Wiesel, 1983). The intrinsic connections are likely more than large enough to connect areas of completely separate receptive fields, though not large enough to account for the maximum values of optically observed point spread area. It seems likely that a combination of the cortical circuitry and subthreshold activation (discussed below) is responsible for the large point spread areas observed with optical recording.

Reliability of amplitude estimates

Many factors affect the reliability of intrinsic signal amplitudes measured by optical imaging. By averaging vector magnitudes, instead of raw signal amplitudes, we avoid some of the variability due to non-stimulus related factors, however our results should be interpreted as no more than an order of magnitude estimate. We present these results partly because there is so little evidence as to whether intrinsic signal amplitudes change linearly with the underlying spiking activity. Our results suggest that there is a significant non-linear component, which we attribute to subthreshold activity, though other mechanisms which use energy locally in a stimulus-dependent manner may also contribute.

Relation to "filling in"

"Filling-in" refers to the percept that occurs in normal monocular vision in the region of the blind spot, and in the vision of patients with focal lesions of the early visual system. The color and texture of the surrounding region is perceived in the region devoid of input. Ramachandran and Gregory (1991) demonstrated that the same effect could be caused artificially by stimuli containing flickering random noise in a retinally stable region of the visual field. Our stimulus is conceptually similar to that which has been shown to induce artificial scotomas. In two experiments, we replaced the neutral gray of the spot region with a flickering random dot field, to make our stimulus exactly identical to that of Ramachandran and Gregory. We did not see any difference in the lateral spread of signal under these conditions, and therefore conclude that our stimulus was identical for the purposes of area 17 physiology. The actual location of the area responsible for the

psychophysical "filling-in" percept cannot, obviously, be answered by this experiment, but our data indicate that already in area 17, cells have access to enough information to generate this percept.

Dynamic receptive field changes

Many investigators have demonstrated the possibility for both excitatory (Nelson and Frost, 1985) and inhibitory (Nelson and Frost, 1978; Gulyás et al, 1987; Hammond and MacKay, 1981) effects of a surround field on single-unit responses. It should not be surprising, therefore, that the actual border of a receptive field should depend critically on the conditions under which it is measured (Cudeiro and Sillito, 1994). It is likewise possible that modification of the receptive field brought about by different stimuli (A,B) shows hysteresis such that if a receptive field is stimulated in the pattern $A_1B_1A_2$ the receptive field measured during the A_1 and A_2 stimuli will not be identical, even over very short time periods (Pettet and Gilbert, 1992; Volchan and Gilbert, 1995). The increase in activity which we observe outside the center region during center presentation, or inside the center region during surround presentation is certainly consistent with an expansion of the receptive fields within those unstimulated regions. Also, the minimum response field technique, used to map the receptive fields shown in fig. 4, does not account for the possibility of conditioned expansion. (It is far from obvious how to properly measure receptive field expansion in such conditions, since, following the hypothesis, the act of measuring the RF itself changes the RF.) Our single-unit data do not support this hypothesis, however, since the average surround response was only 6% of the center

response magnitude (fig. 7B). We must conclude that although a mechanism that could mediate receptive field expansion (the lateral, subthreshold, iso-orientation response) seems to be present over a large cortical area, this mechanism is not activated dynamically in response to fast changes in the visual scene.

Surround effects on center response

Our finding of a biphasic surround effect on the center response is novel in cat cortex. Knierim and Van Essen (1992) and Fries et al, (1977) have observed the suppressive effect of an oriented surround in monkey V1, and have suggested that the maximal effect occurs at similar orientations of center and surround. Such an effect is a prime candidate for mediating perceptual "pop-out" (Bergen and Julesz, 1983; Triesman and Gelade, 1980). However, a shift only in stimulus phase within the center region, which creates pop-out without changing other stimulus attributes, did not show any effects. Similarly, by lowering the detection threshold for iso-orientation stimuli, surround excitation is an appropriate mechanism for mediating the perceptual completion of occluded objects.

Conclusion

We have suggested that primary visual cortex contains subthreshold, stimulus specific information over a much wider area than previously believed. In doing so, we have reconciled the discrepancy between the relatively small point spread area measured with single-unit techniques, and the extremely large area measured with optical techniques. This subthreshold information can be used in either a facilitory or an inhibitory manner.

We have demonstrated single-unit facilitation for low-contrast stimuli and suppression for high-contrast stimuli. Such modulations may generate psychophysical phenomena such as filling-in or perceptual pop-out, or may contribute to the ability of a higher area to do so.

REFERENCES

Albus K. (1975) A quantitative study of the projection area of the central and the paracentral visual field in area 17 of the cat. I. The precision of the topography. *Exp. Br. Res.* 24:159-179.

Arieli A, Shoham D, Hildesheim R, Grinvald A (1995) Coherent spatiotemporal patterns of ongoing activity revealed by real-time optical imaging coupled with single-unit recording in the cat visual cortex. *J. Neurophys.* 73(5):2072-2093.

Bergen JR, Julesz B (1983) Parallel versus serial processing in rapid pattern discrimination. *Nature* 303:696-698.

Bonhoeffer T and Grinvald A (1991) Iso-orientation domains in cat visual cortex are arranged in pinwheel like patterns. *Nature* 353:429-431.

Blasdel GG (1992) Differential imaging of ocular dominance and orientation selectivity in monkey cortex. *J. Neurosci.* 12:3117-3140.

Cudeiro J and Sillito AM (1994) Spatial variation in orientation domain influences on the response of cells in the feline visual cortex. *Soc. Neurosci. Abstr.* 20:314. (137.14)

Das A, Gilbert CD (1995) Long-range horizontal connections and their role in cortical reorganization revealed by optical recording of cat primary visual cortex. *Nature* 375:780-784.

DeAngelis GC, Ohzawa I and Freeman RD (1993) Spatiotemporal organization of simple-cell receptive fields in the cat's striate cortex. I. General characteristics and postnatal development. *J. Neurophysiol.* 69:1091-1117.

Fries W, Albus K, Creutzfeldt OD (1977) Effects of interacting visual patterns on single cell responses in cat's striate cortex. *Vision Res.* 17:1001-1008.

Frostig RD, Lieke EE, Ts'o DY, Grinvald A (1990) Cortical functional architecture and local coupling between neuronal activity and the microcirculation revealed by *in vivo* high-resolution optical imaging of intrinsic signals. *Proc. Nat. Acad. Sci. USA* 87:6082-6086.

Gilbert, CD, Wiesel TN (1989) Columnar specificity of intrinsic horizontal and corticocortical connections in cat visual cortex. *J. Neurosci.* 9(7):2432-2442.

Gilbert CD, Wiesel TN (1983) Clustered intrinsic connections in cat visual cortex. *J. Neurosci.* 3:1116-1133.

Gilbert CD, Wiesel TN (1979) Morphology and intracortical projections of functionally characterised neurones in the cat visual cortex. *Nature* 280(5718):120-125.

Grinvald A, Lieke EE, Frostig RD, Gilbert CD and Wiesel TN (1986) Functional architecture of cortex revealed by optical imaging of intrinsic signals. *Nature* 324:361-364.

Grinvald A, Lieke EE, Frostig RD, Hildesheim R (1994) Cortical point-spread function and long-range lateral interactions revealed by real-time optical imaging of macaque monkey primary visual cortex. *J. Neurosci.* 14(5):2545-2568.

Gulyás B, Orban GA, Duysens J and Maes H (1987) The suppressive influence of moving textured backgrounds on responses of cat striate neurons to moving bars. *J. Neurophys.* 57(6):1767-1791.

Hammond P, MacKay DM (1981) Modulatory influences of moving textured backgrounds on responsiveness of simple cells in feline striate cortex. *J. Physiol. Lond.* 319:431-442.

Hubel DH, Wiesel TN (1974) Uniformity of monkey striate cortex: a parallel relationship between field size, scatter, and magnification factor. *J. Comp. Neurol.* 158:295-306.

Humphrey AL, Sur M, Uhlrich DH, Sherman SM, (1985) Projection patterns of individual X- and Y- cell axons from the lateral geniculate nucleus to cortical area 17 in the cat. *J. Comp. Neurol.* 233:159-189.

Knierim JJ, Van Essen DC (1992) Neuronal responses to static texture patterns in area V1 of the alert macaque monkey. *J. Neurophys.* 67(4):961-980.

Löwel S, Singer W (1993) Monocularly induced 2-deoxyglucose patterns in the visual cortex and lateral geniculate nucleus of the cat: I anaesthetized and paralysed animals. *Eur. J. Neurosci.* 5:846-856.

Nelson JI, Frost BJ (1985) Intracortical facilitation among co-oriented, co-axially aligned simple cells in cat striate cortex. *Exp. Br. Res.* 61:54-61.

Nelson JI, Frost BJ (1978) Orientation-selective inhibition from beyond the classic visual receptive field. *Brain Res.* 139:359-365.

Pettet MW and Gilbert CD (1992) Dynamic changes in receptive-field size in cat primary visual cortex. *Proc. Nat. Acad. Sci. USA* 89:8366-8370.

Ramachandran VS, Gregory RL (1991) Perceptual filling in of artificially induced scotomas in human vision. *Nature* 350:699-702.

Rao SC, Toth LJ, Sur M (1994) Invariance of orientation domains in area 17 of cat visual cortex revealed by intrinsic signal imaging. *Soc. Neurosci. Abstr.* 20, 836.

Tootell RBH, Switkes E, Silverman MS, Hamilton SL (1988) Functional anatomy of macaque striate cortex II: retinotopic organization. *J. Neurosci.* 8:1531-1568.

Toth LJ, Nelson SB, Rao SC, Sur M (1993) Synaptic potentials in visual cortical neurons: temporal variability and spatial structure. *Soc. Neurosci. Abstr.* 19:1576. (648.8)

Toth LJ, Rao SC, Sur M (1994) Orientation-specific spread of activation in primary visual cortex measured by optical recording of intrinsic signals. *Soc. Neurosci. Abstr.* 20:836. (349.2)

Triesman AM, Gelade G (1980) A feature integration theory of attention. *Cognit. Psychol.* 12:97-136.

Tusa RJ, Palmer LA, Rosenquist AC (1978) The retinotopic organization of area 17 (striate cortex) in the cat. *J. Comp. Neurol.* 177:213-236.

Volchan E, and Gilbert CD (1995) Interocular transfer of receptive field expansion in cat visual cortex. *Vision Res.* 35(1):1-6.

FIGURE LEGENDS

Fig. 1 Stimuli used in this experiment, orientation convention, and timing diagram for one stimulus presentation. **A)** "Blank" stimulus, **B)** "Full-field" stimulus, also referred to as "center+surround", **C)** "Center" stimulus, **D)** "Surround" stimulus, **E)** "Perpendicular" stimulus. Data collection occurs at the time of maximum orientation-specific intrinsic signal as determined in pilot experiments, and timed from the start of stimulus motion. (We chose to image responses to moving rather than stationary gratings to make the intrinsic signal as robust as possible.) The stimulus is flashed on 5 sec. prior to the start of the motion, thus reducing the contribution of the onset-response to the signal.

Fig. 2 Summed response to 56 presentations of **A)** center and **B)** surround stimuli. Each map represents the response to 0° divided by the response to 90°. 0° orientation domains appear black, 90° domains appear white. Although retinotopy is evident, the signal is not confined to complementary regions. The stimulus is presented 3° below the horizontal meridian. Anterior is to the right, lateral is to the bottom. Scale bar is 1 mm.

Fig. 3 Summed response to 56 presentations of **A)** center and **B)** surround stimuli from a different animal. Each map represents the response to 0° divided by the response to 90°. The vertical line appearing on the left of the images is artifact from a large blood vessel. **C)** shows the activity border, calculated from the single-condition maps. White regions are points where maximal activity was elicited by a center stimulus, black regions are points where maximal activity was elicited by a surround stimulus. The border runs

approximately through the image center. Notice that the map of surround activity extends throughout the entire cortical region. Anterior is to the right, lateral is to the bottom. Scale bar is 1 mm.

Fig. 4 Maps of the summed orientation vector for **A**) center, **B**) surround, and **C**) full-field maps. Vector angle, coding orientation preference, is shown by color, and vector magnitude, coding strength of orientation-specific signal, is shown by intensity. Brightest intensities are 1 standard deviation above the image mean, and are approximately equal for all three maps. Although the center stimulus is stronger (brighter) at the center of the image, within the center representation, the center stimulus continues to elicit strong, orientation-specific signals outside the center representation. Similarly, the surround elicits strong signals within the center representation, "filling-in" the map of orientation preference. The correspondence of center and surround maps with that of the full-field stimulus indicates that the "filled-in" regions receive iso-orientation activation. Scale bar is 1 mm.

Fig. 5 Single-unit receptive fields recorded from center and surround areas of cortex are shown for two animals. Red indicates recordings from the center representation, and blue indicates recordings from the surround representation. **A** and **C** are plots of visual space with superimposed single-unit receptive fields shown in red and blue, and the border of the center spot shown in black. (A square "spot" was used in these experiments.) **B** and **D** show the location of the electrode penetrations used for the recordings superimposed on a

map of the imaged center/surround border calculated by the same methods as in figure 3C. White represents center dominated regions, black represents spot dominated regions. In the first experiment (A,B) the center stimulus was located 3° below the horizontal meridian; thus the top edge of the stimulus was recorded in the optical image. In the second experiment (C,D) we located the bottom stimulus edge 2° below the horizontal meridian, such that the center stimulus covered the area centralis. Thus, the bottom edge of the stimulus was imaged. Receptive field locations show a clear positional separation. Nearly all receptive fields lay entirely within the appropriate stimulus region. VM, vertical meridian; HM, horizontal meridian; A, anterior; L lateral. All figures drawn to same scale.

Fig. 6 Plot of intrinsic signal magnitude for a region of $1x10^4$ pixels 2-3 mm inside the center representation for the three stimulus conditions in two experiments. **A)** In the first experiment, the magnitude of response to surround, full-field and center stimuli respectively were 1.28%, 1.63% and 1.77%. **B)** For the second experiment, the magnitudes of responses were; surround = 0.139%, full-field = 0.244% and center = 0.267%. These values are shown normalized to the spot response (see text). A value of 0% indicates no orientation-specific component in the signal. The percentages can be thought of as the percent of signal in the total collected light. Mathematically, they are equivalent to the magnitude of the fourier component of 180° periodicity when transformed across the dimension of stimulus angle.

Fig. 7 Summary of single-unit responses from 30 cells with receptive fields positioned in the "center" region. **A)** shows the population histogram of the amount of suppression in each cell created by adding the high-contrast "surround" grating to the "center" grating (full field grating = center grating + surround grating). The suppression index, plotted on the x-axis is calculated by; $suppresion\ index = \frac{full\ field - background}{center - background}$. Values less than one indicate suppression, greater than one indicate facilitation. The average index value is 0.843. **B)** shows a similar population histogram for the amount of spiking response elicited by the surround. The surround index, plotted on the x-axis is calculated by; $surround\ index = \frac{surround - background}{center - background}$. A value of zero indicates no surround response. Values less than zero are possible when the response to the surround is less than the response to the background. The average index value is 0.0682. **C** and **D)** show facilitory and suppressive surround effects in two different cells. The average response to ten stimulus presentations is plotted versus the stimulus type. "Blank", neutral contrast gray screen, taken as background. "LCC", low contrast center grating, no surround. "LCC+HCS", low contrast center, high contrast surround. "Center", high-contrast center, no surround. "HCC+HCS", high-contrast center and high-contrast surround (equivalent to full-field grating). Notice that in both cases, the surround facilitates the response to the low contrast center, but suppresses the response to the high contrast center.

Figure 1.

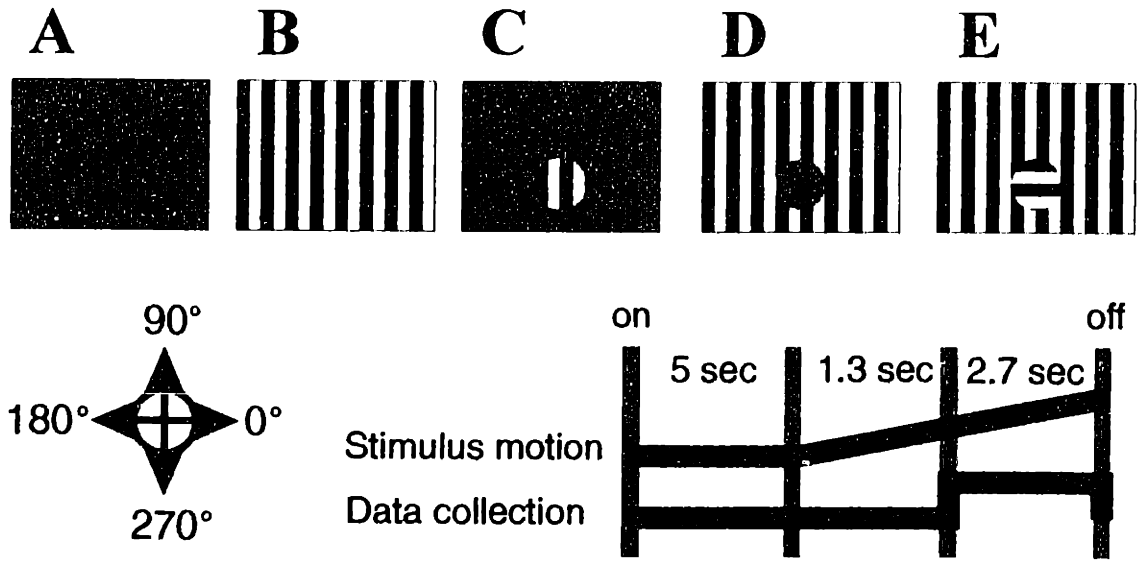
A
B
C
D
E
90°
180°
0°
270°
on
off
5 sec
1.3 sec
2.7 sec
Stimulus motion
Data collection

Figure 2.

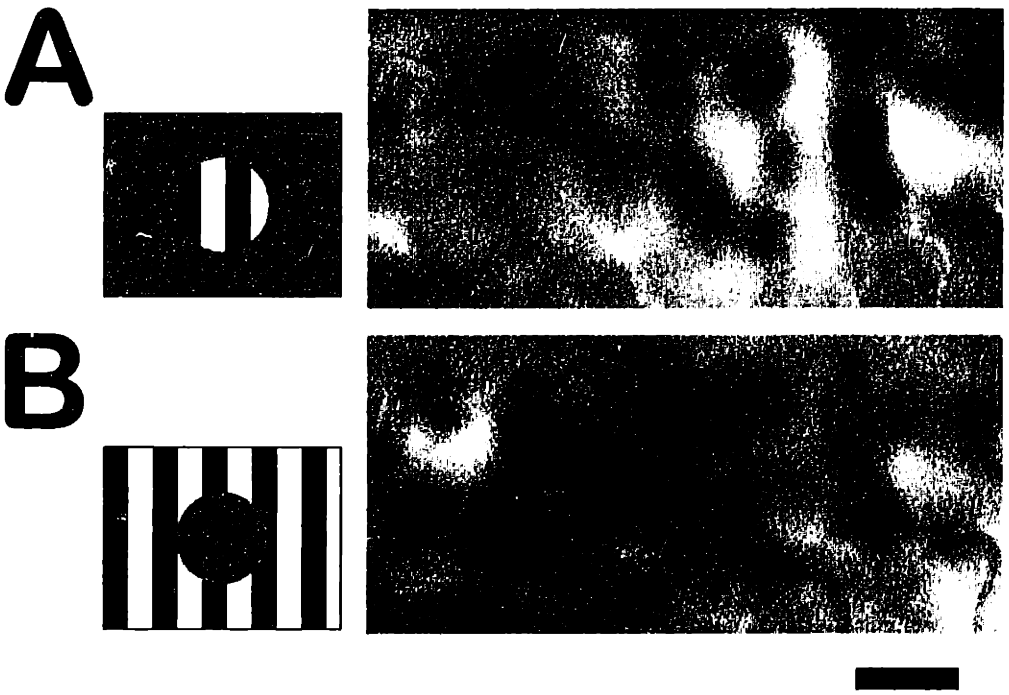

Figure 3.

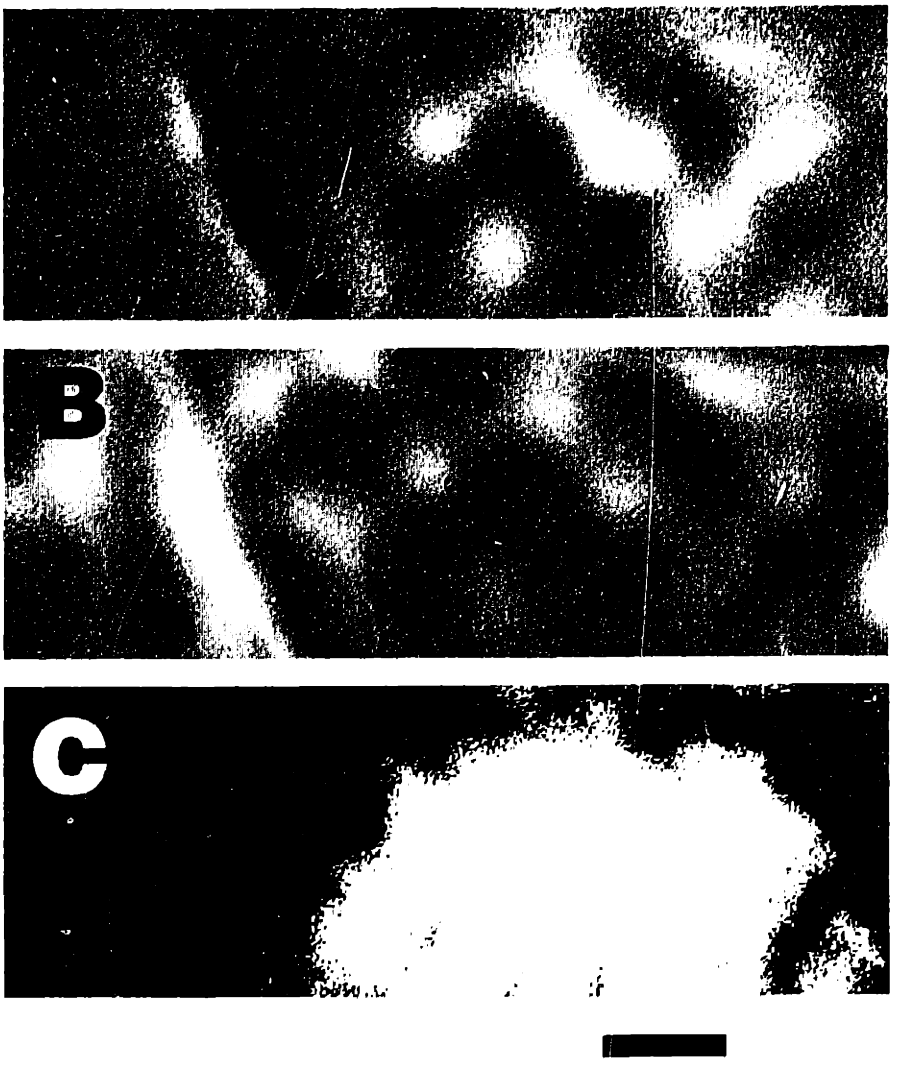

Figure 4.

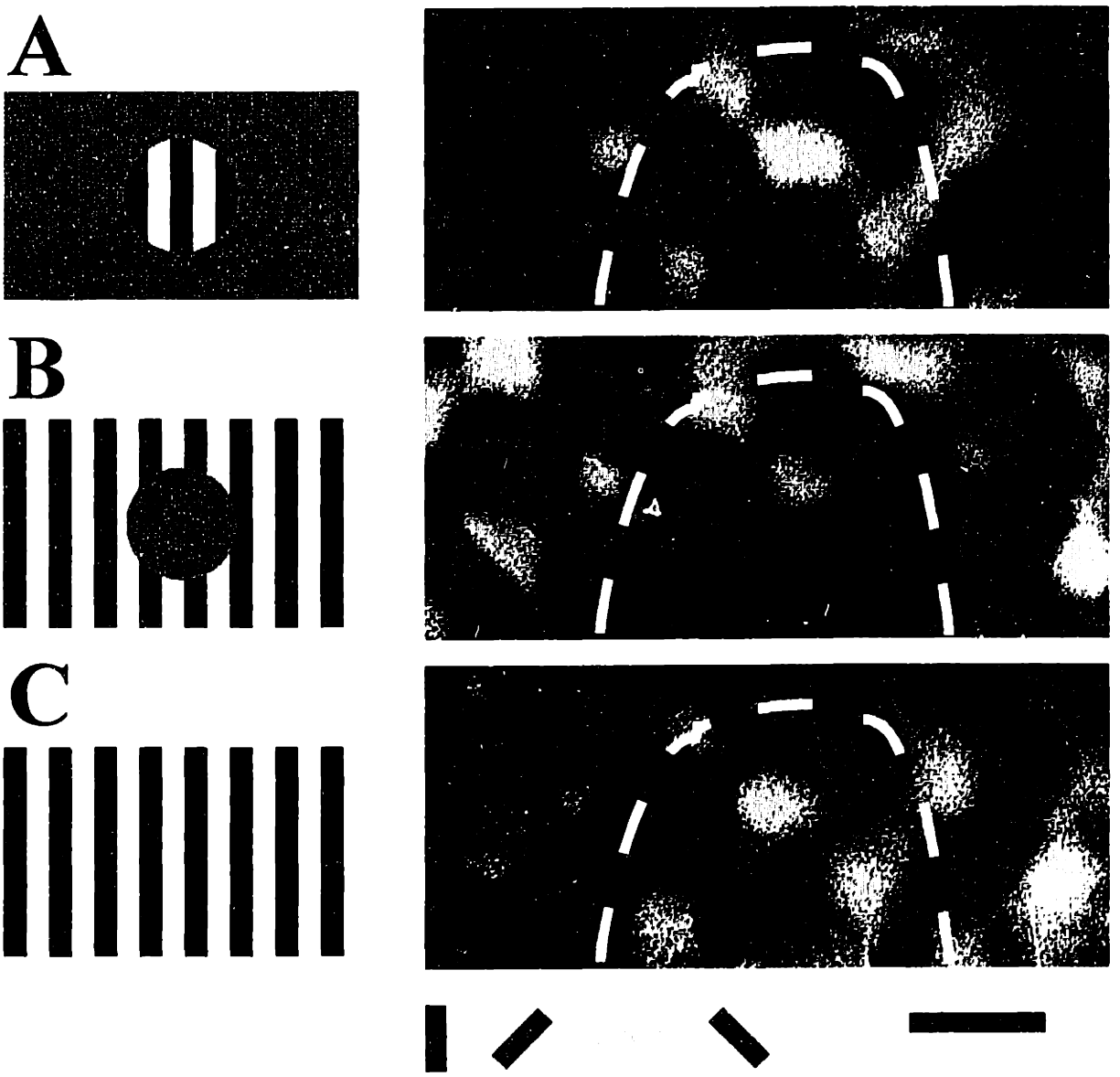

Figure 5.

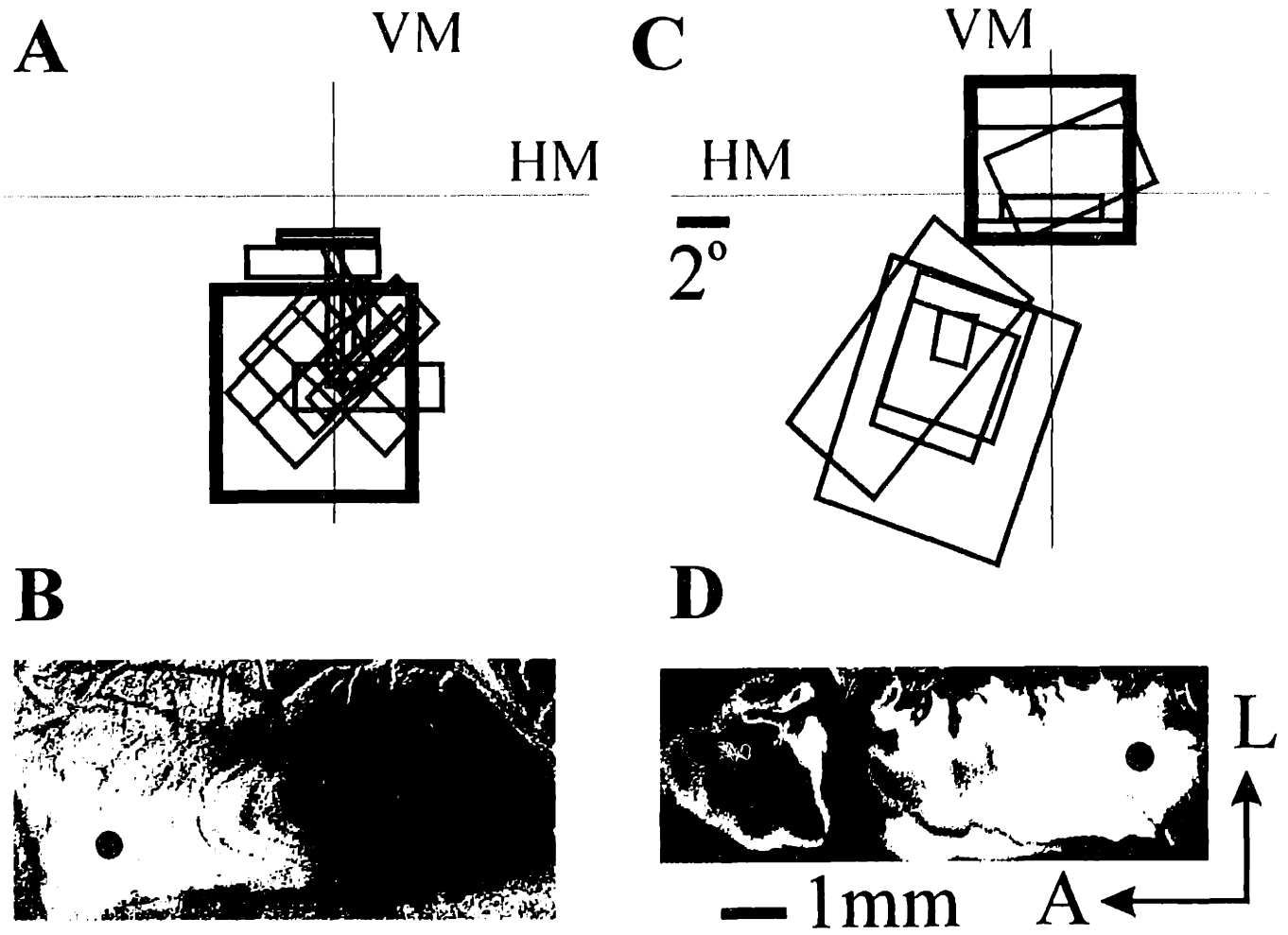

Figure 6.

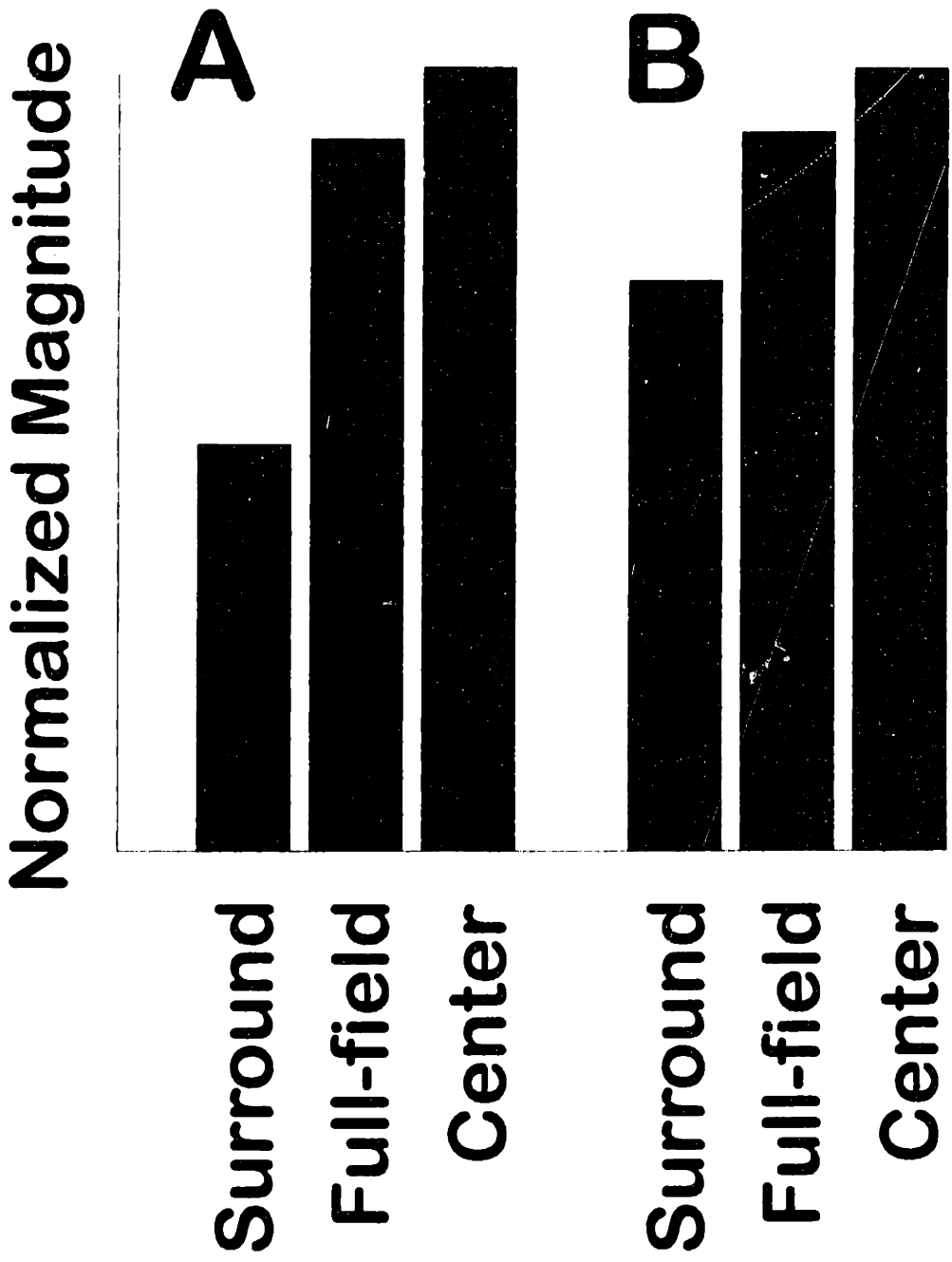
Normalized Magnitude
A
B
Surround
Full-field
Center
Surround
Full-field
Center

Figure 7.

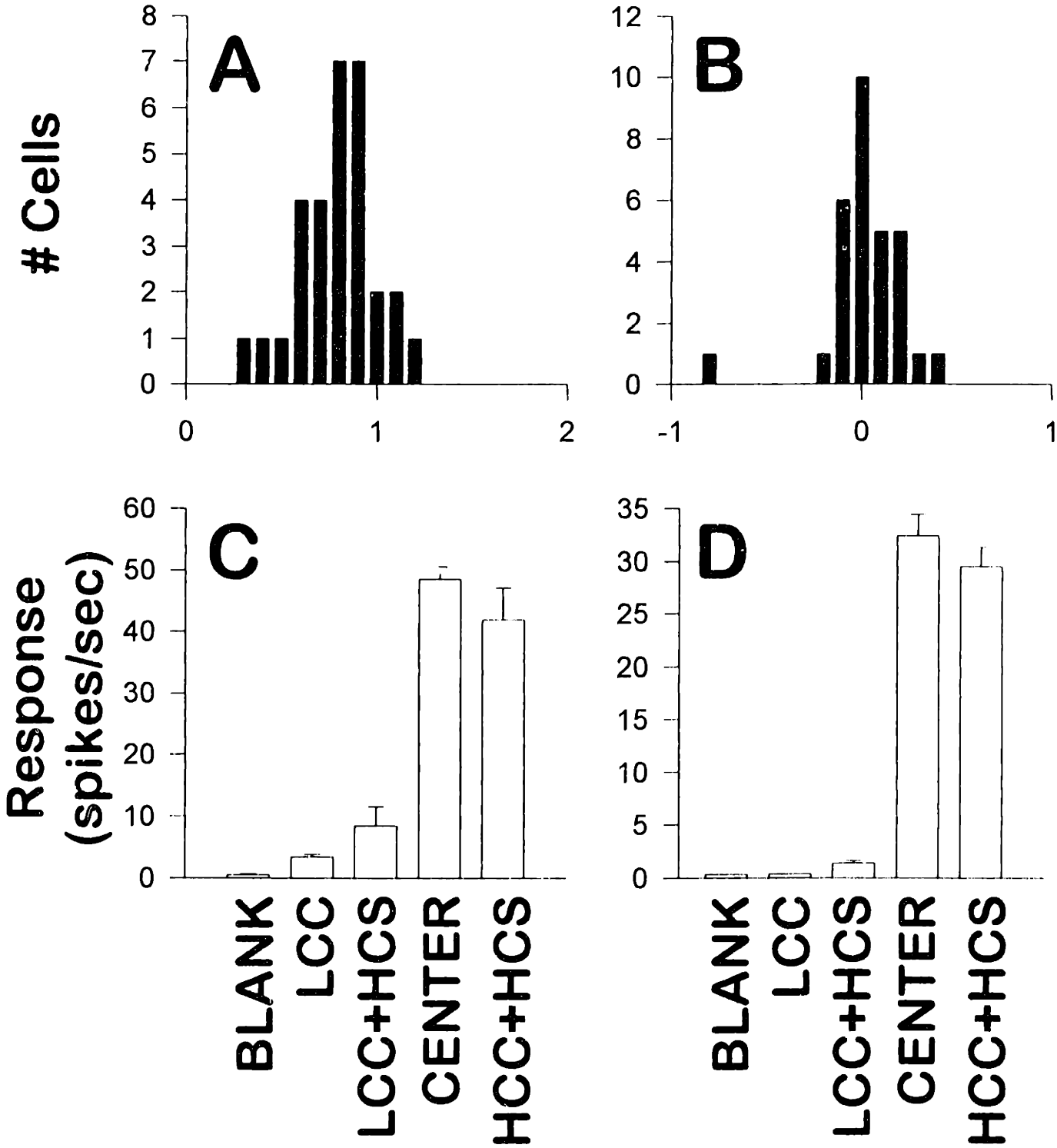
A
B
C
D
Cells
Response (spikes/sec)
BLANK
LCC
LCC+HCS
CENTER
HCC+HCS

Chapter 3

Discrete Latencies and Surround Responses: Subthreshold Effects in Visual Cortex Seen with Whole Cell Recording

ABSTRACT

Using *in vivo* whole-cell recording, we studied the post-synaptic potentials (PSPs) evoked by visual stimuli in primary visual cortex of anesthetized cats. High-contrast moving and stationary bars of optimal size and orientation generated patterns of excitatory (E) and inhibitory (I) PSPs consistent with simple and complex type receptive field organizations and with previous whole-cell studies. Compared to moving bar responses, stationary bars elicited responses that were 1) reliably present from trial to trial, 2) tightly time-locked to the stimulus onset, and 3) were repeatable in amplitude. In contrast, moving bar responses were 1) sometimes absent, 2) more variable in onset latency, and 3) often different in shape from trial to trial. PSPs measured with stationary bars often occurred at multiple, discrete latencies, occurring at a frequency of 7-10 Hz. Inputs from extra-classical receptive field regions evoked late latency PSPs only. We suggest that these discrete latencies are evidence of the brain's mechanism for recognizing different areas of the visual field as one object.

LIST OF COMMON ABBREVIATIONS

CRF	classical receptive field
ECRF	extra-classical receptive field
EPSP	excitatory post-synaptic potential
GABA	γ-aminobutyric acid
IPSP	inhibitory post-synaptic potential
PSP	post-synaptic potential
RMP	resting membrane potential

INTRODUCTION

The concept of a visual "receptive field", a discrete region of visual space over which stimuli are capable of eliciting spike discharges, has been a driving concept of neuroscience since its description in the optic nerve by Hartline (1938). Hubel and Wiesel (1962) first discovered the essential characteristics of receptive fields in primary visual cortex, and much work since then has assumed that the neuron is only interested in stimuli within its receptive field. A growing body of literature is asserting that this is not the case, however (see Allman et al, 1985, for review). While by definition, stimuli outside the classical receptive field (CRF) cannot cause spike discharges in that cell, Jones (1970) discovered that surround stimuli can change the degree of responsiveness to CRF stimuli. Since then, the surround effect of orientation (Blakemore and Tobin, 1972), frequency-modulation (Maffei and Fiorentini, 1976), direction (Fries et al, 1977; Nelson and Frost, 1978) and random dot fields (Hammond and McKay, 1981) have been documented. These effects are mostly suppressive, though can be excitatory under the right conditions. Toth (1995) demonstrates that the effect of surround stimuli can be biphasic; inhibitory if the center contains a high-contrast stimulus, but excitatory if the center contains a low contrast stimulus. Intracellular recording, and whole-cell recording in particular with its advantages of high signal-to-noise, are ideal techniques for viewing the modulatory effects of the surround, or "extra-classical" receptive field (ECRF), since subthreshold inputs that do not lead to spikes can readily be observed. Although *in vivo* sharp electrode (Ferster and Lindström, 1983; Ferster, 1986, 1987, 1988; Douglas et al, 1991) and whole-cell techniques (Ferster and Jagadeesh, 1992; Jagadeesh et al, 1993; Nelson et al, 1994; Pei et

al, 1994) have been applied previously to characterize classical visual responses, we apply the technique of intracellular recording for the first time to study the ECRF of cells, and to compare ECRF-elicited events with those elicited from classical stationary and moving stimuli. These results have appeared previously in abstract form (Toth et al, 1993).

METHODS

Animal preparation

Female cats aged 10 to 16 weeks were initially anesthetized with an i.m. injection of ketamine (15 mg/kg) and xylazine (1.5 mg/kg). A venous cannula was placed through which a 50/50 mixture of 5% dextrose and lactated Ringer's solution was continuously infused, and a tracheotomy performed to facilitate artificial respiration. Anesthesia was then maintained with isofluorane, 0.5-1.5% in 70:30 N_2O:O_2 for the remainder of the experiment, typically 36 to 48 hours. The animal's heart rate and EEG were monitored continuously to ensure adequate anesthesia. End-tidal CO_2 was maintained at 4%. Animals were paralyzed with gallamine triethiodide (10 mg/kg/hr). In some experiments, paralysis was discontinued for several hours to ensure the adequacy of our anesthesia monitoring. A craniotomy and durotomy were performed over area 17. To allow maximum recording stability, a bilateral thoracotomy was performed, and cerebrospinal fluid withdrawn from the cisternum magnum. Finally, a 3% agar mixture was used to seal the craniotomy after the pipette had been placed. Atropine sulfate and phenylephrine hydrochloride ophthalmic solutions were used to dilate the pupils and retract the nictitating membrane. Animals were fitted with appropriate contact lenses such that the back-projection of the retinal vasculature was in focus at the stimulus display monitor, typically 57 cm. Ambient lighting was kept low (~1 cd/m^2).

Whole-cell recording

Whole cell recording was accomplished using a variation of the blind technique popular in slice preparations (Blanton et al, 1989). Pipettes were drawn from filamented, borosilicate tubing (T100F-4, World Precision Instruments) using a Flaming-Brown type puller (model P-80/PC, Sutter Instruments). Our stock solution consisted of 120 mM potassium gluconate, 10 mM potassium chloride, 10 mM HEPES, 5 mM EGTA, and 2 mM magnesium sulfate. Immediately prior to filling, 3 mM ATP (adenosine triphosphate, Sigma) and 1 mM GTP (guanosine triphosphate, Sigma) was added to the solution. The final solution was checked with a freezing-point depression type osmometer (model 3MO, Advanced Instruments Corp.) and typically adjusted to 270 mOsm. Pipettes were coated with Sigmacote (Sigma Corp.) to increase hydrophobicity. Pipettes were attached to a 0.1 gain headstage held on a Leitz micromanipulator of 1μm vertical resolution. We used the Axoclamp-2A voltage-clamp amplifier in bridge mode to control current input and measure the voltage output. A ground wire of AgCl was inserted between dura and skull, where excess saline and cerebrospinal fluid provided a low resistance electrical connection with the recording site. Measured voltage was adjusted to zero extracellularly, and rechecked at the completion of each recording. We required each cell to show a stable resting membrane potential more negative than -45 mV for the duration of the testing.

Stimulus presentation and data collection

Programs for generating moving and stationary bar stimuli were written in C (Microsoft v5.1) on an IBM '486 computer, and displayed at 640x480x16 resolution on a Sony

Trinitron 14" monitor using a 4 MB Sgt. Pepper+ board (Number Nine Corp.). Bars were anti-aliased both spatially and temporally to provide exceptionally smooth edges and motion for any values of orientation and temporal frequency. Data collection was performed on a second '486 computer using a 200 MHz A/D converter (AT-MIO-16-F-5, National Instruments) with software written using Quick Basic (v. 4.5, Microsoft Corp.) and LabWindows (National Instruments) libraries. Data collection was synchronized to the frame rate of the display, and tested by collecting the output of a photodiode as data, to ensure that stimulus on and off times were repeatable to better than 0.5 msec. within trials. Voltage and current traces were also recorded digitally in real time onto a video tape (Neurocorder DR886, NeuroData Inst. Corp.) for later re-collection and analysis. Stimuli were presented monocularly to the dominant eye.

RESULTS

The whole cell recording configuration proved quite difficult to achieve *in vivo*, but once achieved proved quite stable, recordings lasting between 20 minutes and 2 hours. Loss of stable recordings either occurred due to cell death, presumably from injury due to motion, or from electrode clogging, evidenced by a sudden rise in input resistance. Data in this paper are drawn from a population of 19 cells recorded in 9 animals. All recordings presented here represent cells resting at normal membrane potentials, without application of current through the whole-cell pipette.

Moving bar responses

Fig. 1 shows the response of a simple cell to five sweeps of an optimal bar of light moving through the receptive field in the preferred direction, and five sweeps in the reverse direction. The bar was under computer control and synchronized to the data collection, so all trials represent exactly identical input conditions. The cell shows multiple subfields, strong orientation selectivity (data not shown), and mild direction selectivity (direction index $= \frac{\sum preferred - \sum reverse}{\sum preferred + \sum reverse} = 15\%$). Notable is the pattern of input integration that can be observed in these recordings. Each spiking response rides on the crest of several, smaller PSPs, thus showing that the response to a moving bar results from a summation of several smaller inputs. Although the general shape of the response is identical from trial to trial, in detail the shape of the summed responses are very different. The result of this "random" summation is that spike latencies and frequencies are different from trial to trial

under the same input conditions.

IPSPs, though likely present, are difficult to observe directly in this response for two reasons. First, the reversal potential for GABA-mediated currents ($E_{GABA} \approx$ -82 mV) is relatively close to the measured resting membrane potential, -60 mV for this cell, thus providing a low electrochemical gradient. Second, EPSPs and IPSPs are being generated which overlap in time, thus preventing their clean separation in the recording trace.

Another observation from this recording is that the reverse direction response is not a mirror image of the preferred direction response, as would be expected if all inputs sum linearly. Nonlinear, temporal characteristics of the PSPs play an important role in shaping the response profile.

Finally, notice that the summed excitatory potential underlying the spikes is broader than the spiking region itself. Since a cell's receptive field is defined by its spiking response, the presence of these regions raise the question whether the size of the receptive field might change depending on the amount of facilitation or suppression present. Response thresholding may play an important role in determining the limits of a cell's receptive field.

Stationary bar responses

Figure 2 shows responses to a stationary bar flashed in an OFF subfield of the simple cell shown in figure 1. Timing of the 500 msec flash is indicated by the dark line. At this

receptive field position, this cell shows a large net excitatory response to light offset, and a smaller, subthreshold excitatory response to light onset. Unlike the moving bar, the earliest response to the flashed bar is consistent from trial to trial in latency and in amplitude. Later responses are more variable. Figure 3 shows a comparison of the earliest responses in figures 1 and 2 superimposed and at a higher time scale. Stationary bar response latencies fall within 5-10 msec of each other, and the earliest PSPs are within 2 mV amplitude from base to peak between trials. The early latency of the moving bar response, on the other hand, is spread out over 40-60 msec and is not of consistent amplitude. Figure 4 shows a different cell responding to a stationary bar flashed over the receptive field. In this case, the response is entirely subthreshold. The OFF IPSPs observed in this figure, similar to stationary bar evoked EPSPs, also show a consistency of amplitude and latency.

Evidence for discrete latencies

When we compared the timing of stationary responses at different receptive field positions, an interesting pattern emerged. Figure 5 shows the response of a simple cell to moving (fig. 5A) and flashed (fig. 5B, C) stimuli. The moving bar response reveals regions of predominant excitation and inhibition. Stationary stimuli evoked a variety of responses. The CRF, measured extracellularly in cell-attached mode, extended from -4° to +4°, and contained two subfields. Nearly all positions tested contained some visually-evoked PSPs, even though the extreme positions were outside the classical receptive field.

A few positions showed sustained ON responses after a very long latency, similar to what might be expected from a phasic LGN input.

The unexpected finding is that the large majority of visually driven PSPs began in synchrony, at one out of a small number of discrete latencies to the visual stimulus. For the cell in figure 5, there are three discernible latencies to onset responses and four to offset responses. The first latency occurs between 70 and 120 msec after the visual stimulus, and subsequent latencies occur roughly at multiples of these times. Also surprising, is that the latencies for ON and OFF responses are not necessarily equal. In figure 5B, the earliest onset latency is 111 msec while the earliest offset latency is 76 msec. The average time between onset latencies is 107 msec, (9.3 Hz) and between offset latencies 124 msec (8.1 Hz).

Finally, it is worth noting that multiple components of the subthreshold response are present at any one position. For example, the response at -2° has strong EPSPs at all three of the OFF latencies illustrated in fig. B. The response at +6°, outside the CRF, shows a small response at the second and third ON latencies, but no response (except in one trial) at the first ON latency.

Invariance of latencies with stimulus position

In three cells, two simple cells and one complex cell, we tested flashed bar responses several degrees outside the classical receptive field. All three cells showed the

phenomenon illustrated in fig. 6. The receptive field in this case is shown by the moving bar response (figure 6A) and the extracellular, hand-plotted position shown by the dark line above that response. Stationary stimuli were flashed intracellularly at the positions indicated by the rectangles at the bottom of the figure. (Since the bar always swept a constant path under computer control, time and space are related and shown together on the same axis.) The complete set of individual responses, ON and OFF to each stationary stimulus is shown in figure 6B. Again, multiple discrete latencies are seen in the response. The first two are indicated by vertical shaded lines. The earliest latency is seen only in the regions underlying the CRF, and not in regions outside it. As in figure 5, the timing of the latencies is independent of receptive field position, however latencies of ON and OFF responses are different. A plot of the subthreshold receptive field for this cell is constructed in fig. 7. ECRF responses are of comparable magnitudes to CRF responses, and mainly occur at the longer latencies. These data suggest that a cell's spiking response is strongly influenced by the temporal characteristics of its inputs.

DISCUSSION

There are two main conclusions of this study. First, subthreshold responses to stationary bars, though generally of a smaller magnitude, are more reproducible in successive trials of identical stimuli, more tightly time locked to the stimulus, and of a more consistent amplitude than subthreshold responses to moving bars. Second, responses to stationary bars occur at multiple discrete latencies. The latencies vary with the phase of the response (onset or offset) but not with stimulus position. The earliest latency of subthreshold response corresponds with the CRF, but later latencies occur robustly with ECRF stimulation. Interestingly, these multiple latencies have been observed previously (Pei et al, 1994) though it seems fluctuations in the membrane potential prevent them from commenting on the issues of discreteness of latencies. It is also possible that some types of cells show a differing organization of latencies, though we have observed multiple, discrete latencies in both simple cells and a complex cell. To date, the low success ratio of the *in vivo* whole-cell recording technique has precludes large population studies. Another drawback of the whole-cell technique is that it is difficult to know from which cortical layer cells are recorded. A technique has been proposed for locating layer boundaries based on extracellular field potentials (Ferster and Lindström, 1983), however it requires the placement of stimulating electrodes in the LGN and superior colliculus, and the careful extracellular recording of cell types along the penetration.

Artifact considerations

Oscillations at α frequencies (8-13 Hz) can be generated by many different brain mechanisms, so we considered whether the roughly 10 Hz synchronizations we observed could be due to an extrinsic source. Two arguments seem to suggest that the synchronization is in fact stimulus dependent and resides in the cortex. First, we observed the exact frequency of oscillation change over a period of two seconds between the ON and OFF responses. Differing amounts of time between stimuli presentations did not affect the repeatability of the latencies, suggesting that they were, in fact, purely stimulus driven. Second, variations in these rhythms were not seen over the time required to collect the responses, which in the case of the cell in figure 6, was approximately 15 minutes, suggesting that factors such as depth of anesthesia were not directly controlling these responses.

Discrete latencies - how do you get them and what are they good for?

The immediate question, having demonstrated the long latency surround inputs, is where do they come from? A first thought might be that the latencies represent mono-, di- and tri-synaptic inputs. However, this is unlikely. Ferster and Lindström (1983) showed that di- and tri-synaptic latencies arising from electrical stimulation of the LGN are capable of arriving within 10 ms of each other. Since the entire LGN projection to the cortex is excitatory, IPSPs must be at least di-synaptic, yet visually evoked IPSPs also arrive with 70-100 msec latency. Since higher visual areas also receive direct thalamic input in the cat, and the inter-areal latency is also on the order of 10 ms, it is unlikely that the second latency represents a di-synaptic response of a higher area. More likely is the hypothesis

that a flashed stimulus sets up a low frequency oscillation in the cortex. Chagnac-Amitai and Connors (1989) have shown in the neocortical slice preparation that a cortical circuit consisting of middle-layer pyramidal cells driving both excitatory and inhibitory targets can oscillate with a frequency that depends on stimulation intensity. If such a circuit is at work in area 17, it is possible that synchronous excitation and inhibition is generated by the activation of an intrinsic oscillator neuron by the stimulus, and that the time course of the resulting inhibitory PSPs controls the timing of the next EPSP. This theory would also explain the differing values of latency to ON and OFF responses; since the background was black instead of neutral gray, there is a sustained contrast following an light onset, but no such contrast following light offset - the equivalent of less stimulation intensity. Such a mechanism might also be ideal for use in solving the feature binding problem, since one could imagine that stimuli arising from the same "object" could set up similar oscillatory patterns independently across cortex, and that the unique pattern of oscillations thus created could be used to "bind" those responses for the use of a higher visual area. Such arguments are identical to those that have been recently proposed in the case of 30 to 60 Hz cortical oscillations (Gray et al, 1989; König et al, 1995; reviewed by Singer, 1993).

Surround (ECRF) influence on response

We have demonstrated that stimuli inside the CRF generate the earliest latency response, whereas stimuli in the ECRF are capable of generating strong responses at the second and higher order latencies. A direct prediction of this study is that effects of iso-orientation bar stimuli in the surround are not capable of affecting the earliest response of a cell.

ECRF responses may arrive from lateral inputs within area 17, though it is also possible that the response represents a feedback loop from area 18, or even from LGN (Sillito et al, 1994).

In conclusion, we have shown that the ECRF is directly observable using both moving and stationary bars. Flashed stimuli evoke PSPs at multiple discrete latencies, near 10 Hz, the exact frequency of which may depend on specific stimulus features. The earliest latency is generated only by stimuli within the CRF. We suggest that the later latencies represent information arriving via long range lateral connectivity from disparate receptive field regions, the spatial characteristics of which have been explored in chapter 2 of this thesis.

REFERENCES

Allman J, Miezen F, McGuiness E (1985) Stimulus specific responses from beyond the classical receptive field: neurophysiological mechanisms for local-global comparisons in visual neurons. *Ann. Rev. Neurosci.* 8:407-430.

Blakemore C, Tobin EA, (1972) Lateral inhibition between orientation detectors in the cat's visual cortex. *Exp. Br. Res.* 15:439-440.

Blanton MG, Loturco JJ, Kriegstein AR (1989) Whole cell recording from neurons in slices of reptilian and mammalian cerebral cortex. *J. Neurosci. Meth.* 30:203-210.

Chagnac-Amitai Y, Connors BW (1989) Synchronized excitation and inhibition driven by intrinsically bursting neurons in neocortex. *J. Neurophysiol.* 62(5):1149-1162.

Douglas RJ, Martin KAC, Whitteridge D (1991) An intracellular analysis of the visual responses of neurones in cat visual cortex. *J. Physiol.* 440,659-696.

Fernandez JM, Fox AP, Krasne S (1984) Membrane patches and whole-cell membranes: a comparison of electrical properties in rat clonal pituitary (GH_3) cells. *J. Physiol.* 356:565-585.

Ferster D (1988) Spatially opponent excitation and inhibition in simple cells of the cat visual cortex. *J. Neurosci.* 8(4):1172-1180.

Ferster D (1987) Origin of orientation-selective EPSPs in simple cells of cat visual cortex. *J. Neurosci.* 7(6):1780-1791.

Ferster D (1986) Orientation selectivity of synaptic potentials in neurons of cat primary visual cortex *J. Neurosci.* 6(5):1284-1301.

Ferster D, Jagadeesh B (1992) EPSP-IPSP interactions in cat visual cortex studied with *in vivo* whole-cell patch recording. *J. Neurosci.* 12(4):1262-1274.

Ferster D, Lindström S (1983) An intracellular analysis of geniculo-cortical connectivity in area 17 of the cat. *J. Physiol.* 342:181-215.

Fries W, Albus K, Creutzfeldt OD (1977) Effects of interacting visual patterns on single cell responses in cat's striate cortex. *Vis. Res.* 17:1001-1008.

Gray CM, König P, Engel AK, Singer W (1989) Oscillatory responses in cat visual cortex exhibit inter-columnar synchronization which reflects global stimulus properties. *Nature* 338:334-337.

Gulyás B, Orban GA, Duysens J, Maes H (1987) The suppressive influence of moving textured backgrounds on responses of cat striate neurons to moving bars. *J. Neurophysiol.* 57:1767-1791.

Hammond P, McKay DM (1975) Differential responses of cat visual cortical cells to textured stimuli. *Exp. Br. Res.* 22:427-430.

Hammond P, McKay DM (1977) Differential responsiveness of simple and complex cells in cat striate cortex to visual texture. *Exp. Br. Res.* 30:275-296.

Hammond P, McKay DM (1981) Modulatory influences of moving textured backgrounds on responsiveness of simple cells in feline striate cortex. *J. Physiol.* 319:431-442.

Hartline HK (1938) The response of single optic nerve fibers of the vertebrate eye to illumination of the retina. *Am. J. Physiol.* 121:400-415.

Hubel DH, Wiesel TN (1962) Receptive fields, binocular interaction and functional architecture in the cat's visual cortex. *J. Physiol.* 160:106-154.

Jagadeesh B, Wheat HS, Ferster D (1993) Linearity of summation of synaptic potentials underlying direction selectivity in simple cells of the cat visual cortex. *Science* 262:1901-1904.

Jagadeesh B, Gray CM, Ferster D (1992) Visually evoked oscillations of membrane potential in cells of cat visual cortex. *Science* 257:552-554.

Jones BH (1970) Responses of single neurons in cat visual cortex to a simple and more complex stimulus. *Am. J. Physiol.* 218:1102-1107.

König P, Engel AK, Singer W (1995) Relation between oscillatory activity and long-range synchronization in cat visual cortex. *Proc. Nat. Acad. Sci. USA* 92:290-294.

Maffei L, and Fiorentini A (1976) The unresponsive regions of visual cortical receptive fields. *Vis. Res.* 16:1131-1139.

Nelson JI, Frost BJ (1978) Orientation-selective inhibition from beyond the classic visual receptive field. *Brain Res.* 139:359-365.

Nelson S, Toth L, Sheth B, Sur M (1994) Orientation selectivity of cortical neurons during intracellular blockade of inhibition. *Science* 265:774-7.

Palmer LA, Davis TL (1981) Comparison of responses to moving and stationary stimuli in cat striate cortex. *J. Neurophys.* 46(2):277-295

Pei X, Vidyasagar TR, Volgushev M, Creutzfeldt OD (1994) Receptive field analysis and orientation selectivity of postsynaptic potentials of simple cells in cat visual cortex. *J. Neurosci.* 14(11):7130-7140.

Sillito AM, Jones HE, Gerstein GL, West DC (1994) Feature-linked synchronization of thalamic relay cell firing induced by feedback from the visual cortex. *Nature* 369:479-482.

Singer W (1993) Synchronization of cortical activity and its putative role in information processing and learning. *Ann. Rev. Physiol.* 55:349-374.

Squatrito S, Trotter Y, Poggio GF (1990) Influences of uniform and textured backgrounds on the impulse activity of neurons in area V1 of the alert macaque. *Br. Res.* 536.261-270.

Staley KJ, Otis TS, Mody I (1992) Membrane properties of dentate gyrus granule cells; comparison of sharp microelectrode and whole-cell recordings. *J. Neurophys.* 67(5):1346-58.

Toth LJ, Nelson SB, Rao SC, Sur M (1993) Synaptic potentials in visual cortical neurons: temporal variability and spatial structure. *Soc. Neurosci. Abstr.* 19:333. (139.8)

Toth LJ (1995) Lateral connectivity in visual cortex imaged through intrinsic signals: a substrate for extra-classical receptive field influences and psychophysical "filling-in". Chapter 2, Ph.D. Thesis in Brain and Cognitive Sciences, M.I.T., Cambridge, MA.

FIGURE LEGENDS

Fig. 1. Left: Intracellularly recorded responses to a bar of light of optimal size and velocity moving across the receptive field in the preferred direction. Resting membrane potential is -60 mV. **Right:** Responses under identical conditions to a bar moving in the reverse direction. Responses show evidence for PSP summation, random variability, non-linear summation (since the reverse direction response does not mirror the preferred direction response), and thresholding phenomena.

Fig. 2. Five responses of the same cell (fig 1) to identical flashes of a stationary bar of light in the OFF region of the receptive field. Resting membrane potential is -60 mV. The duration of the flash, 500 msec, is indicated by the heavy line. Although the sustained OFF response is the largest component of the response at this position, also present is a small ON response that does not elicit spiking. Vertical lines emphasize the timing of the earliest component of the response. Notice that, in contrast to the moving bar response, an EPSP of approximately constant amplitude is elicited reliably by this stimulus (just right of the first vertical line).

Fig 3. Moving (left side) and stationary (right side) responses of figs. 1 and 2 shown superimposed, and at a much higher time scale. Moving bar responses are the earliest response to preferred (top left) and reverse (bottom left) directions of motion. Stationary responses are to light onset (top right) and offset (bottom right). Vertical scales differ,

(see figs 1 & 2), though the relative offset in membrane potentials between multiple trials is preserved.

Fig 4. Five stationary bar responses from a second simple cell showing inhibitory OFF responses. The shaded vertical line emphasizes the time of the clear OFF IPSP which is present in all five trials, though small relative to the membrane voltage fluctuations. RMP is -48 mV.

Fig. 5. A) Five superimposed responses to a moving bar stimulus. One excitatory and one inhibitory subregion are clearly evident. Subregions were subsequently mapped with stationary stimuli. The region of the moving bar response corresponding to the region from which the stationary responses in part B were derived is shown by the top black line. The positions indicated by the lower black lines indicate positions of an ON subfield (-2°) an OFF subfield (+2°) and a subfield outside the CRF (+6°) shown in part C. The bar, 1°x15°, was moved at a velocity of 8°/sec for 3 sec, thus the total trace represents 25° of the visual field. The dark bar above the response indicates receptive field position measured extracellularly. **B)** A stationary bar was flashed seven times in each of 13 positions covering the range indicated by the first black bar in part A. The duration of the flash is indicated by the grey bar. Each of the 13 superimposed traces represents the average response at a given position. Notice that although all positions are superimposed in this figure, the excitatory responses peak at latencies which are relatively invariant. The arrows point to ON responses at latencies of 76, 228 and 371 msec, and OFF responses at latencies of 111, 191, 295 and 427 msec. **C)** Representative stationary responses in an

ON subfield (-2°), OFF subfield (+2°), and outside the CRF (+6°) are shown. (OFF subfields at +1° and +3° did show suprathreshold activity to flashed stimuli.) Each trace is the superposition of seven repetitions at a single stimulus position. The position of the stimulus (in degrees) is indicated by the number next to each trace, and by the lower stimulus line in fig. A. Duration of the flash is indicated by the gray bar. The latencies are invariant, and remarkably similar even outside the CRF. Notice that the first excitatory latency is absent in the +6° response. In general, we find that the short latency components disappear with increasing distance from the receptive field center. RMP = -55 mV.

Fig 6. A) Averaged response of a complex cell to five presentations of a moving bar of optimal dimensions. The spiking receptive field, measured extracellularly, is indicated by the black bar above the response. Since with each repetition the bar sweeps out identical regions of space at equivalent points in time, the time axis is doubly labeled with a location corresponding to the position of the bar relative to the receptive field at that time. The bar moved at 8° per second, for 3 seconds, about the receptive field center. This response region corresponds with the minimal response field for this cell found by hand plotting. **B)** Stationary bars (1.5° by 15°) were flashed at the positions indicated by the black rectangles (in part A, lower). The ON and OFF components of 10 responses at each position are shown. Faint shaded lines indicate the first two common latencies across responses. The solid line indicates responses within the CRF position. Notice that although the receptive field extends only from -3° to +1°, reliable visually-evoked

potentials can be seen throughout the entire tested range. The shortest latency responses, occurring at positions -3° to +1°, correspond with the CRF, and are approximately 97 ms in each case. Stimulus-locked responses of longer latencies are largely invariant with stimulus position. In this case, the secondary latencies occur at 195 ms and 300 ms for the ON responses and 210 ms and 330 ms for the OFF responses. RMP = -57 mV.

Fig. 7 Receptive field plot of the cell shown in fig. 6 calculated by summing subthreshold responses to the offset of a stationary bar of light (of optimal orientation and velocity and high contrast). The "classical" receptive field, defined by the cell's spiking response to a moving bar, is indicated by the dark line. To generate this graph, the averaged response to 10 stimulus presentations was integrated over 60 msec time periods. The earliest response, averaged from 117 to 177 msec, is plotted in square symbols. Later responses at 212 to 272 msec and 336 to 396 msec are averaged and plotted in triangular symbols. These time periods were chosen to include the majority of the cell's significant responses. The baseline response of the cell over the same time periods is plotted as the first and last points on the graph. Notice that although the position of the early component agrees well with the classical receptive field, there are significant responses, mostly late, that occur well outside that region.

Figure 1.

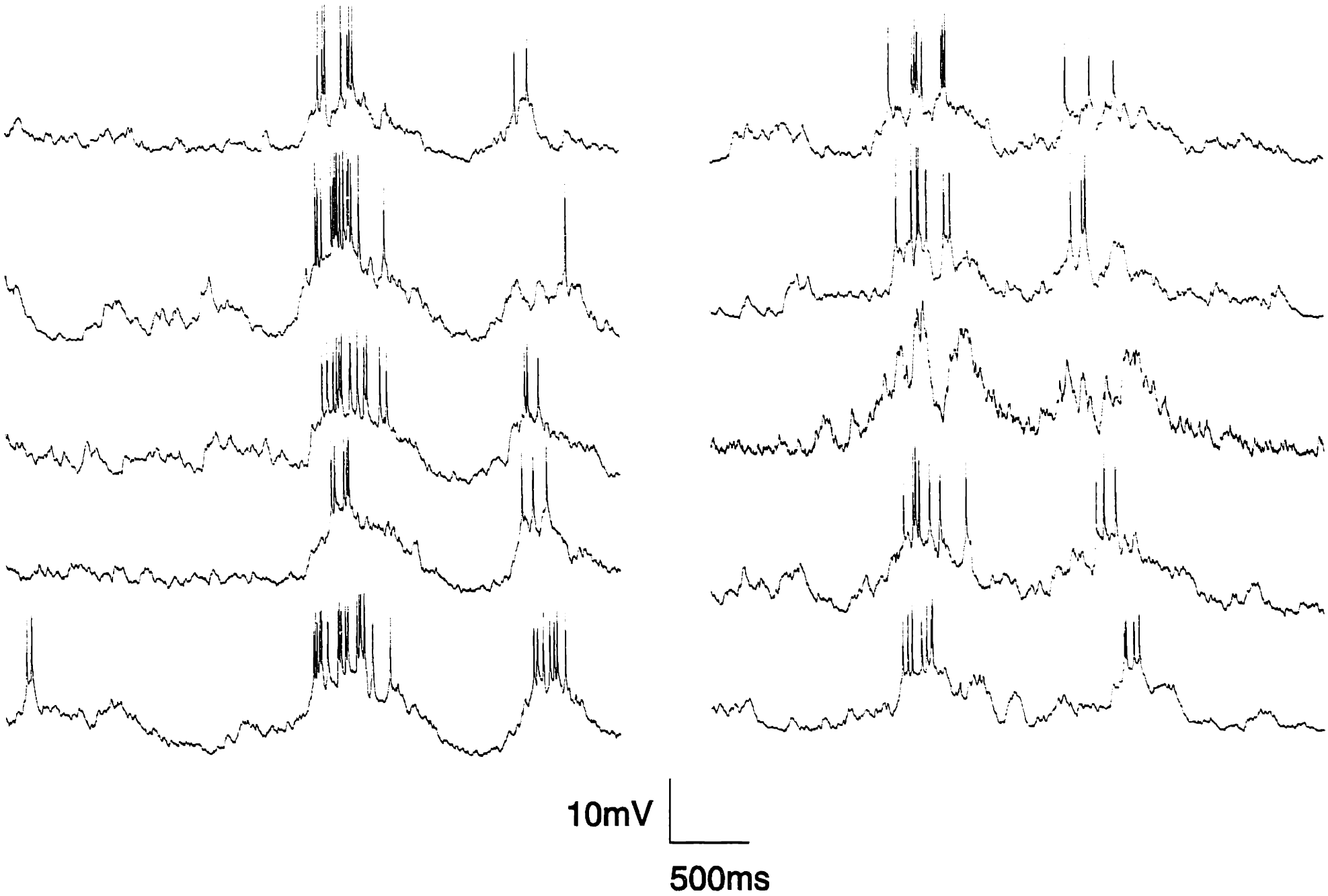

Figure 2.

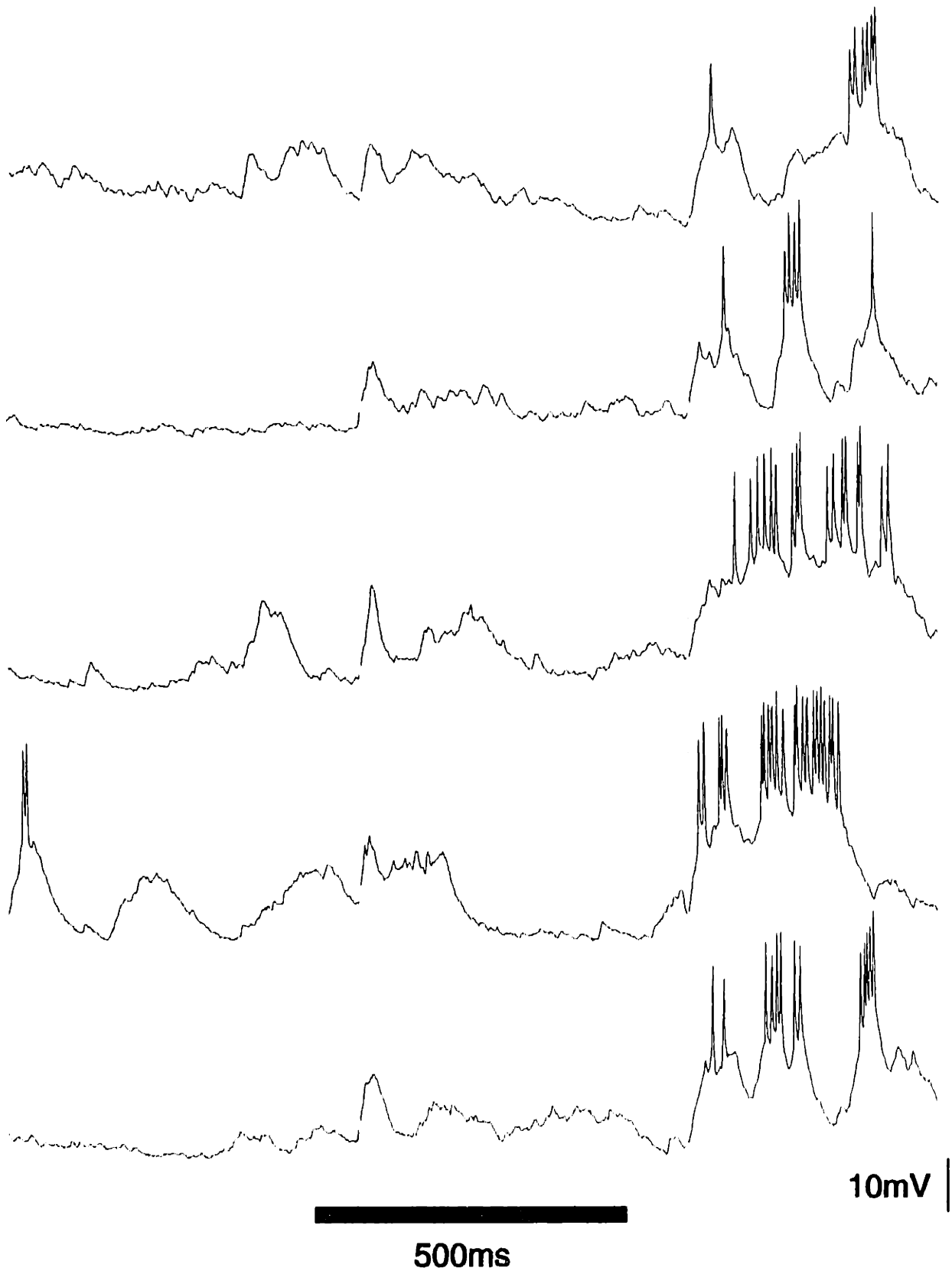

Figure 3.

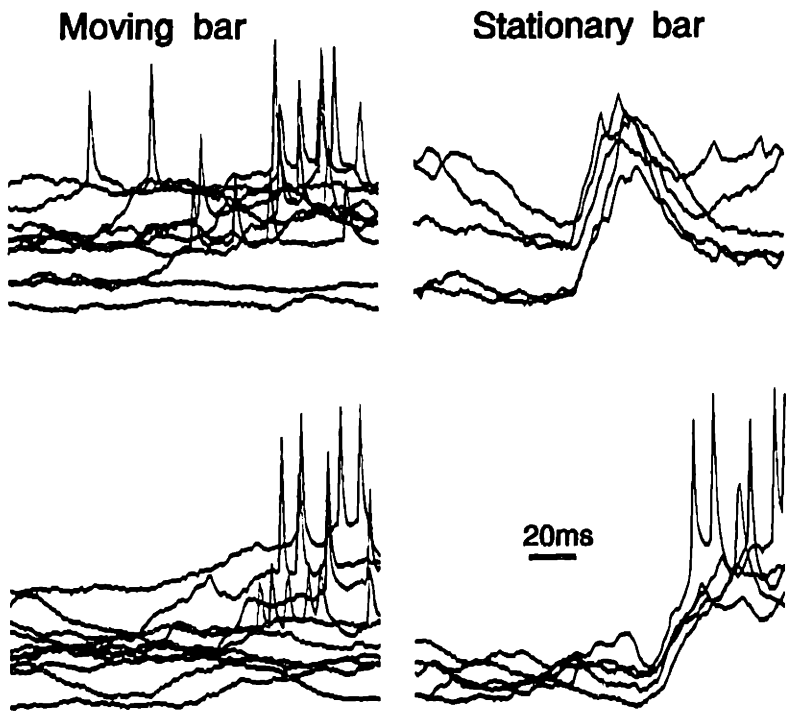

Figure 4.

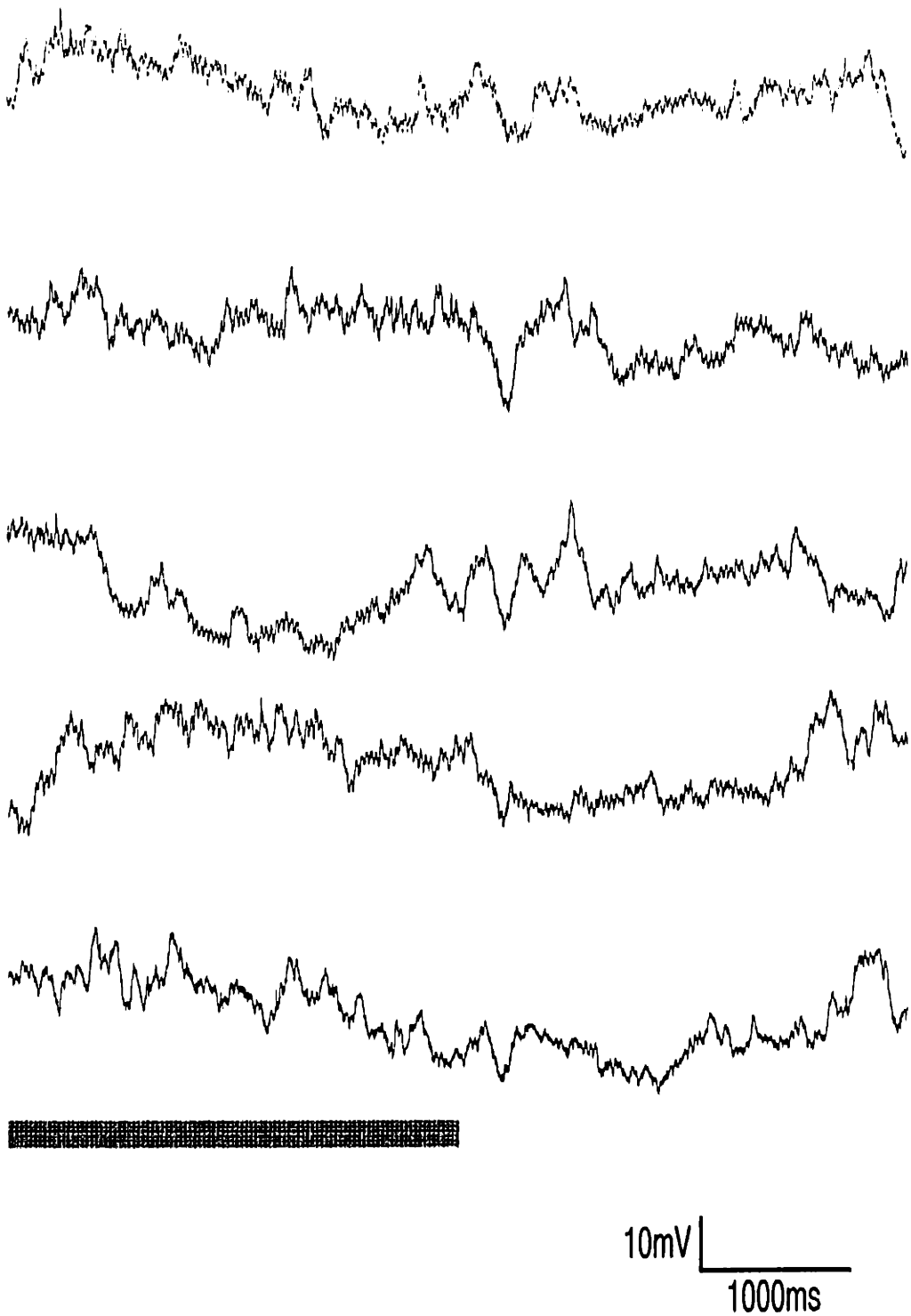

Figure 5.

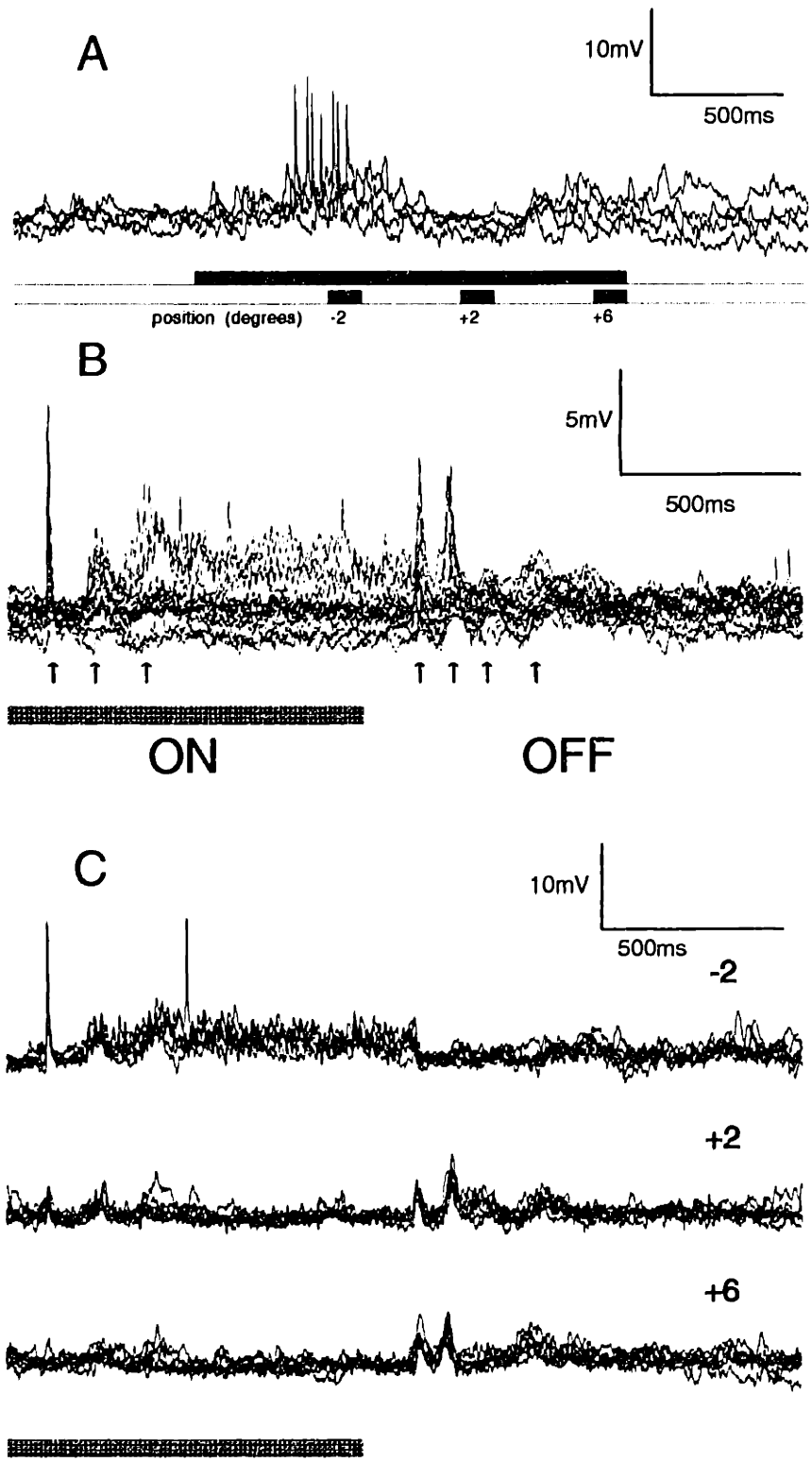
A
10mV
500ms
position (degrees)
-2
+2
+6
B
5mV
500ms
ON
OFF
C
10mV
500ms
-2
+2
+6

Figure 6.

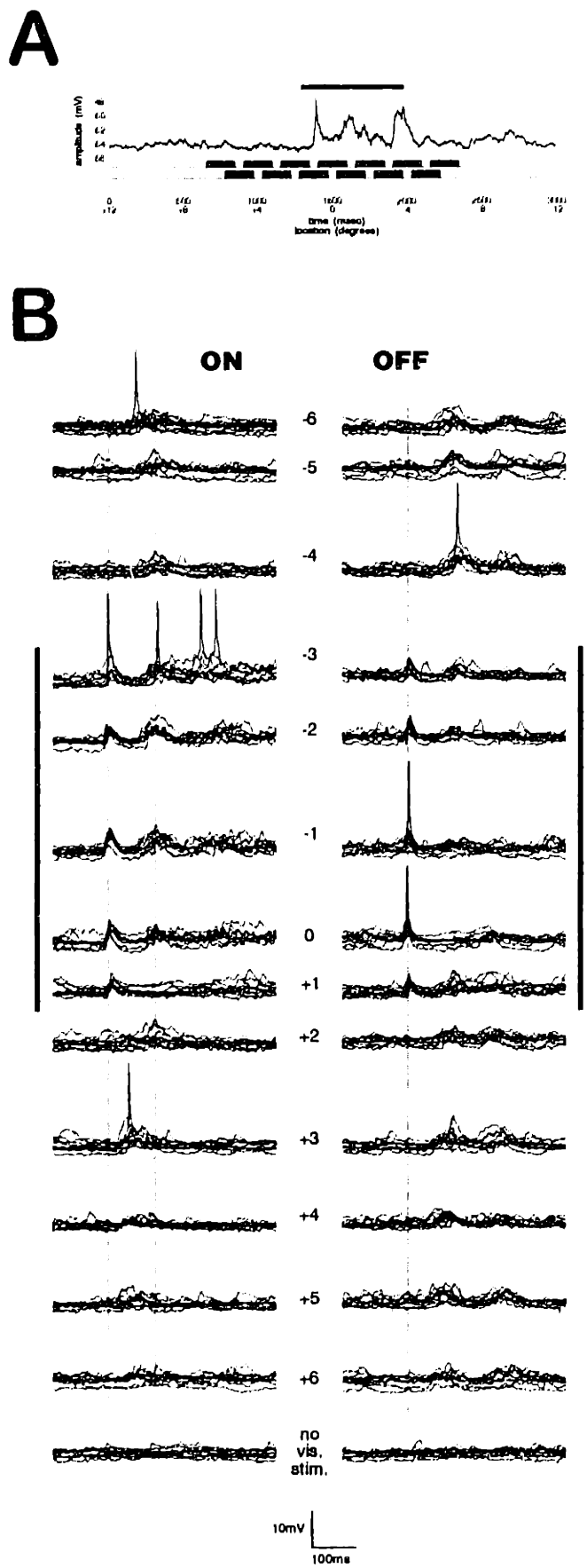

Figure 7.

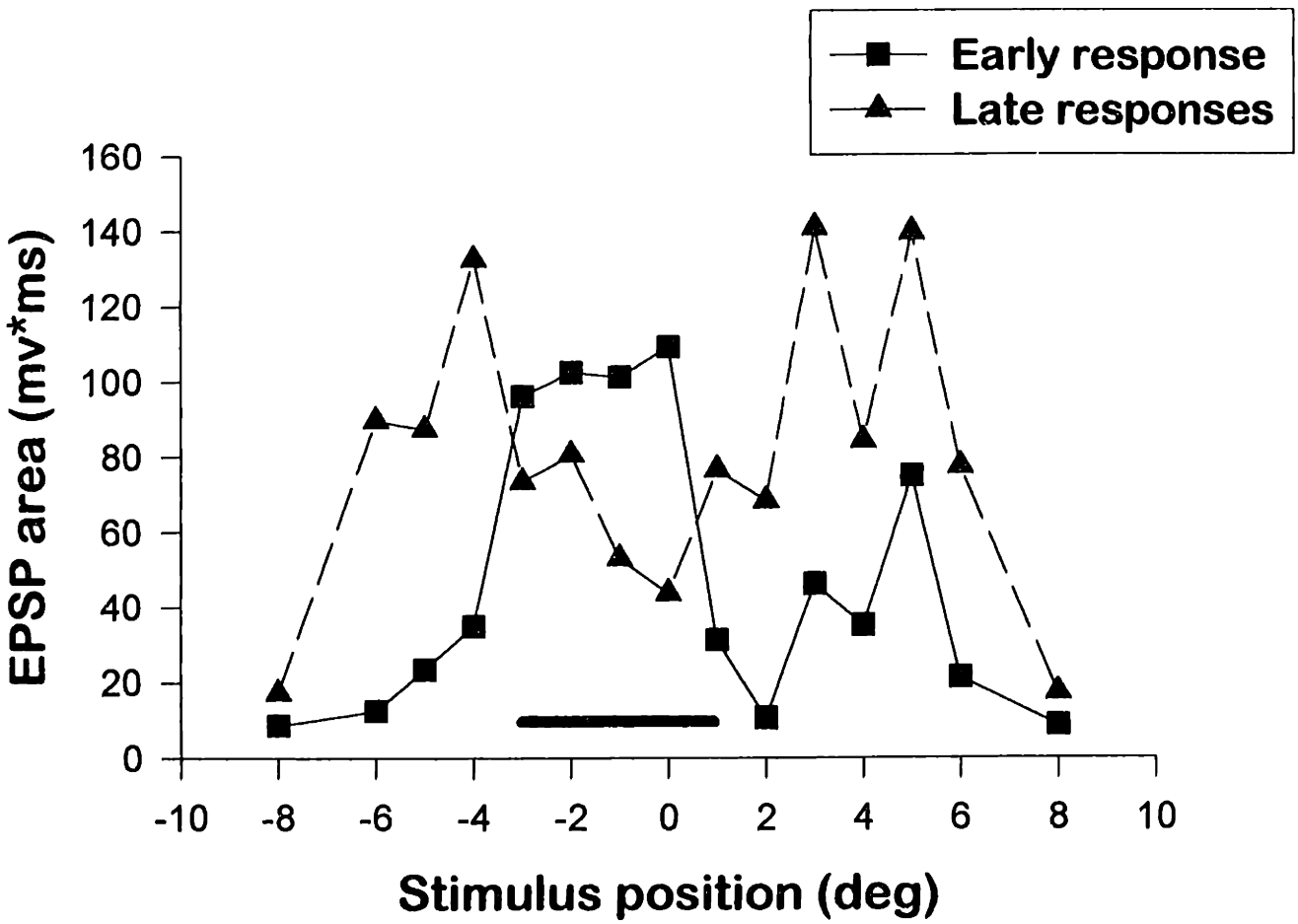
Early response
Late responses
EPSP area (mv*ms)
160
140
120
100
80
60
40
20
0
-10
-8
-6
-4
-2
0
2
4
6
8
10
Stimulus position (deg)

Chapter 4

Altering Cortical Inhibition Disrupts Intrinsic Signal Orientation Maps

ABSTRACT

In the visual system of the cat, layouts of the cortical maps of various physiological properties converge to a stable state within the first few months of life, and thereafter remain largely unchanged. Some properties, such as ocular dominance and orientation selectivity can be altered by appropriate manipulations during the so-called "critical period", however no manipulation has been found that changes the spatial layout of these cortical maps in the adult cortex. By iontophoresis of compounds that act on GABA receptors, we succeeded in altering the map of orientation preference for a region approximately 1.5 mm around the injection site. Bicuculline, a $GABA_A$ antagonist, increased the spatial extent of activity to a stimulus of iso-orientation to the injection region, shifting the orientation vectors in a given cortical region by up to 70°, towards that of the injection site. Iontophoresis of GABA or muscimol (a $GABA_A$ agonist) caused an opposite effect, a shift towards the orthogonal orientation of as much as 50°. These novel effects demonstrate that the map of orientation preference in adult cortex is malleable, and is influenced by the inhibitory circuitry. Furthermore, the intracortical inhibitory circuitry does not show any preferential physiological connectivity across orientation columns, and thus may serve mainly to control the spread of cortical excitation and the range of influence of a cortical cell.

INTRODUCTION

GABA, a ubiquitous neurotransmitter in the cerebral cortex, is of primary importance in providing fast inhibitory influences onto glutamatergic cells. In primary visual cortex, GABA has been demonstrated to affect the organization of several physiological response properties, such as ON and OFF receptive field subregions (Sillito, 1975; Wolf et al, 1986; Rose and Blakemore, 1974), direction selective responses (Rose and Blakemore, 1974; Sillito, 1977, 1984; Wolf et al, 1986), ocular dominance (Sillito et al, 1980b; Sillito, 1984), and orientation selectivity (Pettigrew and Daniels, 1973; Rose and Blakemore, 1974; Sillito 1975, 1984; Tsumoto et al, 1979; Wolf et al, 1986). Though it is perhaps possible to explain the GABAergic effects on receptive field organization and direction selectivity with a simple and plausible cortical circuit (Barlow and Levick, 1965; Reid et al, 1987), GABAergic effects on orientation selectivity have been far more difficult to explain. The experiments of Sillito (1975, 1979) and of Crook et al (1991) seem to suggest a specific role for GABAergic synapses in providing cross-orientation inhibition to sharpen orientation selectivity in target cells. However, this hypothesis did not explain the observations from intracellular and whole-cell recording that 1) inhibitory potentials impinging on a single cell are centered around the preferred, not cross, orientation (Ferster, 1986) and 2) blocking the inhibitory inputs to a single cell does not change its orientation selectivity (Nelson et al, 1993). It may be that the inhibitory network provides a fine degree of orientation tuning by effectively raising the threshold to firing for orientations slightly different from the preferred, or perhaps tuning is controlled by some

other mechanism altogether, and inhibition merely serves a more general purpose of preventing runaway excitatory feedback in cortex (see Somers et al, 1995).

The above history has been mainly concerned with issues of strength of tuning. Manipulations which change the preferred orientation of cortical cells have been much less commonly observed. In fact, recent optical recording studies have demonstrated, remarkably, that the orientation preference of a local region is maintained despite severely disruptive manipulations, such as monocular deprivation (Kim and Bonhoeffer, 1994) and focal retinal lesions (Das and Gilbert, 1995). Single unit studies have suggested that orientation preference may possibly be altered over a long term by stimulus pairing paradigms which may cause long-term potentiation phenomena (Frégnac et al, 1992) or over a short term by presenting bars of non-optimal orientation in the surround (Gilbert and Wiesel, 1990, but see also chapter 2), but the evidence to date suggests orientation maps remain globally stable after an early developmental period. Our result is the first demonstration that the adult map of orientation preference obtained by optical imaging can be changed. We demonstrate that focal application of bicuculline, a GABA antagonist, increases the cortical representation of iso-orientations regions relative to the injection site, and that GABA and muscimol cause an increase in orientations orthogonal to that of the injection site. Rather than interpreting this result as evidence in favor of cross-orientation inhibition, we discuss how it may be a natural outcome of the role of inhibition in limiting the spread of cortical firing.

METHODS

The methods used are identical to those of chapter 2, with the following exceptions.

Craniotomy was centered over area 18, Horsley-Clark A2-3. Area 18 was identifiable by a strong response to gratings of spatial frequency 0.125 cyc/deg and temporal frequency 1.5 cyc/sec, and a weak response to gratings of spatial frequency 0.375 cyc/deg and temporal frequency 0.75 cyc/sec. (Area 17 has the opposite characteristics.)

Stimuli consisted of full-field gratings, presented in 8 orientations (16 directions) spanning 360°. Opposite directions of motion were summed.

A micropipette containing either GABA (γ-aminobutyric acid, 1M in 0.9% saline, pH 3.0, Sigma), muscimol (30 mM in 0.9% saline, pH 3-4, Sigma) or bicuculline (bicuculline methiodide, 20 mM in 0.9% saline, pH 3.0, Sigma) was placed at a shallow angle just beneath the cortical surface in the center of the field of view. Its position was marked by noting the location of the deflection of the cortical surface relative to the cortical vasculature using the signal from the imaging camera. 3% agar was used to cover the cortical surface, and was left in place for the duration of the experiment. The camera output was continuously monitored during data collection. A wick was used to prevent fluid accumulation on the surface of the agar from changing the focal plane of the camera. The focal plane was checked after every hour of data collection, and adjusted if necessary

to lie between 300-500μm below the cortical surface. Signal was summed for 2-3 hours to obtain maps before, during and after drug iontophoresis (BH2 iontophoresis system, Medical Instruments Corp.). A retaining current of -10 mA (all drugs are positive ions at the pHs used) was used for initial and recovery maps, and between, a maximum current of +93 nA was used continuously. At least 30 minutes were allowed prior to collecting the recovery map. Each session lasted 6-12 hours. Multiple drugs were never used in the same animal.

Bicuculline causes increase in visually driven activity

We obtained similar results from focal injections of bicuculline during optical imaging experiments in 2 animals. Fig. 1 shows a complete set of single-condition maps before, during and after injection. Bicuculline causes an orientation-specific increase in the magnitude and area of activation for two of the eight orientations tested (67.5° and 90°), and no appreciable change at the other six orientations. We measured the magnitude of activity within a circle of 500μm radius from the injection site by comparing the summed activity in iso (45°, 67.5°, 90° and 112.5°) and cross orientations (0°, 22.5°, 135° and 157.5°). The results, shown in table 1, suggest that an increase in signal magnitude is present, though the increase is not unusually large.

	Initial	Bicuculline	Recovery
Iso-orientations	1.37±2.33	0.80±1.39	2.62±1.75
Ortho-orientations	1.70±2.26	1.91±1.46	2.89±1.67

Table 1: Magnitude of signal ± pixel standard deviation for a region 500μm around bicuculline iontophoresis. Each value is calculated from the summed activity of four single-condition maps (units are arbitrary). Smaller numbers indicate greater activity. Between initial, bicuculline and recovery conditions, the signal magnitude varies more from extraneous causes than from bicuculline application. The difference in activity between iso and ortho orientations is largest in the case of bicuculline, though not unusually so.

Bicuculline causes a shift in orientation preference

The increase in size of the orientation domain at the site of bicuculline iontophoresis can also be seen in the map of orientation preference. Fig. 2 shows the orientation preference maps calculated as the angle of the vector sum at each point from the data shown in fig. 1. The two orientations that show the most change in fig. 1 are coded in orange and yellow on fig. 2. During bicuculline iontophoresis, a large region of cortex, up to 1.5 mm from the pipette, shifts orientation preference towards the initial value at the injection site. Furthermore, the magnitude of the shift is related to the initial orientation of the region,

and not to distance away from the pipette. The structure of the orientation map is also altered, with several singularities having disappeared, and with some orientation domains (defined at 22.5° intervals) no longer bordering two singularity points, as is always the case in a normal map. The normal map is recovered fully within 30 minutes of cessation of iontophoresis. Fig. 3 shows a graph of the shift in orientation preference in the affected region as a function of the initial orientation preference. Angles orthogonal to the pipette region orientation preference shift in a reversible manner by nearly 90°. The magnitude of orientation shift is directly proportional to the difference between initial orientation preference and orientation preference under the pipette. Since these data are obtained by vector summation, it is possible that the effect seen in fig. 2 is a result of increased responsiveness to the orientation preference under the pipette without an increase in response to intermediate orientations; that is, it is possible that the orientation tuning curve of cells with an initially orthogonal orientation preference to the pipette region become peaked at both iso- and orthogonal orientations without necessarily responding to intermediate orientations.

GABA and muscimol cause reverse effects

In order to say that the shift in orientation preference is a specific effect of modifying inhibitory inputs, we should be able to see the reverse effect when GABA agonists are applied. Similar effects of GABA were seen in two animals. Fig. 4 shows the result of GABA iontophoresis on the orientation preference map. In this case, orientation preference at the pipette site was 22.5° (red). Unlike in the case of bicuculline, the basic

structure of the orientation map is unchanged; orientation singularities occur with the same frequency, and most domains still border two or more singularity points. Shifts in the area and borders of domains, however, can be seen in fig. 4 up to 1.5 mm away from the injection site. The normal map recovers fully 30 minutes after cessation of iontophoresis. In figure 5, the change in preferred orientation for pixels within the affected region is plotted as a function of the pixel's orientation preference in the initial condition, as in figure 3. An inverse effect is seen, with regions iso-orientation to the pipette (including the region under the pipette itself) shifting preferred orientation nearly 50°, and regions of orthogonal preference virtually unaffected. The difference in pixel orientation preference between initial and recovery maps is plotted as a control. It is not practical to use GABA solutions of greater than 1M concentration, and increasing iontophoretic current risks tissue injury and non-specific current effects. Therefore, we switched to muscimol, a $GABA_A$ agonist which is effective in lower concentrations. Figure 6 shows the effect of 30 mM muscimol iontophoresis in a third animal. In this case, the structure of the orientation map is virtually abolished in the affected region. General activity of the cortex is also largely decreased, consistent with muscimol's suppressive influence on cortical responsiveness, such that the magnitude of the orientation-specific signal, coded as color intensity on figure 6B and D, is very weak. Figure 7 shows the plot of change in preferred orientation, calculated by the same method as in figures 5 and 3. Although we have succeeded in disrupting the structure of the orientation map, possibly indicating a more complete stimulation of inhibitory response than in the GABA map, the maximum shift in preferred orientation is still only 50°. The

muscimol effect did not recover over a 3 hour period after injection. We conclude that GABA/muscimol iontophoresis does, in fact, show the converse result to bicuculline iontophoresis, in that the orientation map shifts away from the initial orientation of the pipette region. We were, however, unable to achieve as large a shift in preferred orientation as seen with bicuculline. The area of the affected region is similar for all three drugs.

Relation to single-unit studies

The most surprising result of this study is the supposed shift in orientation preference that occurs for up to three "hypercolumns" away from the bicuculline injection. It was not foreseen despite numerous studies of bicuculline's effects on single-unit responses. For purposes of comparison, we can divide the literature on single-unit responses into three groups; studies in which bicuculline was applied globally, studies in which neurons were recorded at the site of iontophoresis, and studies in which the recording site was distant from the iontophoresis site.

We cannot predict the degree to which orientation shifts occur during global iontophoresis. It seems unlikely that any drug can be applied perfectly uniformly to the cortical surface (especially when relying on the technique of intravenous administration). Perhaps regional "hot-spots" of greater activity occur with the subsequent changes in orientation preference of surrounding areas, or perhaps bicuculline has a more all-or none effect, and regional changes in activity are exactly balanced. The bicuculline single-unit studies in this category (Pettigrew & Daniels, 1973; Rose & Blakemore, 1974) do not cite evidence of changes in preferred orientation (though Pettigrew shows a cell with a shift in orientation preference for spot but not bar stimuli.)

Neurons at the site of bicuculline iontophoresis retain their orientation selectivity. Although most single-unit studies in this category are not quantitative about whether some cells shift their orientation preference, the strong implication is that normal orientation preference is retained, despite an increase in visual responsiveness, an increase in tuning width (when measured as width at half-height), and changes in some receptive field properties (Sillito, 1975; Sillito, 1979; Sillito, 1980a). With regard to orientation preference, our data therefore agree with these studies. The observed increase in tuning width, though harder to compare due to the differences between the techniques, is also not inconsistent with our data.

Neuronal responses away from the site of drug application were examined by Crook et al (1991) using a configuration where electrodes were spaced 500μm around the iontophoresis pipette containing GABA. In that study, half of all cortical neurons showed increased tuning widths and new responses to orthogonally oriented stimuli under GABA. Furthermore, 25% of cells were found to change their orientation tuning. Qualitatively, this experiment supports our findings. Of course since GABA is generally inhibitory to cortical activity, we expect a much fewer number of cells to be affected than if bicuculline would have been used. The comparable study of neuronal responses distant to a bicuculline injection has not been so far attempted.

Circuit level explanations for the orientation shift

We will examine four possible explanations for the observed pattern of optical activity. 1) the observations are merely an artifact of the technique, 2) a large part of the signal is generated in dendritic or axonal arborizations, removed from the locus of iontophoresis, 3) the observed shift in orientation preference is a direct result of modifying levels of cross-orientation inhibition 4) the orientation shift is a result of increasing the average number of cells through which information travels.

Point discrimination threshold of imaging technique

Are the observations an artifact of the technique? We do not know quantitatively the exact degree to which the activity-dependent signal we observe correlates with the actual site of activity. Furthermore, the light scattering properties of the cortex limit the point-discrimination capability of the camera system. One could imagine that the strong signal in the region of the bicuculline application was intensely scattered over the surrounding cortex, and therefore falsely localized. There are three reasons to doubt this explanation. 1) Though the bicuculline signal is strong compared to signals from surrounding orientation domains, the strongest signals in the image actually come from larger blood vessels. That well-structured orientation maps can be obtained from very close to such large signal sources indicates that scattering is not a significant source of error. Furthermore, as shown in table 1, the strength of signal for the case illustrated is not significantly outside the range of signal strengths normally encountered. 2) Much smaller structures, such as orientation columns in monkey V1, can be resolved equally well by the

same intrinsic-signal technique (Frostig et al, 1990; Malach et al, 1994) suggesting that scattering does not limit the resolution of the technique at this level. 3) Though scattering of the bicuculline-elevated signal could be misinterpreted as an orientation specific response, the corresponding lack of scattering of the GABA/muscimol-depressed signal would not lead to an orientation specific response. A different source of error would therefore have to be postulated to account for the GABA/muscimol result. Although the horizontal extent of bicuculline-induced signal seems too large to be explained by scattering, the horizontal range of the effect *is* of the same order of magnitude as horizontal connections made by single cells in cortex, arguing in favor of an anatomical basis for the observed changes.

Possible creation of an epileptic focus

It is well known that substances which decrease inhibitory activity can create foci of epileptiform activity in cortex (Matsumoto and Ajmone-Marsan, 1964; Prince, 1968; Yamamoto, 1972; Schwartzkroin and Prince, 1977,1978, 1980; Wong and Prince, 1979; Dingledine and Gjerstad, 1980; Gutnick et al, 1982). It is possible, in our experiment that bicuculline iontophoresis creates such a focus, which then propagates to give the observed result. However, it should be kept in mind that all the activity observed in for example the single-condition maps of fig. 1 is visually-evoked activity. Baseline subtraction of activity during a blank stimulus is inherent in the imaging technique (see methods and appendix). It is unclear if stimulus-evoked epileptiform bursting (see Misgeld et al, 1982) propagates in a different manner than normal visual signals. Furthermore, a different mechanism

would have to be proposed to explain the converse result obtained with GABA application, as GABA or muscimol have not been shown to induce epileptic foci.

Imaging of subthreshold responses

The second possibility is that only cells (or dendrites?) directly under the pipette are affected, but that these cells (or dendrites) generate intrinsic signals over the entire extent of their axonal (or dendritic) arborization. If the projections from a single point in cortex are labeled, one finds dense connectivity within 200-300μm and patchy connectivity, presumably to iso-orientation columns (Gilbert, 1992) at larger distances. We have estimated under other conditions (chapter 2) that 50% to 70% of the intrinsic signal is generated from subthreshold signals. Although it is possible that the entire observed signal in the regions outside the normal orientation domain boundary represents a subthreshold response, it is more likely that it represents a mixture of sub- and suprathreshold responses.

Why does the magnitude of the orientation shift differ?

We observe that the magnitude of the shift in orientation for bicuculline is greater than that for GABA or muscimol. We will examine three possibilities to account for this observation. The simplest possibility is that there is a dose-response relationship to the orientation shift. The higher the concentration of GABA or bicuculline used, the larger the shift. Unfortunately, it was not possible for us to directly test multiple doses of the same drug in the same animal due to the time required for signal summation. We were

interested to see whether by increasing the GABA dosage, we could obtain a greater shift away from the preferred orientation, equal in magnitude to the 90° shift observed with bicuculline. Our decision to study the muscimol response was motivated by the desire to test an increased dosage, and the fact that GABA is a) much more easily inactivated than bicuculline or muscimol, being an endogenous substance, and b) close to saturation at the concentration and pH used. However, it should be noted that GABA at 1M is twice the concentration used by Crook et al (1991) in their study of single-unit remote inactivation. Muscimol at 30 mM is even more potent and permanent, yet it did not lead to an increased shift in preferred orientation. At this dosage of muscimol, the cortex did not recover over the time of the imaging experiment. Finally, observed effect for all three drugs extended for approximately 1.5 mm away from the injection. It might be expected if a dose-response relationship existed, that the range of the effect, as well as its magnitude, would have varied. Thus, we favor the view there is not a strong dose-response relationship, and that the three drugs act specifically over a comparable area.

A second possibility is that the magnitude of the orientation shift may relate to other features of the map, such as distance of the injection from singularities, or location within areas of high orientation gradient. Examination of these possibilities is dependent on a better understanding of the relation of these map features to the underlying single-unit responses, and is beyond the scope of this study.

The final possibility to account for the greater orientation shift with bicuculline involves a difference in the effect on second-order cells. An unaffected cell receiving inputs from a GABA-affected cell presumably gets less excitation than normal, whereas an unaffected cell receiving inputs from a bicuculline-affected cell gets more excitation. Because levels of spontaneous activity in visual cortex are normally quite low, more excitation represents a stronger signal than less excitation to a cell that is integrating its responses. (Put differently, it is more unusual for a cell to see a strong response than a lack of a response.) Thus, bicuculline has a stronger effect than GABA because second and higher order cells may still be passing on the change in response. This hypothesis therefore explains the fact that GABA/muscimol do not cause as large an orientation change as bicuculline, and implies that the optical signal contains more than just subthreshold responses.

Cross-orientation inhibition

The model of cross-orientation inhibition proposed by Sillito (1984) and Crook et al (1991) requires that the strongest inhibitory influences on a column originate in columns of orthogonal orientation. What, then, is the prediction of this model for the intrinsic signal response? Connectivity from a cortical point is locally diffuse, and patchy at larger distances. A recent experiment which combined optical imaging with labeling of inhibitory neurons (Kisvárday et al, 1994) suggest that inhibitory cells connect locally, in a diffuse manner, to columns of all orientations. When GABA/muscimol is applied at a point, excitatory cells see unusually strong inhibition, which, following the assumption, they must either interpret as cross-orientation, or perhaps as non-specific inhibition. These

excitatory cells would be expected to relay strong signals for iso-orientation stimuli to their long-range targets, which in primary visual cortex are other iso-orientation columns (Gilbert and Wiesel, 1989). Thus, the main effect should be increased patchy activity of iso-orientation domains. The converse experiment, bicuculline iontophoresis, should be seen as a reduction in inhibition either to cross or to all orientations at that point. If the hypothesis is that cross-orientation inhibition aids in orientation selectivity, cells at the point of iontophoresis should thus lose some degree of orientation selectivity. Neither of these predictions are seen; GABA/muscimol leads to a decrease in activity in iso-orientation columns, and bicuculline does not prevent strong orientation-specificity. Thus, we must conclude that our experiment is at odds with the model of cross-orientation inhibition.

Role of inhibition in orientation-selective responses

We are thus left with the hypothesis that inhibition serves to limit the spread of excitation in cortex (see figure 8). The relevant predictions of this hypothesis is that increasing local inhibition (GABA/muscimol) would serve to restrict iso-orientation signals from traveling laterally in the cortex, and that decreasing local inhibition would cause an overrepresentation of iso-orientation signals in the cortex. Both predictions are in agreement with the observed affects. In fact, there is evidence that inhibition plays this role (for example, see Chagnac-Amitai and Connors, 1989); the novel information of this study is that this role, rather than a more specific one, is of prime importance in determining the contribution of inhibition to orientation selectivity. The true origin of

orientation selectivity is still unknown. It may be that, in the course of its non-specific role, GABA circuitry may mediate a thresholding mechanism, that along with feed-forward excitatory circuitry shapes selectivity (Somers et al, 1995), or it may be that selectivity is hard-wired during development, either in the pattern of LGN inputs themselves, in the circuitry of the cortical inputs, or in feedback loops between cortical layers, other cortical areas, or the thalamus.

REFERENCES

Barlow HB, Levick WR (1965) The mechanism of directionally selective units in the rabbit's retina. *J. Physiol.* 178:477-504.

Beaulieu, C, Somogyi, P (1990) Targets and quantitative distribution of GABAergic synapses in the visual cortex of the cat. *Eur. J. Neurosci.* 2:296-303.

Beaulieu C, Kisvarday Z, Somogyi P, Cynader M, Cowey A (1992) Quantitative distribution of GABA-immunopositive and immunonegative neurons and synapses in the monkey striate cortex (area 17) *Cerebral Cortex* 2:295-309.

Chagnac-Amitai, Y and Connors BW (1989) Horizontal spread of synchronized activity in neocortex and its control by GABA-mediated inhibition. *J. Neurophys.* 61(4):742-758.

Crook, JM, Eysel, UT, Machemer, HF (1991) Influence of GABA-induced remote inactivation on the orientation tuning of cells in area 18 of feline visual cortex: a comparison with area 17. *Neuroscience* 40(1):1-12.

Das A, Gilbert CD (1995) Long-range horizontal connections and their role in cortical reorganization revealed by optical recording of cat primary visual cortex. *Nature* 375:780-784.

Dingledine R, Gjerstad L (1980) Reduced inhibition during epileptiform activity in the *in vitro* hippocampal slice. *J. Physiol. (Lond.)* 305:297-313.

Ferster D (1986) Orientation selectivity of synaptic potentials in neurons of cat primary visual cortex. *J. Neurosci.* 6(5):1284-1301.

Frégnac Y, Shulz D, Thorpe S, Bienenstock E (1992) Cellular analogs of visual cortical epigenesis. I. Plasticity of orientation selectivity. *J. Neurosci.* 12(4):1280-1300.

Frostig RD, Lieke EE, Ts'o DY and Grinvald A (1990) Cortical functional architecture and local coupling between neuronal activity and the microcirculation revealed by *in vivo* high-resolution optical imaging of intrinsic signals. *Proc. Nat. Acad. Sci. USA* 87:6082-6086.

Gilbert CD, Wiesel, TN (1989) Columnar specificity of intrinsic horizontal and corticocortical connections in cat visual cortex. *J. Neurosci.* 9(7):2432-2442.

Gilbert CD, Wiesel TN (1990) The influence of contextual stimuli on the orientation selectivity of cells in primary visual cortex of the cat. *Vision Res.* 30(11):1689-1701.

Gutnick MJ, Connors BW, Prince DA (1982) Mechanisms of neocortical epileptogenesis *in vitro*. *J. Neurophysiol.* 48:1321-1335.

Kim DS, Bonhoeffer T (1994) Reverse occlusion leads to a precise restoration of orientation preference maps in visual cortex. *Nature* 370:370-372.

Kisvárday ZF, Kim DS, Eysel UT, Bonhoeffer T (1994) Relationship between lateral inhibitory connections and the topography of the orientation map in cat visual cortex. *Eur. J. Neurosci.* 6:1619-1632.

Malach R, Tootell RBH, Malonek D (1994) Relationship between orientation domains, cytochrome oxidase stripes, and intrinsic horizontal connections in squirrel monkey area V2. *Cereb. Cortex* 4:151-165.

Matsumoto H, Ajmone-Marsan C (1964) Cortical cellular phenomena in experimental epilepsy: interictal manifestations. *Exp. Neurol.* 9:286-304.

Misgeld U, Klee MR, Zeise ML (1984) Differences in baclofen-sensitivity between CA3 neurons and granule cells of the guinea pig hippocampus *in vitro*. *Neurosci. Lett.* 47:307-311.

Nelson S, Toth L, Sheth B, Sur M (1994) Orientation selectivity of cortical neurons during intracellular blockade of inhibition. *Science* 265:774-777.

Pettigrew JD, Daniels, JD (1973) Gamma-aminobutyric acid antagonism in visual cortex: different effects on simple, complex, and hypercomplex neurons. *Science* 182:81-3.

Prince DA (1968) The depolarization shift in 'epileptic' neurons. *Exp. Neurol.* 21:467-485.

Reid RC, Soodak RE, Shapley RM (1987) Linear mechanisms of directional selectivity in simple cells of cat striate cortex. *Proc. Nat. Acad. Sci. USA* 84:8740-8744.

Rose D, Blakemore C (1974) Effects of bicuculline on functions of inhibition in visual cortex. *Nature* 249:375-377

Schwartzkroin PA, Prince DA (1977) Penicillin-induced epileptiform activity in the hippocampal in vitro preparation. *Ann. Neurol.* 1:463-469.

Schwartzkroin PA, Prince DA (1978) Cellular and field potential properties of epileptogenic hippocampal slices. *Brain Res.* 147:117-130.

Schwartzkroin PA, Prince DA (1980) Changes in excitatory and inhibitory synaptic potentials leading to epileptogenic activity. *Brain Res.* 183:61-73.

Sillito AM, (1975) The contribution of inhibitory mechanisms to the receptive field properties of neurones in the striate cortex of the cat. *J. Physiol.* 250:305-329.

Sillito AM (1977) Inhibitory processes underlying the directional specificity of simple, complex and hypercomplex cells in the cat's visual cortex. *J. Physiol.* 271:699-720.

Sillito AM (1979) Inhibitory mechanisms influencing complex cell orientation selectivity and their modification at high resting discharge levels. *J. Physiol.* 289:33-53.

Sillito AM, Kemp JA, Milson JA, Berardi N (1980a) A re-evaluation of the mechanisms underlying simple cell orientation selectivity. *Br. Res.* 194:517-520.

Sillito AM, Kemp JA, Patel H (1980b) Inhibitory interactions contributing to the ocular dominance of monocularly dominated cells in the normal cat visual cortex. *Exp. Br. Res.* 41:1-10.

Sillito AM (1984) Functional considerations of the operation of GABAergic inhibitory processes in the visual cortex. In: *Cerebral Cortex.* Vol. 2, Functional properties of cortical cells (EG Jones, A Peters, eds.) Plenum Press, New York, 91-117.

Somers DC, Nelson SB, Sur M (1995) An emergent model of orientation selectivity in cat visual cortical simple cells. *J. Neurosci.* 15(8):5448-5465.

Tsumoto T, Eckart W, Creutzfeldt OD (1979) Modification of orientation sensitivity of cat visual cortex neurons by removal of GABA-mediated inhibition. *Exp. Br. Res.* 34:351-363.

Wolf W, Hicks TP, Albus K (1986) The contribution of GABA-mediated inhibitory mechanisms to visual response properties of neurons in the kitten's striate cortex. *J. Neurosci.* 6:2779-2795.

Wong RKS, Prince DA (1979) Dendritic mechanisms underlying penicillin-induced epileptiform activity. *Science* 204:1228-1231.

Yamamoto C (1972) Intracellular study of seizure-like afterdischarges elicited in thin hippocampal sections *in vitro*. *Exp. Neurol.* 35:154-164.

FIGURE LEGENDS

Fig. 1 24 single condition maps show the imaged response to eight orientations (one direction only) of full-field gratings shown previous to (**left column**), during (**middle column**), and after (**right column**) iontophoresis of bicuculline. Active regions show darkly. The pipette's location corresponds to the dark patch seen in 67.5° and 90° orientations at the image center. This patch is greatly expanded during bicuculline iontophoresis, though surrounding patches of other orientations are minimally affected. In order to minimize image artifacts, maps are divided by the summed activity within each condition. Scale bar, 2 mm.

Fig. 2 Orientation preference maps (**A**) before, (**B**) during and (**C**) after iontophoresis of bicuculline (20 mM) from a pipette at the site marked by the star. A shift in orientation preference occurs such that nearly the entire cortex for a distance of 1.5 mm around the pipette comes to prefer orientations between 67.5° (orange) and 90° (yellow). These maps show the angle of the vector summation at each pixel, binned in 22.5° increments according to the color key shown. Scale bar, 1 mm.

Fig. 3 The shift in orientation preference is plotted as a function of the initial orientation preference for the region of cortex approximately 1.5 mm around the bicuculline pipette. Values of orientation preference from the vector angle maps shown in figure 2 were subtracted, pixel by pixel, and grouped to the eight values of orientation shown (0°, 22.5°,

45°... 157.5°). The solid line represents the shift in orientation preference between the initial map (fig. 2A) and the bicuculline map (fig. 2B). The dashed line represents the control condition in which the initial map was compared with the recovery map (fig. 2C). Values of $\Delta\theta$ on the X axis represent the difference between the preferred orientation of a given pixel and the preferred orientation of the pipette region; that is, 0° represents a pixel whose orientation preference was equivalent to the injection region (between 67.5° and 90° in this experiment). According to these data, the greatest shifts, 73.2° (at 0°, $\Delta\theta=\pm 90°$) and 69.2° (at 157.5°, $\Delta\theta=67.5°$) occur in columns orthogonal to that of the pipette region. Furthermore, the change in preferred angle is directly proportional to $\Delta\theta$.

Fig. 4 Orientation preference maps (**A**) before, (**B**) during and (**C**) after iontophoresis of GABA (1M) from a pipette at the site marked by the star. In this case, cortex around the pipette shifts its orientation preference away from the initial preference at the pipette region (22.5°, red). Orthogonal orientation columns in the surrounding cortex expand up to 1.5 mm from the injection site. No significant change is seen in iso- or orthogonal columns further away. As in fig. 2, these maps show the angle of the vector summation at each pixel, binned in 22.5° increments according to the color key shown. Scale bar, 1mm.

Fig. 5 The shift in orientation preference caused by GABA is plotted as a function of the initial orientation preference for the region of cortex approximately 1.5 mm around the pipette. Methods as in fig. 2. Values of $\Delta\theta$ on the X axis represent the difference between

the preferred orientation of a given pixel and the preferred orientation of the pipette region (22.5° in this experiment). The dotted line shows the difference between maps pre and post application as a control. The orientation shift for GABA is in the opposite direction from that of bicuculline. Regions iso-orientation to the pipette show the greatest change in orientation. Despite the fact that in this case, the greatest change occurs at the injection site instead of away from the injection site, the magnitude of the shift is less, only 48.6° at maximum. The change in preferred angle at a cortical point is directly proportional to $\Delta\theta$, and not proportional to distance from the injection.

Fig. 6 Orientation preference maps before (**A**, **B**) and during (**C**, **D**) infusion of muscimol (30 mM) at the site marked by the cross. Maps **A** and **C** are vector angle maps. Maps **B** and **D** are identical, except that intensity of color is used to code vector magnitude. One can see the generally depressive effect of muscimol as the dark area surrounding the injection site in map D. Maximum color intensity represents a response three standard deviations above the mean response over the valid region of the map. Responses in D are low enough that image artifacts (masked out for calculations) are clearly seen. Furthermore, as in the case of GABA, a general shift in preferred orientation towards a value of about 120° (greens), orthogonal to that of the pipette location, is visible for a distance of 1.5 mm around the injection site. Scale bar 1mm.

Fig. 7 The shift in orientation preference caused by muscimol (30 mM) is plotted as a function of the initial orientation preference for the region of cortex approximately 1.5 mm

around the pipette. Methods as in fig. 2. Values of $\Delta\theta$ on the X axis represent the difference between the preferred orientation of a given pixel and the preferred orientation of the pipette region (45° in this experiment). Again, the magnitude of the change is small (50.3° maximum at $\Delta\theta$=0°) relative to that caused by bicuculline. The control curve in this case is calculated from a region of the initial and muscimol maps 4 mm away from the injection site, outside the affected region. Muscimol, like GABA, causes a shift away from the preferred orientation of the pipette region.

Fig. 8 Schematic illustrating the proposed non-specific role of inhibitory circuitry in the cortex. Long-range fibers connect cells of similar orientation preference, thus an excitatory signal must traverse several synapses before affecting a cell of cross-orientation. By decreasing inhibition, signals can travel farther in cortex, increasing the representation of the orientation where inhibition was decreased in neighboring cells. On the other hand, when inhibition is increased, cells receive more predominant inputs from other columns, shifting the orientation bias away from the original. Since a decrease of inhibition leads generally to more activity, the effect on orientation preference is larger than when inhibition is increased.

Figure 1.

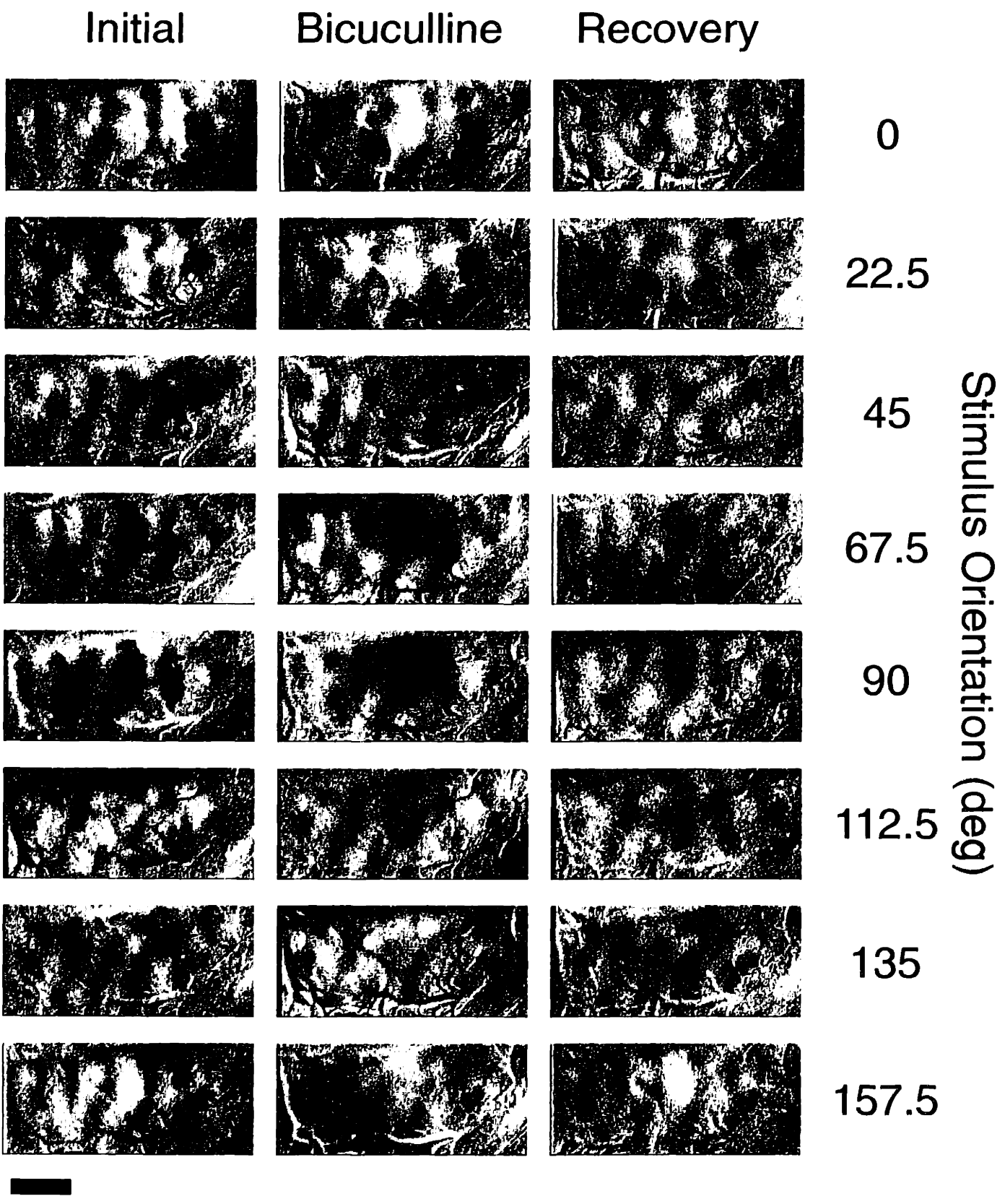
Initial
Bicuculline
Recovery
0
22.5
45
67.5
90
112.5
135
157.5
Stimulus Orientation (deg)

Figure 2.

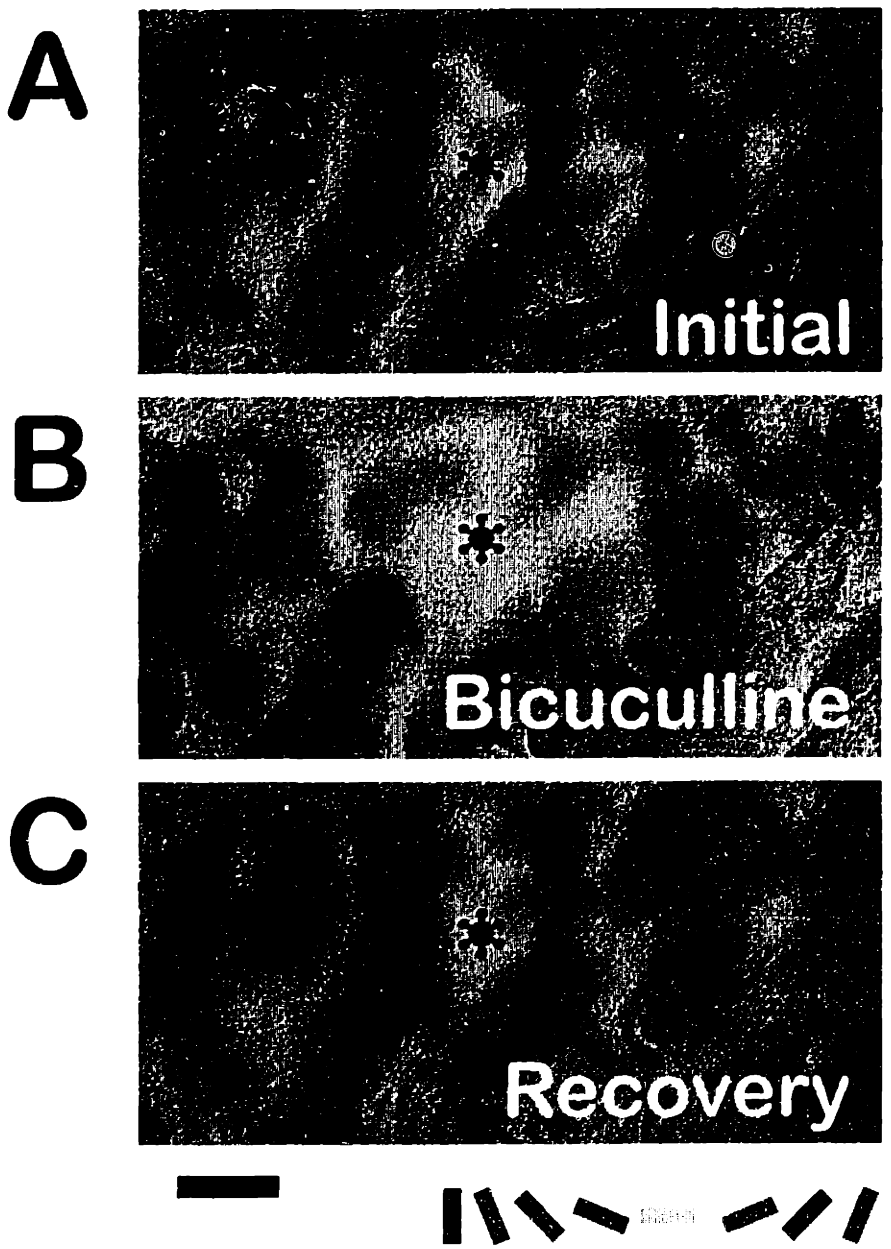

Figure 3.

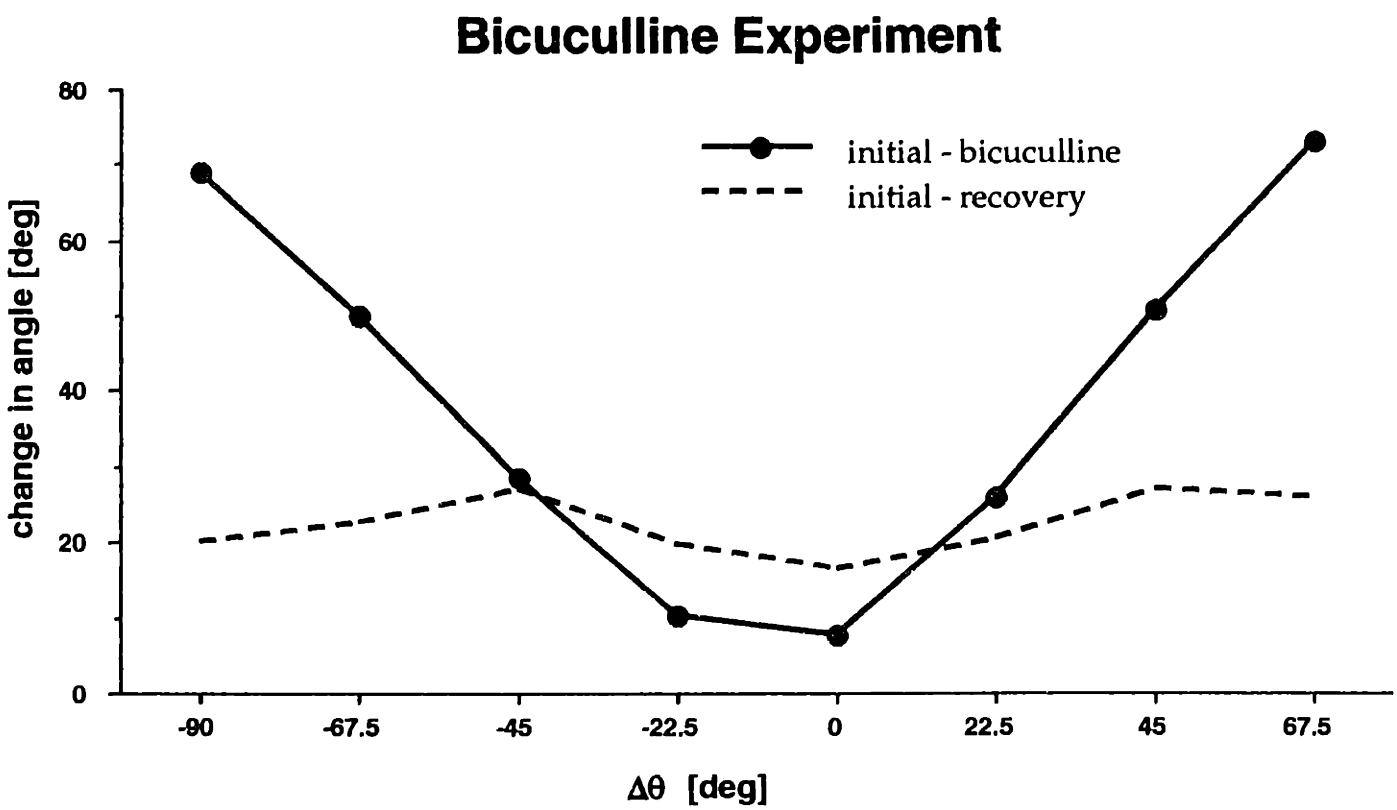
Bicuculline Experiment
initial - bicuculline
initial - recovery
change in angle [deg]
80
60
40
20
0
-90
-67.5
-45
-22.5
0
22.5
45
67.5
Δθ [deg]

Figure 4.

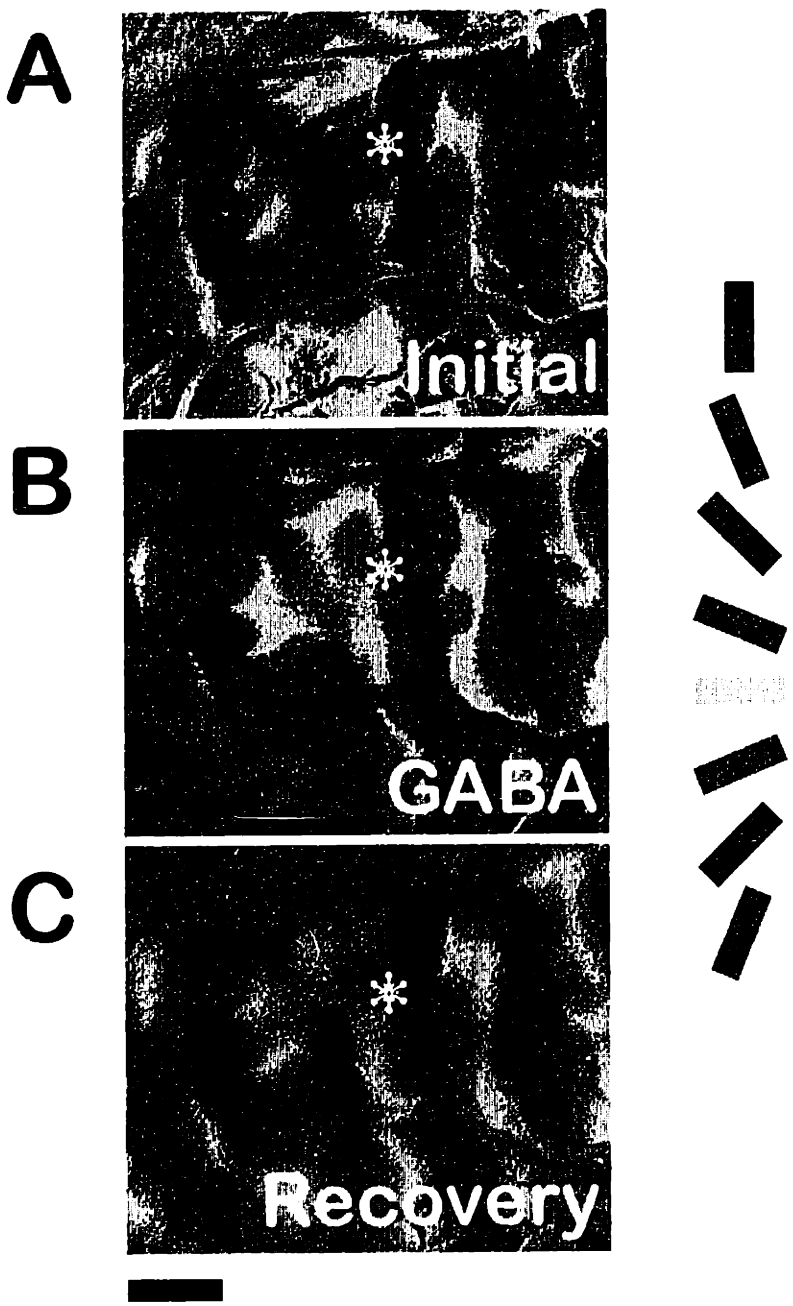

Figure 5.

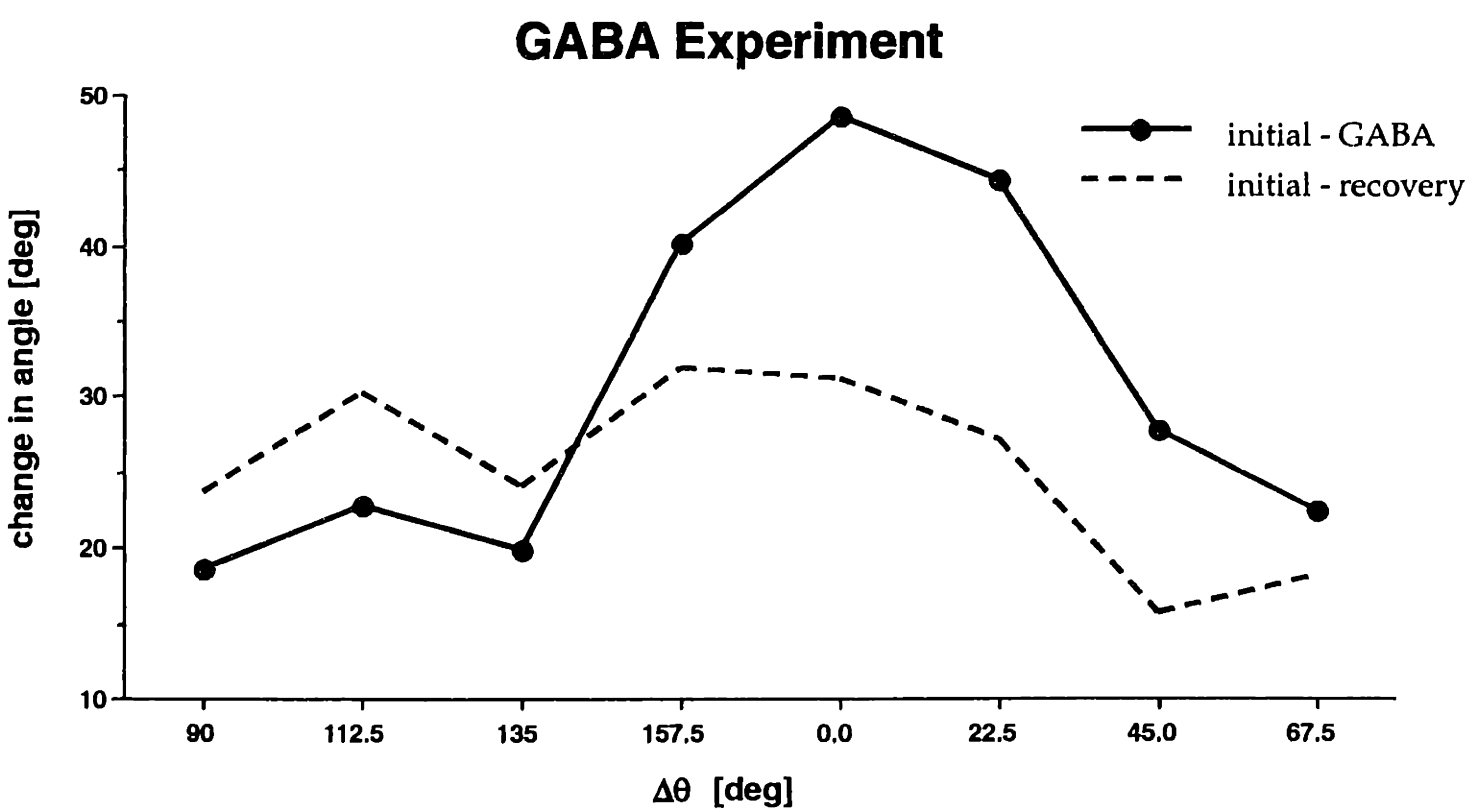
GABA Experiment
initial - GABA
initial - recovery
change in angle [deg]
50
40
30
20
10
90
112.5
135
157.5
0.0
22.5
45.0
67.5
Δθ [deg]

Figure 6.

Figure 7.

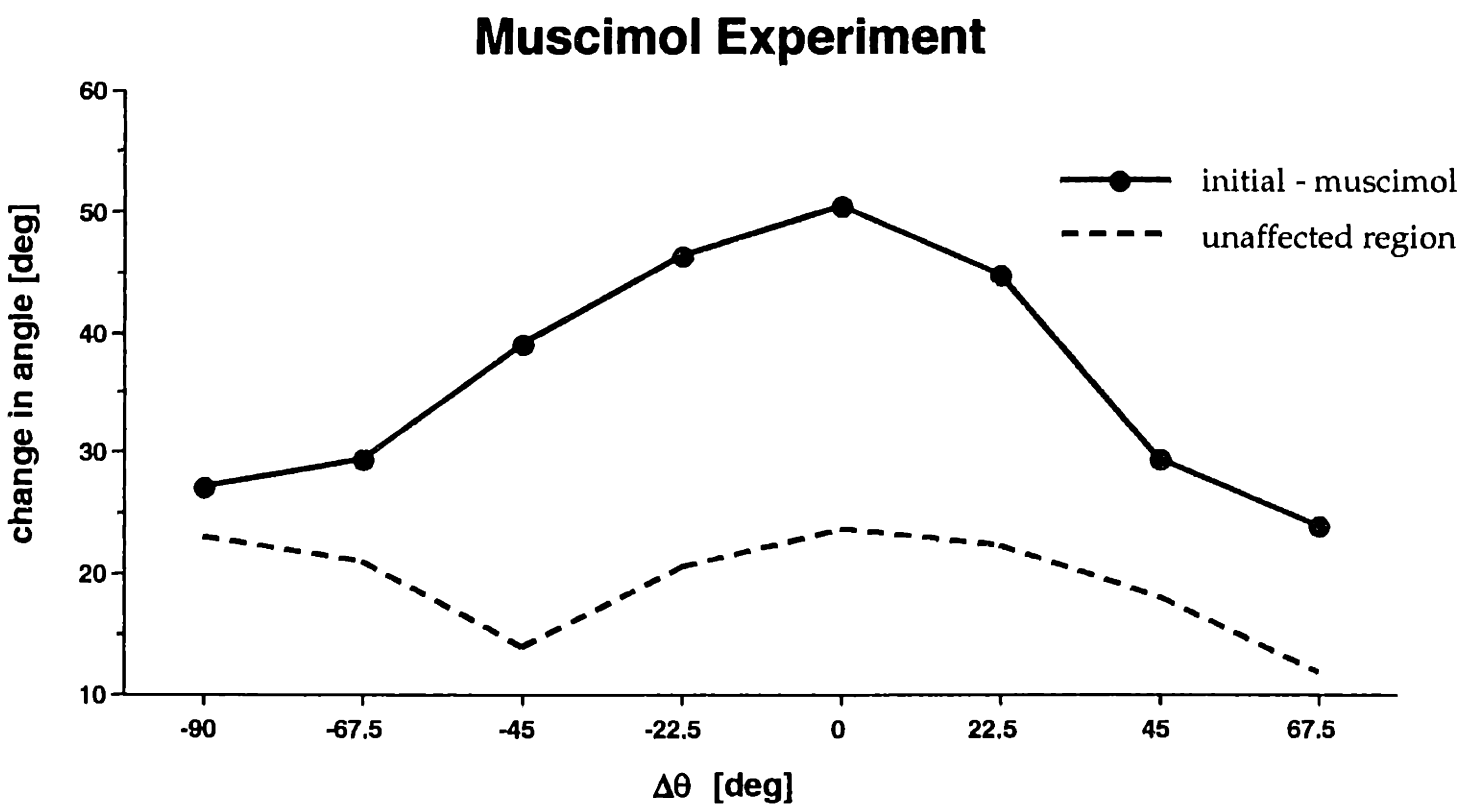
Muscimol Experiment
initial - muscimol
unaffected region
change in angle [deg]
60
50
40
30
20
10
-90
-67.5
-45
-22.5
0
22.5
45
67.5
Δθ [deg]

Figure 8.

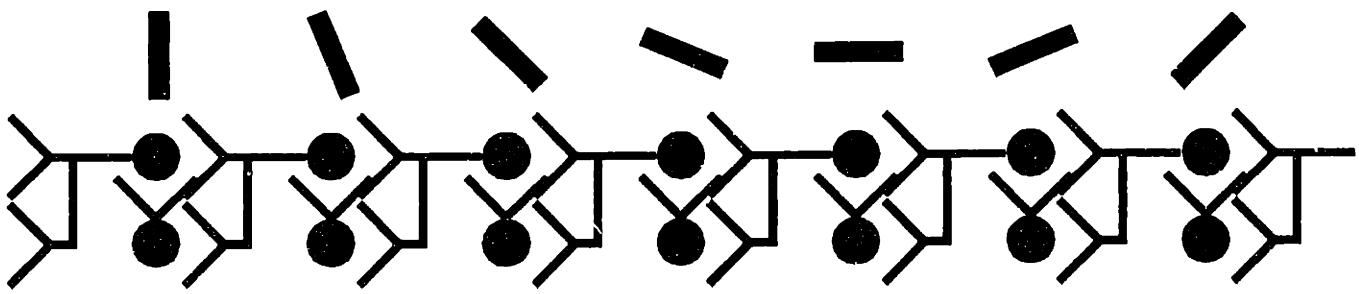

Conclusion: A Physiological Role for Lateral Connectivity in Cortex

It has been suggested that patchy lateral connectivity is a fundamental feature of the organization of all cortical areas (Lund et al, 1993). In primary visual cortex, we are able to relate known physiological properties to the underlying system of lateral connectivity. We propose that the system of lateral connectivity mediates communication that is dynamic and stimulus-specific, but primarily modulatory in nature. Furthermore, since the frequency of patches is remarkably similar across cortical areas, we propose that the distance between cortical patches represents a physical limitation that is relevant in determining the final geometry of cortical maps in the adult (chapter 1).

Long-range lateral connections in primary visual cortex connect domains of iso-orientation preference (Gilbert and Wiesel, 1989; Malach et al, 1993). Furthermore, the range of their connectivity suggests that they connect regions of non-overlapping receptive fields (see LeVay, 1988a), making them prime candidates for mediating effects of the surround, or extra-classical receptive field. Using single-unit recording, we demonstrate that a surround stimulus that by itself causes no suprathreshold responses, can modulate neuronal responses in either an excitatory or an inhibitory manner (chapter 2). Since long-range connectivity has been demonstrated to be excitatory in nature (LeVay, 1988b), this result suggests that surround information can travel either via a long-range connection directly, or indirectly through a local, inhibitory synapse.

Our experiments show that the technique of intrinsic signal imaging is quite sensitive to subthreshold signals. Optical images of responses to localized visual activation

demonstrate that the region of subthreshold effect is 1) very large, extending several millimeters laterally across the cortex, and 2) specific to iso-orientation signals.

A second method of directly observing subthreshold effects is intracellular recording. Using the whole-cell technique in an *in vivo* preparation allowed us to record directly the effect of surround responses in cortical neurons. Responses to flashed stimuli occur at multiple, discrete latencies. Flashed stimuli in the surround were found to generate quite similar post-synaptic potentials to center flashes, with the important difference that the responses only occurred at the second and later latencies. The exact timing of visual latencies may be contrast dependent, but is not position dependent. Since lateral connections are the likely path by which surround stimuli exert their influence, the lateral connectivity may serve to bind stimuli arising from the same source into a temporally locked response.

It has been proposed in the past that lateral connectivity may also mediate the generation of orientation specific responses through an intracortical inhibitory circuit (see Sillito, 1984). We applied GABA agonists and antagonists, and examined the disruption of the orientation map directly using intrinsic signal imaging (chapter 4). The results argue against a direct role of lateral connectivity in generating orientation selectivity, and suggest a general, non-specific role for inhibitory circuitry in containing cortical excitation.

In conclusion lateral connectivity in primary visual cortex mediates orientation-specific surround responses that are primarily modulatory (subthreshold) in nature. Surround effects can be directly excitatory, or inhibitory through a local interneuron. Neither lateral connectivity nor the inhibitory circuitry by itself is responsible for generating orientation selectivity, rather both systems serve to control the spread of information through the cortex. Finally, the range of lateral connectivity may be an important physical constraint which determines features of the layout of cortical maps, such as spacing of iso-orientation domains in primary visual cortex. This thesis is concerned with visual cortex, an area where the ease of providing complex, patterned input has aided our efforts to understand its function. It is hoped that the application of these results to cortical areas not so easily accessible will help uncover the unifying principles of the brain's organization.

REFERENCES

Gilbert CD, Wiesel TN (1989) Columnar specificity of intrinsic horizontal and corticocortical connections in cat visual cortex. *J. Neurosci.* 9(7):2432-2442.

LeVay S (1988a) The patchy intrinsic projections of visual cortex. Chapter 14 in *Progress in Brain Research, vol. 75.* TP Hicks and G Benedek eds. Elsevier.

LeVay S (1988b) Patchy intrinsic projections in visual cortex, area 18, of the cat: morphological and immunocytochemical evidence for an excitatory function. *J. Comp. Neurol.* 269:265-274.

Lund JS, Yoshioka T, Levitt JB (1993) Comparison of intrinsic connectivity in different areas of macaque monkey cerebral cortex. *Cereb. Cortex* 3:148-162.

Malach R, Amir Y, Harel M, Grinvald A (1993) Relationship between intrinsic connections and functional architecture revealed by optical imaging and in vivo targeted biocytin injections in primate striate cortex. *Proc. Nat. Acad. Sci. USA* 90:10469-10473.

Sillito AM (1984) Functional considerations of the operation of GABAergic inhibitory processes in the visual cortex. In: *Cerebral Cortex.* Vol. 2, Functional properties of cortical cells (EG Jones, A Peters, eds.) Plenum Press, New York, 91-117.

Appendix

Standard methods of analysis for optical imaging data

The analysis of imaging data from the visual cortex, whether obtained using intrinsic signal or voltage sensitive dye technique, has been performed using basically the same algorithms by all groups that have published so far. Because some of the mathematics behind these "standard" analysis techniques are somewhat less than obvious, they are detailed here. The hope is that the reader who does not have first-hand experience with these techniques will be able to appreciate the strengths and weaknesses of each of the methods, and thereby be able to judge their appropriateness as the field of optical imaging moves beyond the systems with which it was developed.

Chapters 1,2 and 4 of this thesis are concerned with the intrinsic signal technique. Mention of the peculiar difficulties inherent in that technique can be found therein. For a good, though slightly dated, review of the special problems associated with the voltage-sensitive dye technique, consult Grinvald, 1985.

Single-condition maps

The most basic data that can be obtained from an imaging system is the raw output of the scanning device. Whether such data is meaningful in its raw form depends on the specifics of the experimental setup. In slice or culture experiments using voltage-sensitive dyes, the magnitude of the signal can often be directly related to the underlying voltage change by relatively simple controls. Appropriate controls become difficult when such dyes are used *in vivo*, and the correlation between the optical signals and underlying activity has yet to be demonstrated, but expectations are that it will be quite strong. Similarly, intrinsic

signals are difficult to correlate with exact levels of activity, and are most useful as measures either of spatial differences, or of differences between two or more stimuli.

Intrinsic-signals, being related to blood-flow and/or volume, are indirectly correlated with activity, though this indirect correlation has proved useful for the last several decades in the techniques of positron emission tomography, 2-deoxyglucose radiolabeling, and functional magnetic resonance imaging. The raw data from an intrinsic-signal experiment already contains some assumptions about the time course of the activity, and the amount of activity present. In the visual system, researchers typically integrate data for several seconds after a stimulus onset, and sum over several stimulus presentations to obtain useful data. Several methodological questions are relevant: Is the researcher collecting data around the time of maximal signal? Does the activity in the optical map really reflect the desired neuronal feature, given that the stimulus may last for several seconds? Is there interaction between successive stimuli? These questions can be answered by appropriate controls.

In intrinsic signal experiments, the most useful, unadulterated form of the data is a map of stimulus-driven activity. Such a map must be obtained by mathematically subtracting or dividing, pixel-by-pixel, the image of the stimulus-driven activity, appropriately integrated and summed, by the image of the static brain, not being driven by a stimulus, summed in the same manner. This condition may be one of no stimulation if neurons are being driven electrically, or of background stimulation, as when an animal views a neutral gray screen.

In some systems, the procedure of subtracting a reference condition is accomplished before the data is digitized, in order that the data can be passed in real time through an A/D converter.[1]

One subjective feature in the display of single condition maps is inherent in the choice of color scales. Usually, a linear gray scale is fit to the values ±3 standard deviations around the mean of the image. Closer clipping results in large areas of the image being saturated white or black, and loss of detail in those regions. If single condition maps are to be compared with each other, the clip range, instead of being based on the standard deviation of the image, must be set to equal values for all the images being compared. Finally, since the gray scale is used for the purpose of display, it is desirable that the gray scale *look* linear on the final output. Often, substantial gamma-correction to a mathematically linear color table is needed to achieve a visual linearity.

Differential maps

Differential maps, calculated by mathematically dividing, pixel by pixel, two single condition maps, representing activity from two discrete stimuli. The differential map,

[1] This technique should be obsolete in a few years, as 12 to 16 bit A/D converters fast enough to handle real-time video become available. By subtracting the "blank" or "reference" image prior to digitization, the intrinsic signal, which is at maximum 1/1000 part of the reflected light, can be seen with only 8-bit digitization, whereas the original signal would require an absolute minimum of 10 bits. This technique is used by Optical Imaging's Imager 2001 and the Fuji Deltaron systems. In such systems, the raw data is already a reference-subtracted image. Dividing the reference-subtracted data by an equivalent reference-subtracted reference image (using two separate presentations of the reference image!) can improve the signal by correcting fluctuations that occur prior to digitization. A minimum stimulus configuration becomes, therefore "stimulus", "reference", and "blank", with the single-condition map being computed as $\frac{stimulus - reference}{blank - reference}$.

colored in gray-scale, will be dark where one stimulus is more effective, and light where the opposite stimulus is more effective. It can be used to show spatial segregation of responses, or for comparing response amplitudes. The rules on displaying single-condition images discussed above also apply to differential images, with the exception that it may be fairer to use a mean value of 1.0 to calculate the clip range, rather than the actual image mean. (A mean value of 1.0 would indicate equal activity in both input maps.)

Angle maps

An angle map is calculated usually from eight, but sometimes from four or sixteen single condition maps to stimuli of differing orientations. For the activation of orientation domains, six to eight equally spaced orientations are enough such that any particular region of cortex responds well to at least one of the stimuli. With fewer than four stimuli, the angle map begins to show gross errors, whereas with more than sixteen, the time to run the experiment becomes prohibitive.

Most commonly shown is the vector-angle map. For purposes of explanation, we will assume eight stimulus orientations are being tested, though the procedure is the same for a greater or fewer number of maps. Each pixel of the single-condition maps is treated as a vector, whose magnitude is the strength of the signal (value of the pixel) and whose angle is the angle of the stimulus orientation used to generate the map. For every pixel position in the output map, there are thus eight vectors corresponding to the same pixel position in the input maps. These eight vectors are summed using the coordinate system shown in

fig. A1. Since an orientation of 0° is equivalent to an orientation of 180°, they are made equivalent in the vector sum as well. Vectors with angles 90° apart work to cancel each other. This is the arrangement shown in fig. A1. If it is desired instead to map direction preference, angles are arranged normally, such that 0° and 360° are equivalent, and angles 180° apart cancel each other. From the resultant vector, two maps can be generated; the "angle" map, in which each pixel bears the value of the resultant vector's angle, and the "magnitude" map, in which each pixel bears the length of the resultant vector. The angle map is a form of data interpolation, as it contains a continuous range of angles despite the fact that only a finite number of stimulus angles were tested. It would be wrong to assume from the imaging data alone that the interpolation is necessarily valid.

Angle maps are color-coded either in a continuous range of colors, or in a discrete color "rainbow". Continuous coloration provides the advantage of best showing regions of smooth and sharp change in angle, but only if the color map is selected with extreme care, such that the proportions of all colors look equal in the final output. Most output devices, when given a mathematically exact color palette, exaggerate reds and greens and minimize yellows and light blues, thus negating the visual effect. We prefer the discrete color map, where the number of colors used in the map reflects the number of tested orientations. This minimizes the number of arbitrary, interpolated borders in the image. Be warned that in much of the current literature, angle maps are published which the colors greatly outnumber the actual tested orientations. This practice has the effect of exaggerating the interpolated regions and making the map look smoother than is justifiable.

Polar maps

Since a discretely colored angle map contains a relatively small number of bright colors, one can use the level of color saturation to code for the vector magnitude, and thus obtain a "polar" map. Such a map is merely a visual combination of the angle and magnitude maps described above, and is best used to show regions of strongly selective activity, which appear as the most intensely colored. Two words of caution are necessary about "polar" maps. First, dark regions only imply lack of selective signal, they do not imply lack of signal. A region is dark if the vector magnitude is near zero, but this could arise either from all the input vectors being zero, or from all the input vectors being nearly equal. Second, the color mapping in a polar map, like that of a single-condition map, but unlike that of the angle map, relies on a subjective clipping. Full saturation usually equals a value of between 1 and 3 standard deviations above the mean. If magnitudes across multiple polar maps are to be compared visually, it is important that the value of full saturation be equal in all three maps, even though the standard deviations of those maps may be different. Third, the number of basic colors in a polar map *must* reflect the number of stimuli used. When binning the angle map, it is important that the bins fall equally-spaced around the tested angles. For example, if orientations of 0°, 45°, 90°, and 135° are tested, a polar map must have four basic colors representing vector angles from 157.5° to 22.5°, 22.5° to 67.5°, 67.5° to 112.5°, 112.5° to 157.5°, *not* from 0°-45°, 45°-90°, etc..

REFERENCES

Grinvald A (1985) Real-time optical mapping of neuronal activity: from single growth cones to the intact mammalian brain. *Ann. Rev. Neurosci.* 8:263-306.

Figure 1.

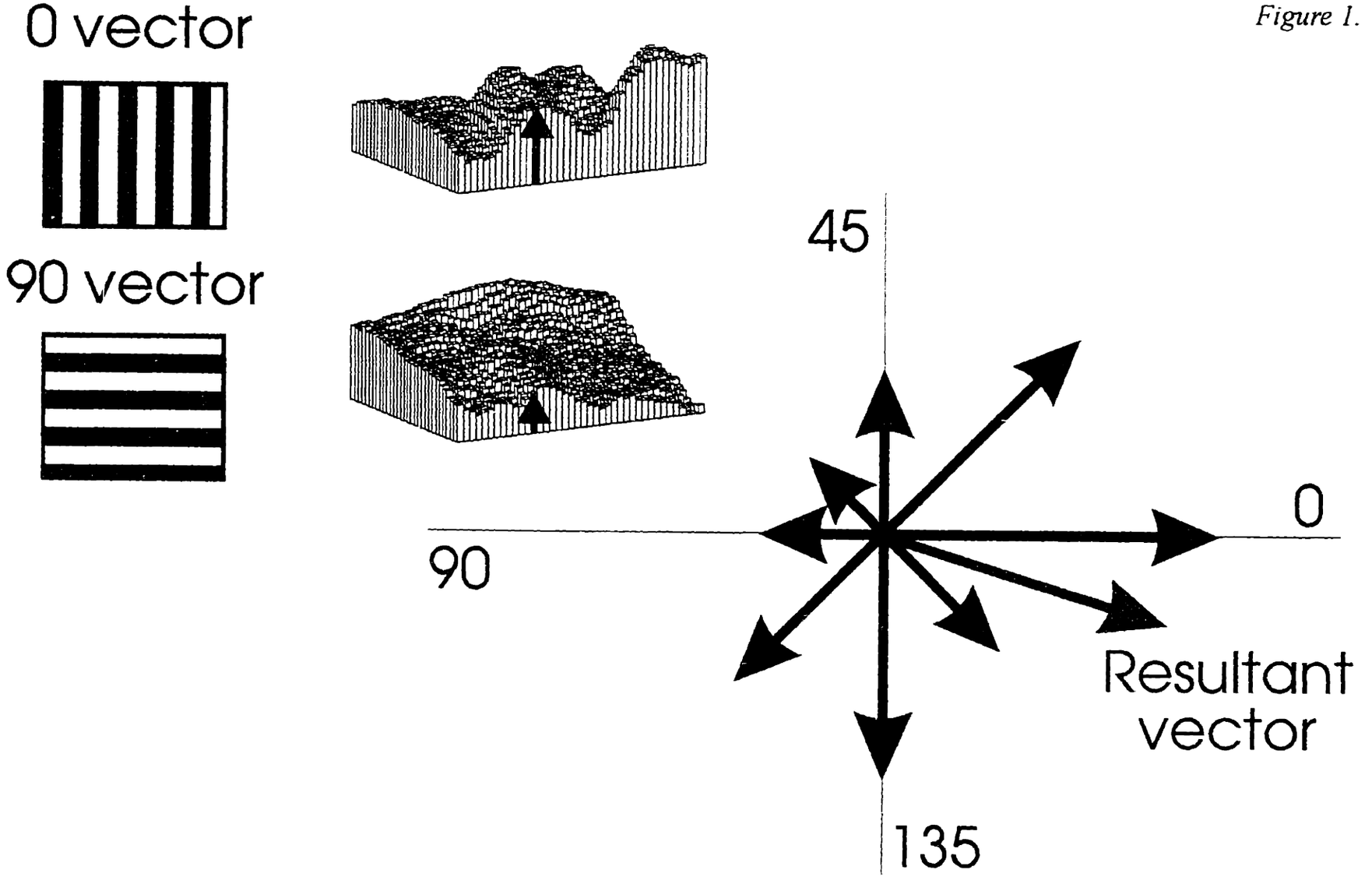

VECTOR AVERAGING METHOD for ORIENTATION